2022-07-20

Development of a Gram-type Specific Method for Detection of Bovine Mastitis Pathogens by Combining Loop-mediated Isothermal Amplification (LAMP) and Split Trehalase Technologies

Miao, Zhuohan

UNIVERSITY OF CALGARY

Development of a Gram-type Specific Method for Detection of Bovine Mastitis Pathogens by Combining Loop-mediated Isothermal Amplification (LAMP) and Split Trehalase Technologies

by

Zhuohan Miao

A THESIS

SUBMITTED TO THE FACULTY OF GRADUATE STUDIES

IN PARTIAL FULFILMENT OF THE REQUIREMENTS FOR THE

DEGREE OF MASTER OF SCIENCE

GRADUATE PROGRAM IN VETERINARY MEDICAL SCIENCES

CALGARY, ALBERTA

JULY, 2022

ABSTRACT

Bovine mastitis, which results mainly from intramammary infections (IMI) caused by Gram-positive or Gram-negative bacteria, is a huge burden on the global dairy industry. Oftentimes the presence of an infection can be deduced by measuring the somatic cell count (SCC) or released enzymes, or directly detected by the presence of mastitis pathogens. While many laboratory diagnostic methods (e.g., SCC determination, bacteria culturing, qPCR) exist, few have been modified and adopted for on-farm use due to the requirement of sterility, dedicated equipment and well-trained personnel for implementation, time restraints, and accuracy. As such, the development of new methods that can sensitively and specifically detect mastitis-causing pathogens on-farm would be very valuable. We aimed to detect and distinguish Gram-positive and Gram-negative mastitis bacteria to inform on the proper and prompter treatment/antibiotic to prescribe through two steps: (i) develop PCR and LAMP assay for a point-of-care (POC) amplification of Gram-positive and Gram-negative bacteria and (ii) use a modified amplicon binding split trehalase assay (ABSTA) to detect this amplification by a specific protein-DNA binding and the complementation of split trehalase. To do this, split trehalase fusion proteins HisTreA-C-SpoIIID and HisTreA-N-SpoIIID were purified, and the binding with modified oligonucleotides incorporated with SpoIII-specific recognition sequences was tested to verify and optimize the complementation conditions. Next, recognition sequences were introduced in Gram-type specific PCR primers, allowing for specific detection of PCR amplicons by ABSTA. We also integrated the recognition sequences in three Gram-type specific LAMP primer sets designed based on the pathogens' 16S rRNA genes,

allowing for specific detection of *Staphylococcus, Streptococcus* and Gram-negative bacteria LAMP products by ABSTA. The salt concentration, protein reagents versus DNA substrate ratio, direction and linker length of tandem recognition sites required for the complementation were optimized. Binding with purified PCR products demonstrated Gram-type detection specificity with the protein reagents, whereas the complementation appeared to be inhibited by agents in unpurified PCR products. The sensitivity of detection of bacterial genomic DNA of *Escherichia coli*, *Staphylococcus devriesii* and *Streptococcus uberis* ranged from 2 to 24. The sensitivity of detection of *E. coli* in spiked milk samples was 11 CFU/ml, but 4.9×10^4 CFU/ml and 2.0×10^5 CFU/ml for *S. devriesei* and *S. uberis*, respectively. The analytical specificity of the newly designed LAMP primer sets was evaluated with ten mastitis isolates at two genomic DNA copy number levels. In conclusion, the combination of bacterial genetic target amplification by LAMP and ABSTA demonstrated high sensitivity and specificity towards genomic DNA of Gram-positive and Gram-negative bacteria, enhancing the potential of developing a timesaving, user-friendly and cost-effective on-farm diagnostic method for educated treatment decisions of bovine mastitis causative pathogens.

ACKNOWLEDGEMENT

I would first like to express my deepest gratitude to my supervisor, Dr. Jeroen De Buck, for showing me the substance of a genius. Thank you for convincingly guiding and encouraging me to be professional and do the right thing even when the road got tough. I am extremely proud of, and grateful for my time working with you.

I would like to thank my committee members, Dr. Dongyan Niu and Dr. Constance Finney, for guiding and supporting me through this journey. Thank you for your encouraging words and thoughtful, detailed feedback.

I would like to thank the De Buck Lab for being the best lab mates to work with and grow together. Thank you for your friendship and company. For your invaluable assistance that you all provided throughout the journey.

Especially, I am indebted to Yongpeng Fu for being the most warmhearted partner to keep encouraging and guiding me to be on the right track. Words cannot express my gratitude and appreciation for having such a family-like friend like you in and out of the lab.

Thank you to James Wang for your assistance and support during my entire degree.

My most tremendous appreciation must go to my parents, Wei Miao and Yan Li. Thank you for your unconditional love and support throughout the entirety of my academic career. I hope to be a son who will not let you two down. I would like to dedicate this thesis to you two.

TABLE OF CONTENTS

LIST OF TABLES

LIST OF ILLUSTRATIONS, FIGURES, AND GRAPHICS

LIST OF SYMBOLS, ABBREVIATIONS AND NOMENCLATURE

Abbreviation	Definition
ABSTA	Amplicon Binding Split Trehalase Assay
BHI	Brain Heart Infusion
BIP	Backward Internal Primer
B3	Backward Outer Primer
BSA	Bovine Serum Albumin
CBMRN	Canadian Bovine Mastitis Research Network
CMT	California Mastitis Test
CNS	Coagulase-Negative Staphylococci
CPA	Cross Priming Amplification
DNA	Deoxyribonucleic Acid
E. coli	*Escherichia coli*
EDTA	Ethylenediaminetetraacetic Acid
ELISA	Enzyme-Linked Immunosorbent Assay
FIP	Forward Internal Primer
F3	Forward Outer Primer
g	Gram
gDNA	Genomic Deoxyribonucleic Acid
HDA	Helicase-Dependent Amplification
HIS	Histidine
HMG	High Mobility Group
hRFX1	Human Regulatory Factor X1
HTH	Helix-Turn-Helix
IMI	Intramammary Infections
IPTG	Isopropyl-β-D-Thiogalactoside
LAMP	Loop-Mediated Isothermal Amplification
LB	Backward Loop Primer
LB	Luria-Bertani
LF	Forward Loop Primer

LoC	Lab-on-Chip
MR	Magnetoresistive
NAS	Non-Aureus Staphylococci
PCR	Polymerase Chain Reaction
PDB	Protein Data Bank
POC	Point-of-Care
RCA	Rolling Circle Amplification
RM	Restriction-Modification
RPA	Recombinase Polymerase Amplification
S. aureus	*Staphylococcus aureus*
S. agalactiae	*Streptococcus agalactiae*
SCC	Somatic Cell Count
SDA	Strand Displacement Amplification
S. devriesei	*Staphylococcus devriesei*
SDS	Sodium Dodecyl Sulfate
S. dysgalactiae	*Streptococcus dysgalactiae*
SEA	Strand Exchange Amplification
SFMT	Surf Field Mastitis Test
S. uberis	*Streptococcus uberis*
TSA	Tryptic Soy Agar
wHTH	‘winged’ Helix-Turn-Helix
3EA	Three-Enzyme Assay

1. INTRODUCTION

1.1 Bovine Mastitis Causative Bacteria

Bovine mastitis, an inflammation of the udder tissue, is a huge burden on the global dairy industry (1). It can be broadly classified into two forms - clinical mastitis and subclinical mastitis (2). Bovine mastitis mainly results from intramammary infections (IMI) by udder pathogens (3). At present, more than 150 bacterial species have been identified as pathogens of mastitis, and both Gram-positive and Gram-negative bacteria can cause IMIs (4). Among them, Gram-positive bacteria are represented by various staphylococci and streptococci, while *Escherichia coli* and *Klebsiella pneumoniae* and other environmental coliforms such as *Enterobacter spp.*, *Serratia* and *Pseudomonas* are considered causative Gram-negative bacteria (5-6). For clinical mastitis, the primary pathogens are *Escherichia coli*, *Staphylococcus aureus*, coagulase-negative staphylococci (CNS) (also called non-aureus staphylococci (NAS)), streptococcal species, especially *Streptococcus uberis*, *Streptococcus agalactiae* and *Streptococcus dysgalactiae* (5, 7-11). On the other hand, minor pathogens, such as *Corynebacterium bovis*, are the main causative microorganisms of subclinical mastitis (12). However, due to different environmental factors and management measures, the distribution of bacterial species and the form of mastitis they cause, could vary between countries and herds (13-14).

1.2 Bovine Mastitis Treatment

The successful cure of bovine mastitis is mainly related to the severity of udder inflammation, precise diagnostic methods, drugs of choice, supportive treatment strategies, and control of the spread of the disease (15). For cases of mastitis during the lactation and dry-off period, it is essential to apply a suitable and effective treatment plan to eliminate the infection before the following lactation. This is especially true for infections at dry-off because the next lactation period will be directly affected by the infection during this period (16). Before the dry-off period, dairy cows need to be diagnosed with mastitis to confirm to be free from infection (17). Subsequently, the dry-cow mammary ducts are infused with antibiotics, and a teat sealant is used to block the teat canals (18). Although there are risks such as antibiotic resistance and antibiotic residues in the milk, currently, the dairy industry worldwide mainly relies on antibiotic administration for the control and treatment of bovine mastitis (19). Before antibiotic treatment, milk in the infected quarters should be excreted as much as possible to ensure that the efficacy of antibiotic therapy will not be hindered or delayed by the remaining pathogens, debris or the toxin produced by bacteria in the milk (20). For subclinical mastitis and mild or moderate clinical mastitis, intramammary injection of antibiotics is a broad route of administration. This route is also used in some acute clinical cases, especially in infections caused by certain Gram-positive cocci (22).

For acute clinical cases, macrolide antibiotics and gentamicin are commonly used for mastitis caused by Gram-positive bacteria, and polymyxin B is the primary choice for Gram-negative infections (21). Penicillin is usually applied to treat infections caused by NAS, *S. agalactiae* and *S. dysgalactiae* due to their sensitivity to penicillin (21). Penicillin also has a certain effect in the treatment of infections caused by *S. uberis*, but the administration time needs to be prolonged. However, since *S. aureus* is often resistant to β-lactam antibiotics, antimicrobial treatment is challenging for this pathogen (23). For mild clinical mastitis caused by Gram-positive bacteria, intramammary injection of bactericidal drugs such as Procaine penicillin, cephalexin, and erythromycin can play a certain role (21). However, for Gram-negative pathogens antibiotics are not suggested for the mild and moderate infections due to the risk of releasing endotoxin (27). In contrast, glucocorticoids are suitable for severe clinical mastitis caused by Gram-negative bacteria, especially endotoxin-producing coliforms (22). For subacute clinical infections, intramammary infusion of cefoperazone with a single dose can improve the treatment outcome of this form of mastitis (24). The treatment of subclinical mastitis is the same as for clinical cases. Generally, it is more economical to use antibiotics during the dry-off period than during lactation and it has a higher cure rate (25). Although antimicrobial therapy is currently the primary treatment strategy for mastitis, the critical prerequisites for selecting and administrating appropriate antibiotics are accurately detecting the involved pathogens and performing drug sensitivity tests (26).

1.3 Bovine Mastitis Diagnosis

1.3.1 Somatic Cell Count (SCC) Indication

Diagnosis is an essential bridge between the cause and treatment of bovine mastitis. The earlier the diagnosis is implemented, the lower economic losses, including treatment, control and management costs, can be (28). Generally, the diagnosis of mastitis can be divided into two categories: (i) detection of disease status and severity indicators and (ii) detection of pathogenic bacteria (29). SCC is the most commonly used indicator determined from milk samples for the presence of mastitis, with an equal to or higher than 200,000 cells/ml (30-31). The direct measurement of SCC includes Coulter counting, methylene blue staining, and automated cell counter-based fluoro-optic electronic cell counting (29). On the other hand, indirect methods include the California mastitis test (CMT), Surf field mastitis test (SFMT), and Fossomatic SCC by disk or flow cytometry. The first two are based on the detection of gel formed by releasing nucleic acids and other cell constituents by adding certain detergents (e.g., sodium dodecyl sulfate (SDS)) to high-SCC samples (32-33). These two tests can lead to false-negative and false-positive results, and they are not capable of giving SCC numerical values and indicating the severity of the disease (34). The principle of Fossomatic SCC is based on flow cytometry, where the fluorescent cells are detected after being excited at a certain wavelength. This technology is faster and more automated, but it is inseparable from the laboratory and requires expensive and complex equipment

(31). However, the above methods based on SCC determination cannot identify specific causative pathogens. Due to the distribution of the mastitis pathogens being diverse, their identification informs treatment strategies, including the choice of antibiotics and management to control the spread of infection. Antimicrobial therapy is currently the most commonly employed treatment strategy for mastitis. Thus, species-identifying diagnosis before treatment greatly helps to avoid the occurrence of multi-drug resistance, reduce the risk of antibiotic residues in milk, and improve the welfare of animals to a certain extent (35-36).

1.3.2 Culture Methods

Pathogen culturing-based technologies rely on culturing milk samples on appropriate media under specific conditions, counting harvested colony forming units (CFU) and assessing colony phenotypes to indicate pathogens. On various general-purpose media (e.g., TSA blood plates), most bovine mastitis pathogens can grow aerobically. However, widespread implementation of pathogen culturing methods is limited due to the lengthy time required and the need for sterile culture environments, experimental equipment and personnel trained to interpret bacterial phenotypes. To make microbial culturing methods more beneficial for on-farm adoption, several on-farm culturing-based kits that incorporate selective media have been developed (e.g., the Accumas™ system) to circumvent the demand for expertise in phenotypic identification (37).

Although the sensitivity and specificity of these kits for the detection of Gram-negative and Gram-positive bacteria have been validated (38), it is undeniable that they are still time-consuming and require special equipment to accommodate their on-farm use.

1.3.3 Molecular Methods: PCR and qPCR

The advent of PCR-based molecular amplification technology shortens the detection of mastitis pathogens to a few hours, and direct detection of target DNA dramatically improves the accuracy of pathogen identification. By amplifying the thermonuclease coding *nuc* gene, which is highly specific for *S. aureus*, a qPCR method can identify this specie in milk samples within 5 hours with high specificity (39). Furthermore, several qPCR-based commercial kits have been developed and adopted to amplify the DNA of mastitis bacteria in milk, such as the qPCR PathoProof Mastitis kit, which showed superior performance in detecting both subclinical and clinical mastitis bacteria compared to traditional culturing methods (40). Nevertheless, implementing an on-farm PCR is challenging, requiring specific laboratory equipment and skilled personnel. PCR is still likely to be inhibited by agents present in milk that are not removed by the DNA extraction step. A lab-on-chip (LoC) device from Magnomics S.A. that combines microfluidics with magnetoresistive (MR) sensors is going through the development phase. This method integrates sample preparation, DNA extraction and amplification steps in a compact disposable box in order to achieve point-of-care

(POC) detection of mastitis bacteria on-farm (41).

1.3.4 Molecular Method: Loop-Mediated Isothermal Amplification (LAMP)

Unlike PCR, which relies on a thermal cycler for denaturation, annealing, and extension, isothermal amplification of DNA can be performed at constant reaction temperatures and offers more potential to be developed as the POC diagnosis. Overall, isothermal technologies can be divided into DNA replication-based amplification and enzyme-based digestion (42). Although the emergence of isothermal amplification of DNA could facilitate the diagnosis of pathogens on-farm at the molecular level, based on a comparison of the sensitivity and specificity of detection, simplicity of reaction conditions, reaction time, and cost of different techniques, some have certain limitations. For example, SEA (strand exchange amplification) and CPA (cross priming amplification), which are one-step methods, are characterized by more straightforward primer designs. However, their detection sensitivity makes them unsuitable for molecular diagnostics on farms (43). On the other hand, RPA (recombinase polymerase amplification), which also uses a uncomplicated primer design, is prone to generating non-specific products in the negative control. Detecting the amplification products also require specialized instruments (e.g., gel electrophoresis apparatus) that are inconvenient to operate on farm (43). Moreover, some of the isothermal reactions are expensive, and the completion of the assay requires additional enzymes, such as DNA

helicase used in HDA (helicase-dependent amplification) to unwind double-stranded DNA and generate single-stranded DNA for the hybridization and extension of primers (42). Additionally, SDA (strand displacement amplification) initially requires a denaturation step at 95ºC, and RCA (rolling circle amplification) requires a special circle template called 'padlock probe' for the exponential amplification phase. These increase the condition complexity and time to results (42, 46). The listed drawbacks of the above-mentioned amplification assays technically limit their on-farm use as portable real-time quantitative methods.

In contrast, LAMP has a huge potential to be developed as an on-farm diagnostic, which was first proposed in 2000 (44). Compared to standard PCR and qPCR techniques, this method is faster, more sensitive and specific with fewer requirements for high-quality template. Most importantly, it is performed at an isothermal condition which can be easily fulfilled by a water bath or heat block set on field (45). In each LAMP reaction, forward internal primer (FIP), backward internal primer (BIP), forward outer primer (F3), backward outer primer (B3), forward loop primer (LF) and backward loop primer (LB) are required. Nagamine et al. (2002) developed a LAMP mechanism using loop primers to accelerate the amplification (46). As such, LAMP primers specifically recognize eight distinct regions flanking the gene of interest, namely F3, F2, F1 and LF regions located at the 5' end of the target gene and B1c, B2c, B3c and LB regions located at the 3' end. F1c is the region on the antisense strand that is complementary to F1. FIP (BIP) is composed of the sequence of F1c (B1c) at the 5' end and F2 (B2) at its 3' end. The sequences of LF and LB are complementary to the regions between F1/F2 and B1/B2, respectively. The size of

target DNA, the primers' sequence, size and GC content, the range of their melting temperature, and the distance between the various primer-bound regions on the same strand, and the limitations of the change in free energy at the primer end, have been previously reviewed (47, 48). More descriptions of the design standards of LAMP primers can be found on the Eiken Chemical Co., Ltd. website (http://loopamp.eiken. co.jp/e/index.html) (49).

Another critical component in the LAMP reaction is the *Bst* DNA polymerase, which has strand displacement activity under a constant temperature condition. According to its participation, LAMP amplification can be divided into the starting structure producing stage and the cyclic stage (50). First, with the assistance of the *Bst* DNA polymerase, one of the internal primers (i.e., FIP) starts regular DNA synthesis to produce the target DNA. Subsequently, the outer primer at the same prime end was added and a new DNA strand is synthesized, releasing the previously synthesized target DNA strand. Therefore, through the action of FIP/F3 and BIP/B3, a single-chain dumbbell-like structure is generated. The complementarity of F1/F1c and B1/B1c forms two loops at both ends of the strand, which are rapidly transformed into a stem-loop-like DNA, serving as the starting material for the next LAMP amplification stage. The next step is also called the cycling stage, in which by-products of various sizes initiate the elongation stage in which the loop primers are employed. Since loop primers are capable of specifically recognizing the stem-loop region in the structure of these by-products, the number of amplification starting sites increases, thereby significantly improving the amplification efficiency. Moreover, the starting materials of the cycling stage also contain these loop primer recognition sites, so it is more difficult to produce non-specific

LAMP products when loop primers are used (46). The products of the LAMP reaction contain stem-loop DNA of various sizes with alternately inverted repeats of the target sequence on the same strand, thus the preliminary characterization of the positive result can be analyzed by electrophoresis. A step-like pattern filling up an entire lane can be observed on the agarose gel. Additionally, magnesium pyrophosphate is a side-product of the LAMP reaction so that the preliminary results can be directly observed with a real-time turbidity meter. The fluorescent dyes such as SYBR green can be added during the preparation to visually detect the changes in fluorescence intensity through a UV light (48).

LAMP has several advantages over conventional PCR and real-time PCR technologies. Firstly, the whole process of amplification can be accomplished within 30 minutes (46). Only a few copies of the genetic target are required at the start to obtain up to 10^9 target copies, corresponding with a higher efficiency. Secondly, in the initial structure generation stage and the elongation stage of LAMP, there are six independent primers and four primers, respectively, involved in amplifying the target gene, so the specificity of LAMP can theoretically be higher as well (51). Moreover, LAMP reaction does not require a laboratory thermal cycler; it only needs a water bath or heating block to meet isothermal conditions. Thus, LAMP can be modified to be a POC application. The final results can be observed as a change in fluorescence or turbidity, avoiding the need for more complex analysis (45, 48).

Based on the considerable potential of LAMP as a diagnostic tool, several studies have developed

LAMP methods to identify various causative pathogens of bovine mastitis. Aiming at the main pathogenic bacteria, *S. aureus*, Zhang et al. focused on the species-specific *nuc* gene encoding thermonuclease (52). They designed a set of LAMP primer without loop primers. A highly specific LAMP assay was then developed to detect *S. aureus* in natural mastitis milk samples within 45 minutes at 62.5°C. At the same time, they compared the sensitivity of LAMP with conventional PCR and found that the detection limit of the former was 1×10^2 CFU/ml of concentration in the bacterial culture, which was 100-fold more sensitive than conventional PCR. The addition of the fluorescent dye SYBR Green I allowed the positive results to be more readily distinguished by the naked eye under UV light, demonstrating the potential of this technology to be applied to the rapid detection of *S. aureus* (52). Aiming at the specific DNA sequence of *S. agalactiae* in the 16S rRNA gene, a LAMP primer set containing six primers was also previously generated. This LAMP assay has the capability of detecting the extracted *S. agalactiae* genomic DNA with a sensitivity of 20 pg per reaction within 1 hour at 64°C. In addition, among the 13 known bovine mastitis pathogens, only *S. agalactiae* was positive for this developed LAMP assay, indicating its high specificity. This research supported using LAMP for on-farm control of mastitis by a rapid screening of bacterial pathogens (53). Furthermore, *S. uberis* genes encoding superoxide dismutase A (*sodA*), plasminogen activator A (*pauA*), and chaperonin Cpn60 (*cpn60*) were selected for the design of another LAMP primer set specific for these bacteria. The minimum detection limit of this assay was determined to be 12 fg of extracted genomic DNA per reaction, and the detectable amplification appeared as soon as 8 min. Based on raw milk samples from farms infected and uninfected with *S. uberis*, both the sensitivity and specificity of the test reached 96.0% (42).

Mycoplasma bovis (*M. bovis*) genome *gyrB*, *uvrC* and 16S rRNA sequences were the target of another LAMP assay. Research in 2017 by Aqeela et al. demonstrated that, compared to conventional PCR using one pair of primers, these newly developed LAMP assays presented higher sensitivity and specificity in detecting the genomic DNA extracted from standard isolates of *M. bovis* and spiked pasteurized milk (28).

1.4 Protein-DNA Binding

The interactions of DNA and proteins play a critical role in most cellular biochemical activities, such as DNA transcription, replication, packaging, and repair (54). DNA-protein interactions can be classified as DNA sequence-specific and non-sequence-specific. For non-sequence-specific recognition, base-pair specific recognition of protein is absent during the formation of the DNA-protein complex structure, or the protein binds multiple sites on double-stranded DNA (55-56). Three classes non-sequence-specific binding proteins have been studied. The first is HMG-D, which originates from the subfamily of chromosomal protein and binds to DNA with the high mobility group (HMG) domain (57); the second is the nucleosome, a basic unit of eukaryotic chromatin formed by the core histone and peripheral-wrapping multiple base pairs (56); the third is the Sso7d protein from *Sulfolobus solfataricus*, which is categorized as histone-like DNA-binding protein (58). As mentioned, the above-mentioned proteins non-specifically distinguish

DNA strands for binding. In contrast, type II restriction endonucleases and transcription factors were considered to be examples of proteins capable of recognizing DNA sequences specifically. Type II restriction endonucleases are an essential component of bacterial restriction-modification (RM) systems. This group of proteins can respond to specific recognition sites in foreign DNA and bind before cleaving the DNA (59). Sequence-specific transcription factors are another critical group of DNA-binding proteins in the cellular environment. They specifically recognize and bind to transcriptional regulatory regions on homologous DNA for the purpose of initiating the regulation of target gene expression (60).

According to the architectures of the proteins in the protein-DNA complexes, these proteins are categorized into a system at group and family levels in the Protein Data Bank (PDB) (54). In this classification system, DNA-binding proteins are defined into the following groups: helix-turn-helix (HTH) proteins (including the 'winged' version), zinc-coordinating proteins, zipper-type proteins, other α-helix proteins, β-sheet proteins, β-hairpin/ribbon proteins, and other proteins and enzymes. Based on the structural environment of amino acids in the secondary structure of DNA-binding domains, homologous families were identified by further subdividing the above-mentioned protein into family tiers (61). Additionally, according to the degree of dominance of the secondary structure (such as α-helix and β-sheet) in the DNA-recognition domains of the protein, these proteins can also be classified into the following four categories: α-dominant, β-dominant, α/β-mixed and multi-domain proteins (62). This classification strategy is similar to the previous one. For example, a few same secondary structures such as the HTH motif can be found in the

DNA-binding domains of proteins with different helix dominance.

As one of the most common recognition elements in the binding region of proteins that form complexes with DNA, the HTH motif mainly exists in enzymes and transcription regulators of prokaryotic and eukaryotic genomes (62-63). As the name suggests, the structure of HTH motif contains two helices, but only the second helix is capable of recognizing the DNA, so it is usually termed the recognition helix or probe helix. In most cases, the amino acid side chains on the second helix are in direct contact with the exposed bases in the major grooves of DNA through hydrogen bonds and hydrophobic interactions, thereby embedding in the major grooves. The role of the first helix is mainly to maintain the stability of the interaction between the DNA backbone and the protein and has no specific recognition function (54, 63). But in some exceptional cases, such as in human DNA repair protein AGT, HTH motif can also be utilized to bind the minor groove of DNA (64). Although structures other than HTH motif lack homology between different protein families, the structure of HTH motif is highly consistent within these families (65). The 'winged' helix-turn-helix (wHTH) motif is a representative family in the HTH group, which carries a third α-helix and a reversely parallel β-sheet, which are wing-like (66). In most cases, the wing-like structure functions to increase contact with minor grooves in the DNA backbone without affecting the recognition of DNA by the second helix. But the human regulatory factor X1 (hRFX1) is an exception, using β-sheet to bind the major groove in DNA as a new way of identifying DNA by wHTH motif (67). Generally, both prokaryotic and eukaryotic DNA-binding proteins are able to bind DNA through monomers or dimers, but there are differences in the recognized DNA

sequences. The former mainly recognizes palindrome DNA sequences, while the latter mainly recognizes non-symmetrical target regions (54). Although the interaction between the HTH motif-carrying prokaryotic and eukaryotic proteins and DNA differs, the HTH motif in both cases contributes to the favorable contact structure between recognition helix presented on the protein surface and DNA backbone.

Research on the specificity of protein-DNA binding is at the forefront of structural biology. On average, each contact between protein and DNA comprises more than 20 protein residues and more than 10 bases. These contacts are often responsible for preferential sequence specificity between protein and DNA (68). Different binding specificities of different proteins in a superfamily are based on these specific combinations. For example, in the homeodomain proteins superfamily, asparagine at position 51 and glutamine at position 50 have affinity for AT-rich sequences and a specific conserved binding site, respectively (69-70). In addition to the interplay with bases, another contact that contributes to the site-specificity of protein-DNA binding occurs between the protein and the DNA backbone. Most of the DNA backbone contacts are mediated by the formation of hydrogen bonds, and the rest are mediated by hydrophobic interaction. Backbone contacts assist the protein in settling in the major groove of DNA so that its recognition structure (such as HTH motif) does not deviate from the preferred binding site, thereby enhancing the specificity of this interaction (71). Moreover, in the same protein family, the supporting role of the backbone contacts determines the consistent orientation of binding to ensure family specificity (72).

1.5 SpoIIID

Under nutrient deprivation, Gram-positive *Bacillus subtilis* undergoes a series of endospore formation processes regulated by the expression of cognate genes to achieve a state of survival (73). First, the original cell undergoes morphological changes, that is, a septum is asymmetrically generated between two compartments by way of polarity division. These two compartments are called mother cells and endospores, and each contains an identical genome copy. The membrane subsequently migrates to internalize the endospore in the mother cell, forming a double membrane structure. The space between the double membranes is then filled with peptidoglycan cortex, and the coating protein is also synthesized on the surface of the endospores. Finally, with the lysis of the mother cell, the mature spore is released from it. This complex sporulation process of *Bacillus subtilis* is inseparable from the strict regulation of a gene expression program, which is a cell-type-specific pathway containing a series of δ subunits of RNA polymerase (RNAP) (74). Temporal regulation in gene expression is controlled by four types of RNAP, which are δ^F, δ^E, δ^G, and δ^K in the order of appearance, among which δ^E and δ^K are mother cell-specific (75). SpoIIID is a transcription factor that activates and represses gene expression driven by δ^E and δ^K RNA polymerase. It can specifically recognize and bind to the sequence located in the promoter regions and open reading frames of several genes. For example, SpoIIID is capable of activating the transcription of *spoIVCA* and *sigK* regulated by δ^E RNA polymerase in vitro but presents a

depressing effect on *bofA* and *spoVD* (76-77). After alignment analysis of the binding sites of SpoIIID in these genes, a consensus sequence was obtained, 5‘-WWRRACAR-Y-3’ (W = A or T, R = A or G, Y = C or T). Interestingly, this sequence is similar to the promoter region bound by δ^E and δ^K RNAP. Moreover, the recognition helix of SpoIIID and these two RNA polymerases have an identical amino acid residue at the same position, which is prone to forming hydrogen bonds with the consensus sequence (76). In subsequent studies, it was further demonstrated that SpoIIID can bind the consensus sequence with a high affinity. This idealized sequence of 10 bp was determined to be 5’-TAGGACAAGC-3’ (78).

SpoIIID has a putative HTH motif, which indicates that it uses a recognition helix to bind to DNA. Furthermore, a C-terminal basic region was found in SpoIIID, which is involved in cooperative binding of the conserved DNA and was functionally similar to the 'wing' domain of the winged-HTH motif (78-79). In *Bacillus* and *Clostridium*, the recognition helix and C-terminal basic region involved in DNA recognition in SpoIIID orthologs are highly conserved; the recognized nucleic acid sequence is also highly conserved in many sporulating bacteria (80). As previously mentioned, the DNA sequences bound by prokaryotic transcription regulators are mainly palindromic (54). Nevertheless, the above-mentioned conserved sequence specifically recognized by SpoIIID is non-palindromic. Another noteworthy point is that unlike most bacterial transcription regulators binding to DNA as a homodimer, the binding of SpoIIID to this 10 bp DNA was predicted to be in a monomeric form. The analysis of the monomer status came from a gel filtration chromatography study based on SpoIIID purified from sporulating *B. subtilis* (Zhang and Kroos, unpublished) (78).

As mentioned previously, eukaryotic homeodomain proteins with HTH motifs mainly bind to DNA in monomeric form, owing to the fact that the N-terminal arm interacts to the minor groove of DNA, which plays an assisting role in monomeric binding (81). However, SpoIIID being a prokaryotic DNA binding protein which has only one HTH motif and no N-terminal arm, binds to DNA in a monomer form with high affinity as well. It was found that the α helix located adjacent to the HTH motif occupies the space normally occupied by the N-terminal arm, so that SpoIIID is unable to use the arm to recognize DNA in a monomer form cooperatively. Nevertheless, after reversing several highly conserved charges located in the C-terminal basic region and knocking out the C-terminus, the expression of binding-related genes was significantly depressed. This indicates that the C-terminal basic region of SpoIIID is functionally similar to the N-terminal arm, assisting in generating an additional interaction between SpoIIID and DNA (78). Therefore, the recognition helix of HTH motif and the C-terminal basic region collaborate to support SpoIIID binding to DNA with high affinity in a monomeric form.

1.6 Trehalase

Over the years, various analytical methods have been developed which take advantage of specific enzyme catalytic reactions. For example, in enzyme-linked immunosorbent assays (ELISAs) and polymerase chain reaction (PCR), enzymes respectively play a role in generating detectable signals

and catalyzing the amplification of target DNA strands (82). Similarly, glucose produced by enzymatic catalysis is considered to have great potential as a reporter to be easily and quickly detected by current handheld glucometers. The trehalases discussed here are a group of glucose hydrolases that is able to catalyze the hydrolysis of trehalose, a non-reducing disaccharide, by inversion of the anomeric configuration, breaking it down into two glucose monomers (83-84). Trehalases are found in bacteria, fungi, yeasts, insects, plants and mammals. Human trehalases are locally expressed on the intestinal mucosa and the renal brush border and appear to play the role of stress-protein in the kidney and participate in the gluconic transmembrane transport (85-86). In insects, trehalases universally exist in hemolymph and have a critical role in carbon metabolism during various physiological activities (87). Hence, inhibition of insect trehalases have become a significant target in pest control strategies.

Trehalases have been isolated and characterized from several bacterial species, including *Mycobacterium smegmatis* and *Mycobacterium tuberculosis*, and corynebacterial, *E. coli*, *Rhizobium* sp. and so on (88-91). In *E. coli*, TreA and TreF represent two different trehalases, their expression is subject to a similar regulation pathway, but both are capable of hydrolyzing trehalose (92). TreA, as a periplasmic trehalase, can assist in hydrolyzing the intracellular trehalose exported to the periplasm into glucose to alleviate the high osmolar pressure in the growth media, while it also allows trehalose synthesized in the cytoplasm to be used as a carbon source for *E. coli* at a high osmolarity (82, 93). On the other hand, TreF, as a highly homologous protein of TreA, only participates in trehalose metabolism in the cytoplasm. It ensures that *E. coli* cells are able of

processing redundant internal synthesized trehalose after recovering from high to low osmolarity (94). However, even in low osmotic strength, the enzymatic capability of TreA is higher than that of TreF. Moreover, only in the absence of background activity of TreA, the hydrolysis of trehalose by TreF with low activity can be observed (93).

The three-dimensional structure of TreA reveals that it contains an $(\alpha/\alpha)_6$ toroid fold and utilizes an aspartic acid at residue 312 as the catalytic acid and a glutamic acid at residue 496 as the catalytic base to catalyze glycoside hydrolysis through an inversion of the anomeric configuration. The binding of trehalose by TreA is achieved by multiple hydrogen bonds. The optimal temperature and pH for the catalytic reaction are 37°C and pH 5.5, respectively, in a buffer containing bovine serum albumin (BSA) (84). Based on a published study in 2018, TreA can be experimentally split into two complementary units, N domain and C domain with each fused with a 6× His-tag. The trehalase enzymatic capacity can be conditionally restored after incubating the split TreA fusion proteins with anti-His monoclonal antibodies, which indicates the occurrence of complementation of N and C domains. Since the glucose resulting from split enzyme complementation can be detected by the commercially available glucometer, this split enzyme technology displays a significant potential to be developed as a novel platform for rapid detection of immunoglobulins, pathogens of specific diseases, intermolecular interactions and more (95).

2. HYPOTHESIS

We hypothesize that complementation of recombinant fusion proteins HisTreA-C-SpoIIID and HisTreA-N-SpoIIID can be conditionally triggered by binding of protein SpoIIID with SpoIIID-specific recognition sites incorporated in tandem on hairpin formed oligonucleotides and double-stranded DNA. The complementation will cause the restoration of trehalase enzymatic activity which can be quantified by a colorimetric enzymatic assay. This protein-DNA binding can be affected by different conditions (e.g., salt concentration, protein reagents versus DNA substrate ratio, direction and linker length of tandem recognition sites), whose optimal values can be determined.

We hypothesize that tandem SpoIIID-specific recognition sites can be introduced to colony PCR products by incorporating the tandem SpoIIID-specific recognition sequences into Gram-type specific PCR primer pairs, allowing for the Gram-type specific detection through the restoration of trehalase enzymatic activity.

We hypothesize that Gram-type specific LAMP primer sets can be designed based bacterial 16S rRNA gene alignments and incorporated with tandem SpoIIID-specific recognition sequences, allowing for the Gram-type specific detection through the restoration of trehalase enzymatic activity.

3. SPECIFIC AIMS

The objective of this project is to develop a Gram-type specific method for detection of bovine mastitis pathogens by combining LAMP and split trehalase technologies. To achieve this, we aimed to:

1. Assess complementation of recombinant proteins HisTreA-C-SpoIIID and HisTreA-N-SpoIIID with modified oligonucleotides/DNA incorporated with SpoIIID-specific recognition sequences in tandem.
2. Incorporate tandem SpoIIID-specific recognition sequences into Gram-type specific PCR primers and assess complementation of recombinant proteins HisTreA-C-SpoIIID and HisTreA-N-SpoIIID with PCR products of *S. devriesei* and *E. coli* colonies.
3. Design *Staphylococcus*, *Streptococcus* and Gram-negative bacteria-specific LAMP primer sets incorporated with tandem SpoIIID-specific recognition sequences.
4. Assess sensitivity of detection of Gram-type specific LAMP with designed LAMP primer sets and DNA extracted from bacterial culture and bacteria-spiked milk samples through analysis of complementation of recombinant proteins HisTreA-C-SpoIIID and HisTreA-N-SpoIIID.
5. Assess specificity of detection of Gram-type specific LAMP with designed LAMP primer sets and DNA extracted from bacterial culture through comparison of amplification curves.

4. MATERIALS AND METHODS

4.1 Bacterial Strains and Culture Conditions

The bacterial strains used in the course of this study are *Staphylococcus devriesei* 41816325, *Staphylococcus aureus* USA300, *Streptococcus uberis* 10501290, *Streptococcus dysgalactiae* 20304478, *Streptococcus* spp. 10107041, *Corynebacterium* spp. 40200255, *Escherichia coli* DH10β, *Escherichia coli* 10109298, *Klebsiella* spp. 10116692 and *Enterobacter* spp. 11104490. Strains *S. devriesei*, *S. aureus* and *E. coli* DH10β were preserved in glycerol stocks at -80ºC in our lab. The remaining strains were purchased from the Canadian Bovine Mastitis Research Network (CBMRN), Faculty of Veterinary Medicine, University of Montreal, where the isolates were lyophilized and stored below 4ºC. The preserved glycerol stock of *S. devriesei*, *S. aureus* and *E. coli* DH10β was inoculated and cultivated aerobically in 10 ml LB broth in a 50 ml sterile conical tube shaking at 170 rpm at 37ºC for 18 h to harvest the bacterial cultures. Each freeze-dried strain from CBMRN was revived in 500 µl of Luria-Bertani (LB) broth (Thermo Fisher, Mississauga, Canada), inoculated 100 µl of the suspension onto the Tryptic Soy Agar (TSA) plate with 5% sheep blood (Hardy Diagnostics, California, USA) and incubated at 37ºC for 18-24 h until individual colonies appeared. Individual colonies of *S. uberis*, *S. dysgalactiae*, and *Streptococcus* spp. were scraped off the agar and inoculated into 14 ml Brain Heart Infusion (BHI) broth (Becton, Dickinson and Company, Sparks, USA) in a sterile 15 ml conical tube with cap tighten and grown in a 37ºC

incubator for 18-24 h (96). A single colony of *Corynebacterium* spp. was grown aerobically in 10 ml BHI broth in a 50 ml sterile conical tube at a 30ºC shaker for 18 h (170 rpm) (97). A single colony of *E. coli* 10109298, *Klebsiella* spp. or *Enterobacter* spp. was inoculated in 10 ml LB broth in a 50 ml sterile conical tube and aerobically cultivated for 18 h at 37ºC for the former two isolates and 30ºC for the latter (170 rpm) (98). The bacterial cultures of all the above-mentioned strains were used for the genomic DNA (gDNA) extraction. A 500 µl volume of the bacterial culture was gently mixed with 500 µl of 50% glycerol in a 2 ml sterile tube and stored at -80ºC.

4.2 DNA Extraction

4.2.1 DNA Extraction from Bacteria Culture

The gDNA from bacterial cultures was extracted with the DNeasy Blood & Tissue Kit (QIAGEN, Toronto, Canada). Following the manufacturer's protocols, 1 ml of Gram-positive bacterial overnight culture was centrifuged at 17,900 *g* for 5 min. After removing the supernatant, the cell pellet was resuspended in 1× PBS followed by the addition of 20 µl of proteinase K and 200 µl of Lysis Buffer (Buffer AL). Then, 0.5 g of autoclaved silica beads (Zymo Research, Irvine, USA) was added to the sample and submitted to the bead beater (BioSpec Products, Bartlesville, USA)

for two 5-min rounds. Afterwards, the sample was centrifuged at 16,000 *g* for 5 min and the supernatant was pipetted into a new tube with 200 µl of absolute ethanol (96%-100%) and mixed thoroughly. The solution was subsequently transferred into the provided QIAamp mini spin column in a 2-ml collection tube, followed by centrifugation at 6,000 *g* for 1 min. The spin column was transferred to a new collection tube. Then, 500 µl of wash buffer 1 (buffer AW1) was added before centrifugation at 6,000 *g* for 1 min. In the second round, the sample was washed with 500 µl of wash buffer 2 (buffer AW2) by centrifugation at 20,000 *g* for 3 min and another for 1 min under the same conditions. Subsequently, the mini spin column was placed into a new 1.5-ml microcentrifuge tube. To recover DNA, 50 µl of elution buffer (buffer AE) was added to the mini spin column, which was allowed to stand for 10 min at R/T and centrifuged at 6,000 *g* for 1 min. For DNA extraction from Gram-negative bacterial cultures, the use of autoclaved silica beads and bead beater was omitted. The concentrations, 260/280 and 260/230 ratios of extracted gDNA were measured by the NanoPhotometer™ NP80 UV/Vis spectrophotometer (Implen, California, USA). The DNA preparation was stored at -20℃. All the centrifugations in this section were performed at R/T.

4.2.2 DNA Extraction from Milk Samples Spiked with Bacterial Culture

Pasteurized milk was purchased from a local retail outlet. To prepare a milk aliquot, 1.8 ml of

pasteurized milk was transferred to a 2-ml microcentrifuge tube. For *Staphylococcus* and *Streptococcus*, milk aliquots were spiked with 200 µl of undiluted bacterial culture of OD_{600} at 1, 18 µl of undiluted culture and its 10-fold serial dilutions. For Gram-negative bacteria, milk aliquots were spiked with 18 µl of undiluted bacterial culture (OD_{600} = 1) and its dilutions. After mixing thoroughly by pipetting, the spiked milk aliquot was centrifuged at 6,700 *g* for 10 min. After removing the upper fatty layer and supernatant, 500 µl of 0.9% sterile NaCl solution was added to resuspend the pellet, and the mixture was centrifuged at 6,700 *g* for 5 min. Afterwards, the pellet was resuspended in 500 µl TENS buffer [10 mM Tris-HCl (pH 8.0), 1 mM EDTA, 150 mM NaCl, 0.5 % SDS]. Proteinase K (1.5 mg/ml) was then added to the suspension and incubated at 56ºC for 1 h. Autoclaved silica beads (0.5 g) were subsequently transferred to the solution and the tube was shaken for 5 min in a bead beater, twice, and centrifuged at 12,000 *g* for 10 min in order to collect the supernatant in a fresh tube. The supernatant was supplemented with an equal volume (500 µl) of phenol: chloroform: isoamyl alcohol (25:24:1) and mixed gently and centrifuged at 12,000 *g* for 10 min. The upper aqueous phase was transferred to a new tube to combine with an equal volume (500 µl) of chloroform: isoamyl alcohol (24:1), mixed gently and centrifuged at 12,000 *g* for 10 min. The aqueous layer was collected in another new tube followed by the addition of 600 µl of R/T 100% 2-propanol, gentle mixing, and centrifugation at 12,000 *g* for 10 min. After discarding the supernatant carefully, the pellet was resuspended in 1 ml of ice-cold 100% ethanol, mixed gently and stored at -80ºC for 30 min. The sample was then centrifuged at 20,000 *g* for 20 min. The resulting DNA pellet was washed with 600 µl of room temperature 70% ethanol and centrifuged at 12,000 *g* for 10 min. After air-drying, the DNA pellet was resuspended in 50 µl of

sterile water and stored at -20ºC. All the centrifugation in this section was performed at R/T.

4.3 Oligonucleotides

The oligonucleotides used in the optimization of fusion proteins-DNA binding detection were designed to contain specific recognition sites in tandem. In order to form a hairpin structure at both ends of the oligonucleotide with double-stranded DNA that specifically binds to SpoIIID, two recognition sequences A, and two reverse complement sequences B were connected by linkers.

The recognition sequence A and its reverse complement sequence B were combined in the manner ABAB and named ABABspoIIID (Figure 4c, d, e) (Table 1). In the oligonucleotide ABABcont, four consecutive bases GGCA in the recognition sequence A were replaced with TTGT (Table 1). The corresponding bases in the sequence B were also changed to the complementary ACAA accordingly (Figure 4).

The oligonucleotides other than ABABspoIIID were generated as three different combinations of the recognition sequence A and the reverse complement sequence B. The linker length between the formed double hairpin remained unchanged. These three oligonucleotides were named ABBAspoIIID, BABAspoIIID and BAABspoIIID (Figure 8a-d) (Table 1).

DG74 is a universal primer for the broad-range detection of Gram-type-specific PCR (99) (Figure 10a) (Table 1). Six oligonucleotides were derived from DG74 by the 5' end addition of two specific recognition sequences in tandem and the extension of the linker between recognition sequences from originally 4 thymines to 5, 10, 15, 25 and 30 thymines. The derived oligonucleotides were named FF_DG74, FF_DG74+5T, FF_DG74+10T, FF_DG74+15T, FF_DG74+25T, FF_DG74+30T, while their complement sequences were named FF_DG74c, FF_DG74+5Tc, FF_DG74+10Tc, FF_DG74+15Tc, FF_DG74+25Tc and FF_DG74+30Tc (Figure 10b-c) (Table 1).

The primers used for the PCR of Gram-positive and Gram-negative bacteria in this study were previously described (99). The Gram-positive specific forward primer was named Gram+, while the Gram-negative specific forward primer was named Gram-. FF_DG74 was used as a universal reverse primer for the Gram type-specific PCR. The oligonucleotide sequence FR_DG74 was generated by replacing the downstream recognition sequence of FF_DG74 with its reverse complement sequence (Figure 12) (Table 1).

The primer sets for LAMP assays were designed using the NEB LAMP primer design tool (https://lamp.neb.com/#!/) on alignments of 16S ribosomal RNA genes. Recognition sequences were then added in tandem to the loop primers. All the oligonucleotides in this study were synthesized by Integrated DNA Technologies (Coralville, USA).

4.4 Expression of Recombinant Proteins

The recombinant proteins HisTreA (His-tagged intact TreA), HisTreA-C-SpoIIID and HisTreA-N-SpoIIID were expressed in *E. coli* BL21(DE3) △TreA under the control of the T7 *lac* promoter in the pETDuet-1 vector. The transformed BL21△TreA cells stored as glycerol stocks in -80°C freezer were cultured overnight in 10 ml LB medium (100 μg/ml ampicillin), then transferred to 300 ml LB medium (100 μg/ml ampicillin), and shaken at 225 rpm at 37°C until the OD_{600} reached 0.5. The recombinant proteins were expressed by induction with 0.5 mM of isopropyl-β-D-thiogalactoside (IPTG) for 5 h at 37°C. Bacterial lysates were harvested by centrifuging the induced cultures at 3,000 *g*, 4°C for 20 min. Pellets were washed twice with 40 μl 1× PBS with the same centrifugation conditions.

4.5 Protein Purification

The ÄKTA Go chromatography system (Cytiva, Marlborough, USA) was used to purify the recombinant proteins. Washed cell pellets from section 4.4 were resuspended in 40 ml of 6 M guanidinium buffer (6 M guanidinium-HCl; 25 mM imidazole; PBS 1×). The resuspended cells

were then sonicated with the following program and setting: 10 s pulse-on, 5 s pulse-off for a total of 2 min at amplitude 60. The resulting cell lysates were centrifuged at 3,000 *g*, 4°C for 20 min and the supernatants were then filtered using 0.45 μm pore size syringe filters.

4.5.1 Purification using Denaturing Conditions

Recombinant proteins were purified on the 1 ml HisTrap HP column using the ÄKTA Go system according to a user-defined protocol. Briefly, proteins in filtered lysates were bound to the column, equilibrated by 6 M guanidinium buffer, washed with the same buffer, and then eluted in Denaturing Elution buffer (6 M guanidinium-HCl; 500 mM imidazole; PBS 1×) for the dialysis-refolding.

To obtain a higher yield of the purified proteins, dialysis-refolding was used to gradually exchange the denaturing buffer by dilution of the refolding buffer. Denatured protein samples in Denaturing Elusion buffer were transferred as aliquots of 500 μl into microcentrifuge tubes treated each with a 6-7 mm diameter hole in the lid for the installation of SnakeSkin™ dialysis membrane, 7K MWCO (Thermo Fisher, Mississauga, Canada). Then, the protein aliquots were gradually refolded by dialysis against 1 L of sodium maleate buffer (50 mM, pH 6) with a magnetic stirring speed of 200 rpm at 4°C for 24 h to remove guanidinium and imidazole. The dialysis membranes were renewed every 4-6 h during the refolding to avoid the dialysis membrane being blocked by the

protein aggregation during refolding

4.5.2 Protein Concentration Determination

After dialysis, the refolded protein samples were centrifuged at 300 rpm for 1-2 min to separate the precipitated protein. The supernatants were then harvested as soluble fusion proteins for downstream experiments. To determine the protein concentration, Qubit™ Protein Assay Kit (Thermo Fisher, Mississauga, Canada) was used. Following the manufacturer's instructions, 5 µl of protein sample was added and incubated in the dark for 20 min at R/T. The protein concentrations were then read by Qubit™ 2.0 Fluorometer (Thermo Fisher, Mississauga, Canada).

4.5.3 SDS-PAGE

4.5.3.1 HisTreA-C-SpoIIID

Purified protein samples were subjected to 10% resolving gel in SDS-PAGE running at constant

200 V for 40 min by Mini-PROTEAN Tetra Cell gel electrophoresis system (Bio-Rad, Mississauga, Canada). Precision Plus Protein Kaleidoscope Standards (10-250 kD) (Bio-Rad, Mississauga, Canada) were used as the ladder to monitor protein separation. Proteins in polyacrylamide gels were stained with Bio-Safe Coomassie blue G-250 (Bio-Rad, Mississauga, Canada). The recombinant protein HisTreA was used as the positive control.

4.5.3.2 HisTreA-N-SpoIIID

Purified protein samples were submitted to 12% resolving gel in SDS-PAGE running at constant 100 V for 70 min by the above gel electrophoresis system. The sizes of proteins were indicated by the same prestained protein ladder and visualized by the same Coomassie blue dye. The recombinant protein HisTreA was used as the positive control.

4.6 Optimization of Fusion Protein-DNA Binding Detection

4.6.1 Colorimetric Enzymatic Assay

After the concentrations of fusion proteins were determined, 5 µg HisTreA-C-SpoIIID fragment was added to each assay, whereas the addition volume of HisTreA-N-SpoIIID fragment was adjusted in accordance with the HisTreA-C-SpoIIID to maintain the molar ratio of 1:1. Glucose oxidase (1 mg/ml), horseradish peroxidase (20 U/ml), o-Dianisidine (12 mg/ml) and trehalose were added to each assay at respective final concentrations of 0.1 mg/ml, 0.2 U/ml, 0.12 mg/ml and 0.25 M in sodium maleate buffer (50 mM, pH 6). All the assays were performed at a final volume of 150 µl in a 96-well microplate. This colorimetric enzymatic assay was also known as the three-enzyme assay (3EA). When applied to amplicons of PCR and LAMP, this assay was named the Amplicon Binding Split Trehalase Assay (ABSTA).

The assay mix was incubated in a spectrophotometer BioTek Synergy H1 (BioTek Instruments, Winooski, USA) for 90 min at R/T. The production of glucose in each assay was indicated by the absorbance at 450 nm of wavelength (OD_{450}) each minute by a kinetic scanning mode programmed by BioTek Gen5 software. Statistical analyses for comparison of colorimetric enzymatic assay signals were performed using Microsoft Excel and R (version 4.2.0).

4.6.2 Complementation Experiments of DNA-binding Split Trehalase Fusion Proteins with Specific and Control Oligonucleotides

To form hairpins at both ends, 5 µl of the oligonucleotide ABABspoIIID (1 mM) with specific recognition sequences (TAGGACAAGC) and the oligonucleotide ABABcont (1 mM) with the control sequences (TATTGTAAGC), were added in 1× NEBuffer 3.1 buffer (10×) in a final reaction volume of 50 µl (Table 1). The following protocol was performed using a thermocycler: heating to 95ºC for 7 min, cooling to 56ºC at a rate of 1ºC/min, equilibrating at 56ºC for 5 min, and finally cooling down to 25ºC at a rate of at 1ºC/min and hold for 5 min. Consequently, the final concentrations of ABABspoIIID and ABABcont with hairpin structures were both 100 µM.

The addition of ABABspoIIID and ABABcont (with hairpins) to each 3EA was done at molar ratio of 1:1 to both fusion proteins. The final NaCl concentration gradient (from 4 M stock solution) used in the comparison of the oligonucleotides was 0, 50 mM, 100 mM, 200 mM, 300 mM, 400 mM, 500 mM, and 600 mM.

4.6.3 Salt Titration Test

The molar ratio of hairpin-formed ABABspoIIID and both fusion proteins in each assay was

prepared to be 1:1. The final NaCl concentration gradient (from 4 M stock solution) used in the titration was 0, 200 mM, 400 mM, 600 mM, 800 mM and 1 M.

4.6.4 Characterization of Optimal Ratio of Split Trehalase Fusion Proteins and DNA Substrate

ABABspoIIID was selected as the binding partner of the fusion proteins to characterize the protein reagents versus DNA substrate ratio. In this test, the final molar ratios of fusion proteins and the ABABspoIIID (with hairpin) were 1:0.2, 1:0.4, 1:0.6, 1:0.8, 1:1 and 1:1.2. The final molar concentration of NaCl in the assays above was 600 mM.

4.6.5 Complementation Experiments of Split Trehalase Fusion Proteins with Oligonucleotides Variants

Oligonucleotides ABABspoIIID and three other oligonucleotides, ABBAspoIIID, BABAspoIIID and BAABspoIIID, were added in 1× NEBuffer 3.1 buffer and thermal cycling program was used to form double hairpin structures following the procedure described in section 4.6.2. The final

concentration of hairpin-formed ABABspoIIID, ABBAspoIIID, BABAspoIIID and BAABspoIIID products used in the assays was 100 μM.

Three-enzyme assays were performed at 1:0.4 of the molar ratio of both fusion proteins to one of the above-mentioned hairpin-formed oligonucleotides at 600 mM of the final molar concentration of NaCl.

4.6.6 Complementation Experiments of Split Trehalase Fusion Proteins with Double Stranded DNA with Tandem Recognition Sites and Different Linker lengths

Oligonucleotides with two specific recognition sequences and different linker lengths FF_DG74, FF_DG74+5T, FF_DG74+10T , FF_DG74+15T, FF_DG74+ 25T, and FF_DG74+30T were annealed with their complementary chains, respectively, FF_DG74c, FF_DG74c+5T, FF_DG74c+15T, FF_DG74c+25T and FF_DG74c+30T in 1× NEBuffer 3.1 buffer to form double-stranded DNA linkers at 1 mM, using a thermal cycler through the procedure previously mentioned. The final concentration of harvested double-stranded DNA fragments, namely dsFF_DG74, dsFF_DG74+5T, dsFF_DG74+10T, dsFF_DG74+15T, dsFF_DG74+25T and dsFF_DG74+30T, was 50 μM.

The above-mentioned reagents were added to each 3EA at the final NaCl concentration of 600 mM, the molar ratio of both fusion proteins to double-stranded DNA with different linker lengths was maintained at 1:0.4.

HisTreA was used as the positive control protein for all the tests of sections 4.6.2 to 4.6.6, replacing HisTreA-C-SpoIIID, HisTreA-N-SpoIIID fragments, without any NaCl, hairpin-formed oligonucleotides and DNA substrate. For the negative controls, the hairpin-formed oligonucleotides and DNA substrate were omitted and the final concentration of NaCl was 600 mM except for 1 M for section 4.6.3. All the above-mentioned 3EAs were set up as described in section 4.6.1 and conducted in triplicate.

4.7 Complementation Assessment with PCR Products from S. devriesei and E. coli colonies with ABSTA

4.7.1 Modification of Gram Type-Specific PCR

To test the amplification specificity of Gram-type specific primer pairs incorporated the SpoIIID recognition sequences in tandem, primer pairs DG74/Gram+, DG74/Gram-, FF_DG74/Gram+,

FF_DG74/Gram-, FR_DG74/Gram+ and FR_DG74/Gram- mentioned in section 4.3 were employed to amplify the colonies of Gram-positive bacteria *S. devriesei* and Gram-negative bacteria *E. coli*.

The colony PCR was performed using the *Taq* PCR Master Mix Kit (QIAGEN, Toronto, Canada) in a 50 µl volume consisting of 25 µl of 2× *Taq* PCR Master Mix (final concentration at 2.5 U of *Taq* DNA Polymerase; 1.5 M $MgCl_2$; 200 µM of each dNTP), 2 µl of each of the forward and reverse primers (final concentration at 0.4 µM), one single colony as the template and 19 µl of RNase-free water was added to the final volume. The amplification was carried out in the Applied Biosystems™ Veriti™ 96-Well Thermal Cycler (Thermo Fisher, Mississauga, Canada) as follows: initial denaturation at 95°C for 5 min; followed by 50 cycles of denaturation at 95°C for 30 s, annealing at 65°C for 30 s, and extension at 72°C for 1 min; and 72°C for 2 min at the end of the reaction. The amplified products (10 µl) were then analyzed by electrophoresis on a 1% agarose gel containing 1× SYBR™ Safe DNA gel stain (concentration 10,000×; Thermo Fisher, Mississauga, Canada) and a 1Kb plus DNA ladder molecular weight ladder (concentration 0.1 µg/µl, 5 µl per lane; Thermo Fisher, Mississauga, Canada). The expected size of PCR products for *S. devriesei* amplified by primer set DG74/Gram+ was 355 bp, amplified by primer set FF_DG74/Gram+ was 381 bp and for *E. coli* amplified by primer set DG74/Gram- was 353 bp, amplified by primer set FF_DG74/Gram- was 379 bp.

4.7.2 Specific Detection of Purified PCR Products with Recognition Sites Incorporated in Tandem

To demonstrate the specific detection of the binding of fusion proteins HisTreA-C-SpoIIID and HisTreA-N-SpoIIID to Gram-specific PCR amplicons with incorporated tandem recognition sequences, purified and concentrated PCR products were added to the colorimetric enzymatic assay mix at a maximal volume.

Primer pairs DG74/Gram+ and FF_DG74/Gram+ were used for the *S. devriesei* colony PCR, while primer pairs DG74/Gram- and FF_DG74/Gram- were used for the *E. coli* colony PCR. The above-mentioned four PCR reactions were performed in quadruplicate. The purification and concentration of PCR product were carried out by the QIAquick™ PCR Purification Kit (QIAGEN, Toronto, Canada), followed the manufacturer's instruction. A high concentration of each type of colony PCR amplicon was obtained as follows: two 50 µl PCR product aliquots were pipetted into the first QIAquick column, and another two 50 µl product aliquots were pipetted into the second QIAquick column; the same procedures were performed on the two columns until the elution phase; at the elution phase, 50 µl of DNA-free water was added into the first QIAquick column which was then placed to stand for 10 min and then centrifuged at 17,900 *g* for 1 min; the elution was transferred to the second QIAquick column and performed the same standing and centrifugation as the first one. The final concentration in ng/µl of purified and concentrated PCR product was

measured by the spectrophotometer. The molar concentration of the PCR product was calculated using the Bioline Weight to Molar Quantity online calculator (https://www.bioline.com/media/calculator/01_07.html).

To accommodate a maximum volume of PCR amplicon in the ABSTA reaction mix, higher concentrations of glucose oxidase (10 mg/ml) and horseradish peroxidase (40 U/ml) were used to prepare the master mix while also removing any additional water. The final concentrations of all components of the master mix in a 150 µl volume assay were still maintained. Accordingly, the PCR amplicon with the recognition sites introduced was added to each assay with the maximum volume. Based on this adding volume, the final molar concentration of the purified PCR product was calculated and adjusted to be close to the optimal concentration of hairpin-formed ABABspoIIID determined in section 4.6.4.

As a positive control for the specific detection of the complementation of split trehalase fusion proteins using DNA incorporated tandem recognition sites, the double-stranded fragment dsFF_DG74 was used at the final molar concentration determined in section 4.6.4. The double-stranded fragment dsFR_DG74 was used at the same final molar concentration. The negative control was conducted by replacing the DNA substrate with water. Consistent with the previous colorimetric assays, the final concentration of NaCl in all assays was set to 600 mM except for the second positive control using HisTreA. All the colorimetric enzymatic assays were carried out in triplicate following the methods described in section 4.6.1.

4.7.3 Dilution Test of Purified PCR Products with Recognition Sites Incorporated in Tandem

To demonstrate the optimal composition of split trehalase fusion proteins and PCR amplicons with tandem recognition sites incorporated, dilutions of a high concentration purified Gram-specific PCR product resulting from a *S. devriesei* colony PCR, were subjected to the ABSTA.

S. devriesei amplicons were obtained by PCR reactions using primer pairs DG74/Gram+ and FF_DG74/Gram+. The purification and concentration strategies, measurement of concentrations of eluted PCR products and calculation of the molar concentrations were performed as described in section 4.7.2.

The master mix of the ABSTA was prepared consistent with the test described in section 4.7.2. At the maximal adding volume to each assay, the final molar concentrations of undiluted PCR products obtained with primers DG74/Gram+ and FF_DG74/Gram+ were adjusted to approximate the determined optimal concentration of the hairpin-formed ABABspoIIID. In this test, the purified PCR products produced with primer pair FF_DG74/Gram+ were further diluted two times and five times in sodium maleate buffer (50 mM, pH 6), respectively. The obtained 1/2 dilution, 1/5 dilution and the undiluted PCR products produced with primer pair DG74/Gram+ were added to each assay

at the maximum adding volume. HisTreA was used as the positive control for the ABSTA master mix. The final concentration of NaCl in all assays was maintained at 600 mM except for the positive control where no NaCl was added. The DNA substrate was replaced by water in the negative control assay. All the assays were carried out in triplicate following the methods described in section 4.6.1.

4.7.4 Use of EDTA to Counter Inhibition of ABSTA by PCR Reagents

To demonstrate the inhibition of the ABSTA by PCR reagents, EDTA (Ethylenediaminetetraacetic acid) was allowed to incubate with the PCR reagents of *S. devriesei* colony PCR with primer pair FF_DG74/Gram+ and added to the colorimetric assay to compare its ability to alleviate this inhibition at different final concentrations. The PCR reagents were prepared as described in section 4.7.1. EDTA was added to the prepared PCR reagents and mixed well to set the final molar concentrations in a gradient. Subsequently, the above mixtures were incubated on ice for 30 min. Afterwards, 20 µl of PCR reagents with 0, 0.1 and 0.5 mM EDTA from the mixtures were added to the corresponding colorimetric enzymatic assays.

In this test, the double-stranded dsFF_DG74 was used as a DNA substrate. In the non-PCR reagents assay, PCR reagents assay without EDTA, PCR reagents assay containing 0.1 mM EDTA

and PCR reagents assay containing 0.5 mM EDTA, the final concentration of dsFF_DG74 was adjusted to be close to the determined optimal concentration of the hairpin-formed ABABspoIIID. The preparation of the 3EA master mix, the positive control with HisTreA, the negative control without DNA substrate and the NaCl final molar concentration setup were consistent with section 4.7.2. Sodium maleate buffer (50 mM, pH 6) was used to make up to 150 µl per assay. All the assays were carried out in triplicate following the methods described in section 4.6.1.

4.7.5 Titration Test of Unpurified PCR Products with Recognition Sites Incorporated in Tandem

In the titration experiment of unpurified PCR products, *S. devriesei* colony PCR using primer pair FF_DG74/Gram+, and *E. coli* colony PCR using primer pair FF_DG74/Gram- were performed with the procedure described in section 4.7.1. The obtained two Gram-type of PCR products were added to the ABSTA at a gradient volume. Double-stranded fragment dsFF_DG74 was employed in the positive control for the complementation of the SpoIIID fusion proteins, and its final molar concentration was adjusted to be close to the determined optimal concentration of the hairpin-formed ABABspoIIID. The preparation of the master mix, the positive control with HisTreA, the negative control without DNA substrate and the NaCl final molar concentration setup were consistent with section 4.7.2. Likewise, sodium maleate buffer (50 mM, pH 6) was used to make

up to 150 µl per assay. All the assays were performed in triplicate following the methods described in section 4.6.1.

4.7.6 Use of EDTA to Counter Inhibition of ABSTA by Unpurified PCR Products

To investigate the inhibition of the ABSTA by unpurified PCR products, colony PCR products incorporated with tandem recognition sites were incubated with increasing molar concentrations of EDTA and then added as the DNA substrate to the ABSTA.

Unpurified PCR products from *S. devriesei* and *E. coli* colonies were obtained with the primer pairs FF_DG74/Gram+ and FF_DG74/Gram-, respectively. For each Gram-type bacteria, the final molar concentrations of EDTA in the PCR products were set as a gradient. The PCR products above were incubated under the same condition mentioned in section 4.7.3. Subsequently, 30 µl of EDTA-treated PCR products were added to the corresponding ABSTA. The preparation of the master mix, the positive controls with dsFF_DG74 and HisTreA, the negative control without DNA substrate and the NaCl final molar concentration setup were consistent with section 4.7.2. Sodium maleate buffer (50 mM, pH 6) was used to make up the final reaction volume of 150 µl. All the assays were performed in triplicate following the methods described in section 4.6.1.

4.8 Optimization of LAMP Primer Sets Design

To optimize LAMP primer sets to specifically amplify DNA of bovine mastitis pathogens of different Gram types, an attempt was made to design as few primers as possible to the target gene while ensuring specificity and sensitivity. At this point, a merging strategy was used in which several of the 6 primers of a single LAMP reaction serve as universal primers, thereby reducing the total number of primers required for the two Gram-type LAMP assays. This strategy is described below.

First, the 16S ribosomal RNA genes of three staphylococcus strains (*S. cohnii*, *S. aureus*, *S. arlettae*), three streptococcus strains (*S. uberis*, *S. dysgalactiae*, *S. agalactiae*) and three Gram-negative pathogenic strains (*Klebsiella*, *Enterobacter*, *E. coli*) were sourced from GenBank nucleotide database. The six Gram-positive bacteria genes and the three gram-negative bacteria genes were aligned separately or combined, thus generating three sets of nucleotide alignments, respectively, alignment+, alignment- and alignment±. For the optimization of the Gram-positive specific primer set design, several homologous regions from streptococcus alignment, which were generally about 280 bp in length and have weak consensus identity with Gram-negative bacteria's 16S rRNA genes in alignment± but relatively conservative in the alignment+, were uploaded as candidate regions to the online NEB LAMP primer design tool. Next, following the basic primer

design guidelines recommended by Eiken genome site (http://loopamp.eiken.co.jp/e/lamp/primer.html), multiple parameters that influence primer performance, for example, the length of primers, the distance between primer regions, and the stability of the primer ends, were specifically modified to preferred values. Then, the resulting multiple core primers were used for loop primers generation and finally, the possible LAMP primer set containing 6 primers was then submitted to IDT OligoAnalyzer (https://www.idtdna.com/calc/analyzer) to check the formation of internal or external secondary structures, such as hairpin, self-dimer and hetero-dimer.

Afterwards, the checked primer set was aligned with the alignment+ and assessed in the following manner. The first step was to confirm the single positions that have different bases in the streptococcal alignment. These positions were subsequently replaced with degenerate bases in the corresponding primers to ensure the detection sensitivity for different streptococcal species. In a second step, according to the consensus identity with staphylococcus strains, the highly conserved primer sequences of the streptococcal primer set were regarded as universal primers for both *Staphylococcus* and *Streptococcus*, while the remaining primer sequences were modified as *Staphylococcus* specific. The putative secondary structure of the staphylococcal primer set was then checked by IDT OligoAnalyzer. These primers were then subjected to alignment± to confirm that similarity with the corresponding Gram-negative strain fragments was lacking, thus obtaining less than 12 primers in total for the LAMP assays of *Streptococcus* and *Staphylococcus*. The same strategy was applied to the primer set design of Gram-negative strains, and an additional set of 6

LAMP primers was generated.

Finally, the SpoIIID recognition sequences were incorporated in tandem at both the 5' ends of the loop forward and loop backward primers. Consequently, three primer sets were obtained, namely LAMPstaph, LAMPstrep and LAMPneg (Table 1). However, it should be clarified that when a single specific primer set was aligned against the opposite Gram-type alignment, loop primers with more than 4-base complementarity at the 3' end were avoided because the detection specificity between different Gram-types of strains could be reduced by the common presence of tandem recognition sites. All the nucleotide alignment analysis in this section was done by Geneious version 9.0.5.

4.9 Sensitivity of Detection of Gram-type Specific LAMP followed by ABSTA

4.9.1 Sensitivity Test with Genomic DNA Extracted from Bacterial Culture

The sensitivity of detection discussed in section 4.9 was defined as the limit of detection of ABSTA, or when the ABSTA signal level became significantly different from the negative control. To test this limit of detection of the ABSTA with gDNA, bacterial cultures of *S. devriesei*, *E. coli* DH10β

and *S. uberis* were used for the gDNA extraction. The concentration of gDNA eluates was adjusted to 50 ng/µl. Afterwards, 50 ng/µl DNA solution was 10-fold serially diluted with sterile water to 10^{-1} to 10^{-7} concentrations, respectively. One µl of gDNA from each dilution was used as the DNA template for the Gram-type specific LAMP assays. The starting copy number for each assay was calculated by an online copy number calculator (http://www.scienceprimer.com/copy-number-calculator-for-realtime-pcr) based on the genome median total length of 2,376,740 bp of *S. devriesei* (https://www.ncbi.nlm.nih.gov/genome/?term=txid586733[Organism:noexp]), 1,925,500 bp of *S. uberis* (https://www.ncbi.nlm.nih.gov/genome/?term=txid1349[Organism:exp]), and 4,686,137 bp of *E. coli* DH10b (100), respectively. Sterile water was used in the non-template control of three LAMP assays. Primer set stocks of LAMPstaph, LAMPstrep and LAMPneg were prepared in the ratio specified by the WarmStart™ LAMP kit (New England Biolabs, Whitby, Canada). Following the manufacturer's protocols, a 25 µl reaction was set up with provided reagents and then subjected to the CFX96 Real-Time PCR detection system (Bio-Rad, Mississauga, Canada) programmed to keep the temperature at 65ºC for 30 min. The resulting LAMP product (5 µl) was submitted to 1% agarose gel electrophoresis for confirmation of amplification. The remaining product (5 µl) was used in ABSTA to determine the signal resulting from the complementation of fusion proteins caused by the binding with LAMP products which had tandem-recognition-sites incorporated. The LAMP assay and the ABSTA were performed in triplicate. The methodological workflow of this experiment is explained in Figure 1a.

4.9.2 Sensitivity Test with DNA Extracted from Spiked Milk Sample

To investigate the detection limit of the ABSTA for bacterial DNA in milk samples after amplification by Gram-type specific LAMP primer sets, strains *S. devriesei* and *E. coli* DH10β were cultured in LB broth, and strain *S. uberis* were cultured in BHI broth until their OD_{600} was equal to 1. Each bacterial culture with an OD_{600} of 1 was 10-fold diluted serially in 1× PBS. For the experiment with staphylococci and streptococci, seven milk aliquots of 1.8 ml were used. Aliquots 1 and 2 were spiked with 200 µl and 18 µl of the corresponding bacterial culture at OD_{600} = 1, respectively. Aliquots 3 to 6 were spiked with 18 µl of 10-fold to 10^4-fold dilutions, respectively. Aliquot 7 was spiked with 18 µl of 1× PBS as a negative control. For the Gram-negative experiment, eight milk aliquots of 1.8 ml were used. Aliquots 1 to 7 were spiked with 18 µl of *E. coli* culture at OD_{600} = 1 and its 10-fold to 10^6-fold dilutions, respectively. Aliquot 8 was spiked with 18 µl of 1× PBS. For CFU/ml calculation of the corresponding bacteria in spiked milk samples, 100 µl of undiluted cultures of OD_{600} = 1 and the dilutions were plated on LB agar （Thermo Fisher, Mississauga, Canada） plates for *S. devriesei* and *E. coli*, and TSA blood agar plates for *S. uberis*. Plated bacteria were incubated at 37ºC overnight until colonies appeared. The colonies on the countable plate (30 - 300 colonies) were counted for the calculation of the real CFU/ml in each spiked milk sample. The methodological workflow for this experiment is explained in Figure 1a.

The DNA extraction from spiked milk samples was performed as in the above-mentioned methods in section 4.2.2. The maximal volume of 9.5 µl of DNA was used in each LAMP assay with a total volume of 25 µl. The preparation of LAMP primer set stocks of LAMPstaph, LAMPstrep and LAMPneg, and the programming of the Real-Time PCR detection system were consistent with section 4.9.1. Sterile DNA-free water was utilized in the non-template control for the LAMP assay corresponding to these three primer sets. After the LAMP reaction was complete, agarose gel electrophoresis was conducted as mentioned in the previous section, and 5 µl of each LAMP product was subsequently added to the ABSTA to be detected by fusion proteins HisTreA-C-SpoIIID and HisTreA-N-SpoIIID and to investigate the detection limit (as CFU/ml) of Gram types of bacteria in milk samples. The LAMP assay and the ABSTA were performed in triplicate.

4.10 Specificity of Detection of Gram-type Specific LAMP

To investigate the specificity of detection of the LAMP primer sets LAMPstaph, LAMPstrep and LAMPneg for gDNA of specific Gram-type bacteria, bacterial cultures of *S. devriesei*, *S. aureus*, *S. uberis*, *S. dysgalactiae*, *Streptococcus* spp., *Corynebacterium* spp., *E. coli*, *Klebsiella* spp., and *Enterobacter* spp. were prepared for DNA extraction as mentioned in section 4.1. The concentration of the gDNA obtained from each bacterial isolate was adjusted to 10^6 copies and 10^3

copies per microliter, calculated by the online copy number calculator based on the genome median total length of the above-mentioned bacteria. The LAMP reaction was set up following the guide of WarmStart™ LAMP kit. For the LAMP assay with each primer set, gDNA preparations corresponding to two copy numbers of all the above-mentioned bacteria was used in 1 µl template for each reaction. Non-template control with water was performed with each LAMP primer set. Subsequently, 5 µl of each obtained LAMP product was submitted to agarose gel (1%) electrophoresis for confirmation of amplification. The LAMP assay for each primer set was performed in triplicate. The specificity discussed in this study is defined as the analytical specificity determined using the above-mentioned bacteria isolates in conditions of section 4.10. High specificity corresponds with the absence of a signal when amplifying nontarget isolates at both copy numbers was defined as for each LAMP primer set. The methodological workflow for this experiment is explained in Figure 1b.

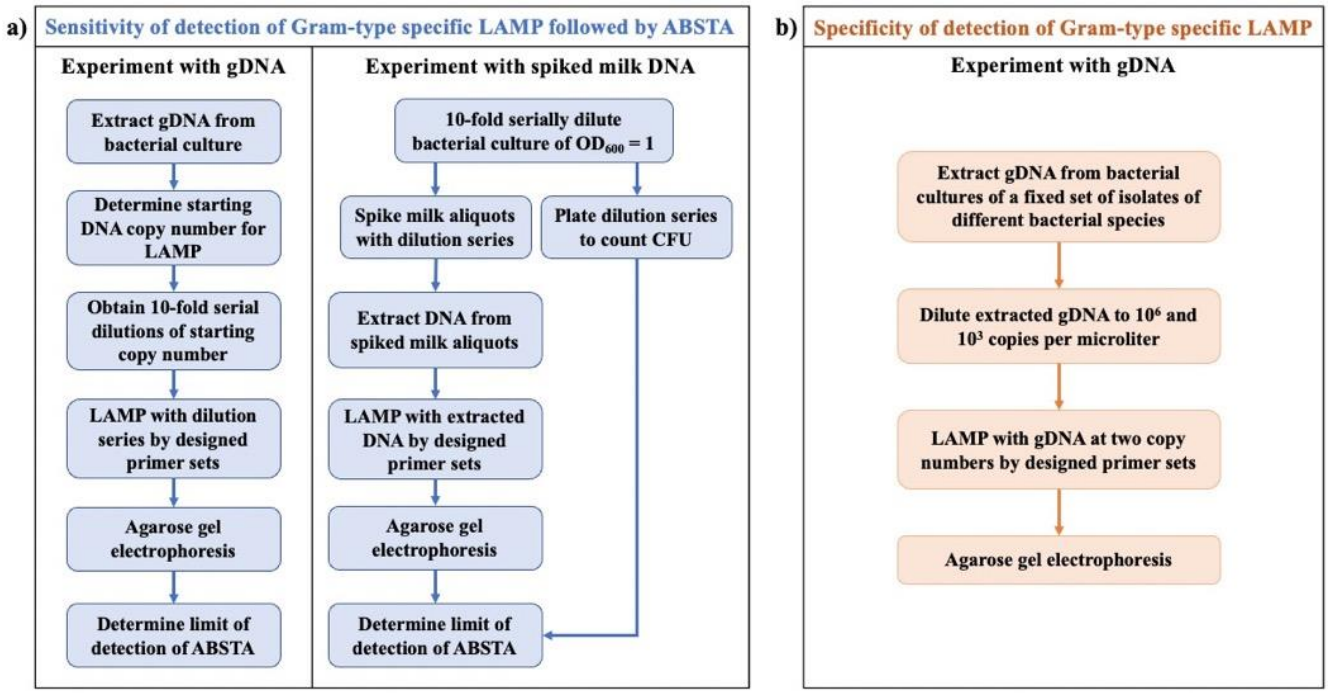

Figure 1. Methodological workflow of assessing sensitivity and specificity of detection of Gram-type specific LAMP. (a) The workflow of sensitivity determination experiment using gDNA is listed on the left, which should be followed step-by-step starting with the 'extract gDNA from bacterial culture' blue box. The workflow of experiment using DNA extracted from spiked milk is listed on the right, which should be followed step-by-step starting with the '10-fold serially dilute bacterial culture of OD_{600} = 1' blue box. A blue arrow from 'Plate dilution series to count CFU' blue box to the last step indicates that the limit of detection of ABSTA is interpreted as the bacterial CFU/ml in a spiked milk sample. **(b)** The workflow of specificity evaluation experiment using gDNA is listed as four steps, which should be followed starting with the 'extract gDNA from bacterial cultures of a fixed set of isolates of different bacterial species' orange box.

Table 1 List of oligonucleotides

Name	*Sequence*
Oligonucleotides for Protein-DNA Binding Optimization	
ABABspoIIID	AATTAGGACAAGCGC GCAGC GCGCTTGTCCTAATT TTT AATTAGGACAAGCGC CGACG GCGCTTGTCCTAATT
ABBAspoIIID	AATTAGGACAAGCGC GCAGC GCGCTTGTCCTAATT TTT GCGCTTGTCCTAATT CGACG AATTAGGACAAGCGC
BAABspoIIID	GCGCTTGTCCTAATT GCAGC AATTAGGACAAGCGC TTT AATTAGGACAAGCGC CGACG GCGCTTGTCCTAATT
BABAspoIIID	GCGCTTGTCCTAATT GCAGC AATTAGGACAAGCGC TTT GCGCTTGTCCTAATT CGACG AATTAGGACAAGCGC
ABABcont	AATTATTGTAAGCGC GCAGC GCGCTTACAATAATT lTTT AATTATTGTAAGCGC CGACG GCGCTTACAATAATT
FF_DG74+5T	ATTAGGACAAGC TTTTTTTTT TAGGACAAGC AGGAGGTGATCCAACCGCA
FF_DG74+10T	ATTAGGACAAGC TTTTTTTTTTTTT TAGGACAAGC AGGAGGTGATCCAACCGCA
FF_DG74+15T	ATTAGGACAAGC TTTTTTTTTTTTTTTTT TAGGACAAGC AGGAGGTGATCCAACCGCA
FF_DG74+25T	ATTAGGACAAGC

	TTTTTTTTTTTTTTTTTTTTTTTTTTTT TAGGACAAGC AGGAGGTGATCCAACCGCA
FF_DG74+30T	ATTAGGACAAGC TTTTTTTTTTTTTTTTTTTTTTTTTTTTTTTT TAGGACAAGC AGGAGGTGATCCAACCGCA
FF_DG74c	TGCGGTTGGATCACCTCCT GCTTGTCCTA AAAA GCTTGTCCTAAT
FF_DG74+5Tc	TGCGGTTGGATCACCTCCT GCTTGTCCTA AAAAAAAAA GCTTGTCCTAAT
FF_DG74+10Tc	TGCGGTTGGATCACCTCCT GCTTGTCCTA AAAAAAAAAAAAAA GCTTGTCCTAAT
FF_DG74+15Tc	TGCGGTTGGATCACCTCCT GCTTGTCCTA AAAAAAAAAAAAAAAAAA GCTTGTCCTAAT
FF_DG74+25Tc	TGCGGTTGGATCACCTCCT GCTTGTCCTA AAAAAAAAAAAAAAAAAAAAAAAAAAAA GCTTGTCCTAAT
FF_DG74+30Tc	TGCGGTTGGATCACCTCCT GCTTGTCCTA AAAAAAAAAAAAAAAAAAAAAAAAAAAAAA GCTTGTCCTAAT
PCR Primers	
DG74 (99)	AGGAGGTGATCCAACCGCA
FF_DG74	ATTAGGACAAGC TTTT TAGGACAAGC AGGAGGTGATCCAACCGCA
FR_DG74	ATTAGGACAAGC TTTT GCTTGTCCTAAT AGGAGGTGATCCAACCGCA

Gram+ (99)	GAYGACGTCAARTCMTCATGC
Gram- (99)	AYGACGTCAAGTCMTCATGG
LAMP Primer Set for *Staphylococcus* and *Streptococcus* (LAMPstaph and LAMPstrep)	
F3	TGCCCCTTATGAYYTGG
B3	GAACGTATTCACCGYR
FIP_staph	TTTGCWTGACCTCGCGG CTACACACGTGCTACAATG
BIP_staph	TCCCATAAAGTTGTTCTCAGTTCGG CGATTACTAGCGATTCCAGCTTC
FIP_strep	TTAGCTTGCCGTCACCG CTACRCACGTGCTACAATG
BIP_strep	TCTCTTAAAGCCAATCTCAGTTCGG CGATTACTAGCGATTCCGACTTC
LF_Ext_staph	ATTAGGACAAGC TTTT TAGGACAAGC TTTMGCTGCCCTTTGTATTGT
LF_Ext_strep	ATTAGGACAAGC TTTT TAGGACAAGC GCTTGCGACTCGTTGTACCAA
LB_Ext	ATTAGGACAAGC TTTT TAGGACAAGC TAGKCTGCAACTCGMCTACA
LAMP Primer Set for Gram-negative Bacteria (LAMPneg)	
F3_neg	TGGGATTAGCTWGTWGGTG
B3_neg	TTCAYACACGCGGCATG
FIP_neg	AGTGTGGCTGGTCATCCTC GGTAACGGCTCACCW
BIP_neg	GGAACTGAGACACGGTCCA GCTGCATCAGGCTTG
LF_Ext_neg	atTAGGACAAGC TTTT TAGGACAAGC AGACCAGCTAGGGATCGTCG
LB_Ext_neg	atTAGGACAAGC TTTT TAGGACAAGC

TGGGGAATATTGCACAATGGGC

All oligonucleotides are listed 5’→3’

5. RESULTS

5.1 Fusion Proteins Expression and Purification

The production of fusion proteins HisTreA-C-SpoIIID and HisTreA-N-SpoIIID was verified by SDS-PAGE gel according to protein standards. The size of HisTreA-C-SpoIIID (predicted to be 64.86 kDa) was verified on the 10% resolving gel referring to the positive control HisTreA (60 kDa) and protein standards ladder (Figure 2). The fusion protein HisTreA-N-SpoIIID migrated to the bottom boundary of the stacking gel, coinciding with the bromophenol blue dye. After using 12% resolving gel, reducing the constant voltage from 200 V to 100 V and extending the run time from 40 to 70 min, a band representing HisTreA-N-SpoIIID was visible on the gel. Compared with the positive control and protein standards, the mass of the protein HisTreA-N-SpoIIID was verified to be approximately 20 kDa, consistent with its predicted size of 20.78 kDa) (Figure 3).

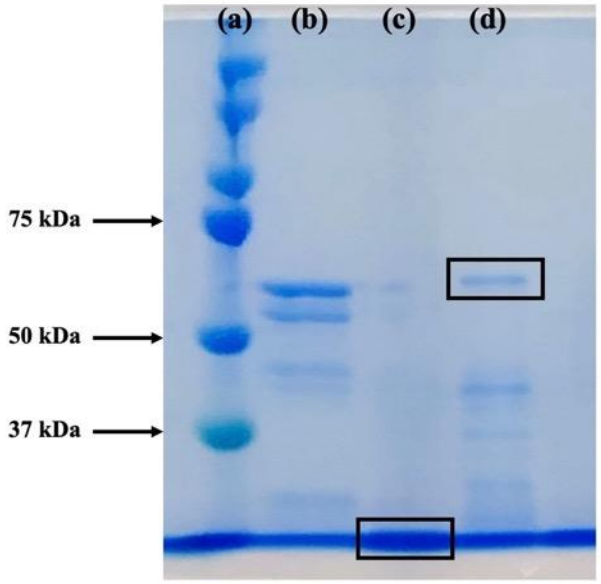

Figure 2. SDS-PAGE confirmation of production of the fusion protein HisTreA-C-SpoIIID using 10% resolving gel running at 200 V for 40 min. (a) Protein standards (10-250 kDa) **(b)** Protein HisTreA as the positive control with a band corresponding to 60 kDa. **(c)** Protein HisTreA-N-SpoIIID purified under denaturing conditions appears a band at the gel bottom boundary, showing in the black box. **(d)** Protein HisTreA-C-SpoIIID purified under denaturing conditions with a band corresponding to 64.86 kDa, showing in the black box.

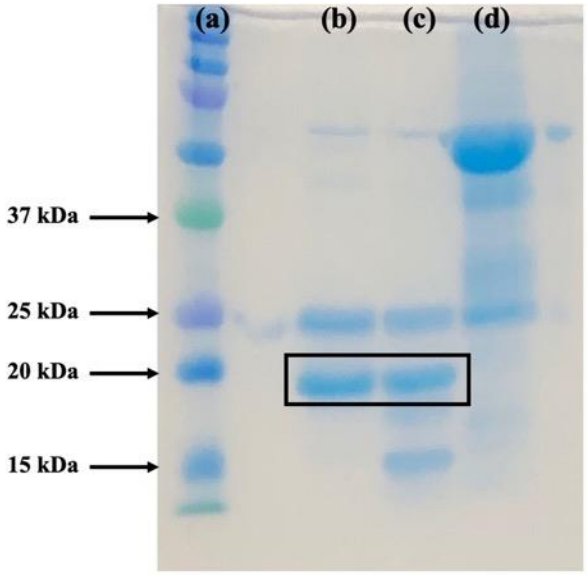

Figure 3. SDS-PAGE confirmation of production of the fusion protein HisTreA-N-SpoIIID using 12% resolving gel running at 100 V for 70 min. (a) Protein standards (10-250 kDa). **(b) (c)** Protein HisTreA-N-SpoIIID purified under denaturing conditions with bands corresponding to 20.78 kDa, showing in the black box. (d) Protein HisTreA as the positive control, with a band corresponding to 60 kDa.

5.2 Complementation Assessment with Modified Oligonucleotides

5.2.1 Complementation Test Comparing Oligonucleotides with and without Recognition Sequences with Increasing Salt Concentrations

The ability of the oligonucleotide ABABspoIIID, which forms two hairpins at both ends generating the double-stranded recognition sequences, to complement the split TreA fusion proteins was assessed at different salt concentrations. The specificity of the interaction of the SpoIIID fragments with the recognition sequences was assessed comparison with oligonucleotide ABABcont which lacks the recognition sequences (Figure 4). The colorimetric enzymatic assay was read by the absorbance at 450 nm wavelength after a 90 min incubation. For all tested NaCl concentrations (0 to 600 mM), the OD_{450} after 90 min for all the reactions involving control sequence ABABcont remained the similar level as that of the negative control reaction without DNA, indicating that this hairpin-formed sequence did not interact with the fusion proteins HisTreA-C-SpoIIID and HisTreA-N-SpoIIID in the system (Figure 5). On the contrary, the OD_{450} after 90 min of incubation of the reactions with oligonucleotides ABABspoIIID increased as the NaCl concentration increased for all concentrations up to 600 mM. The difference between the two oligonucleotides indicates that only the double-stranded specific recognition sequences were capable of specifically binding to the SpoIIID domain of the fusion proteins, thereby linking the split trehalase fragments and restoring the enzymatic activity of the split trehalase. The salt concentration in the reaction

mixture positively affected the protein-DNA binding (Figure 5).

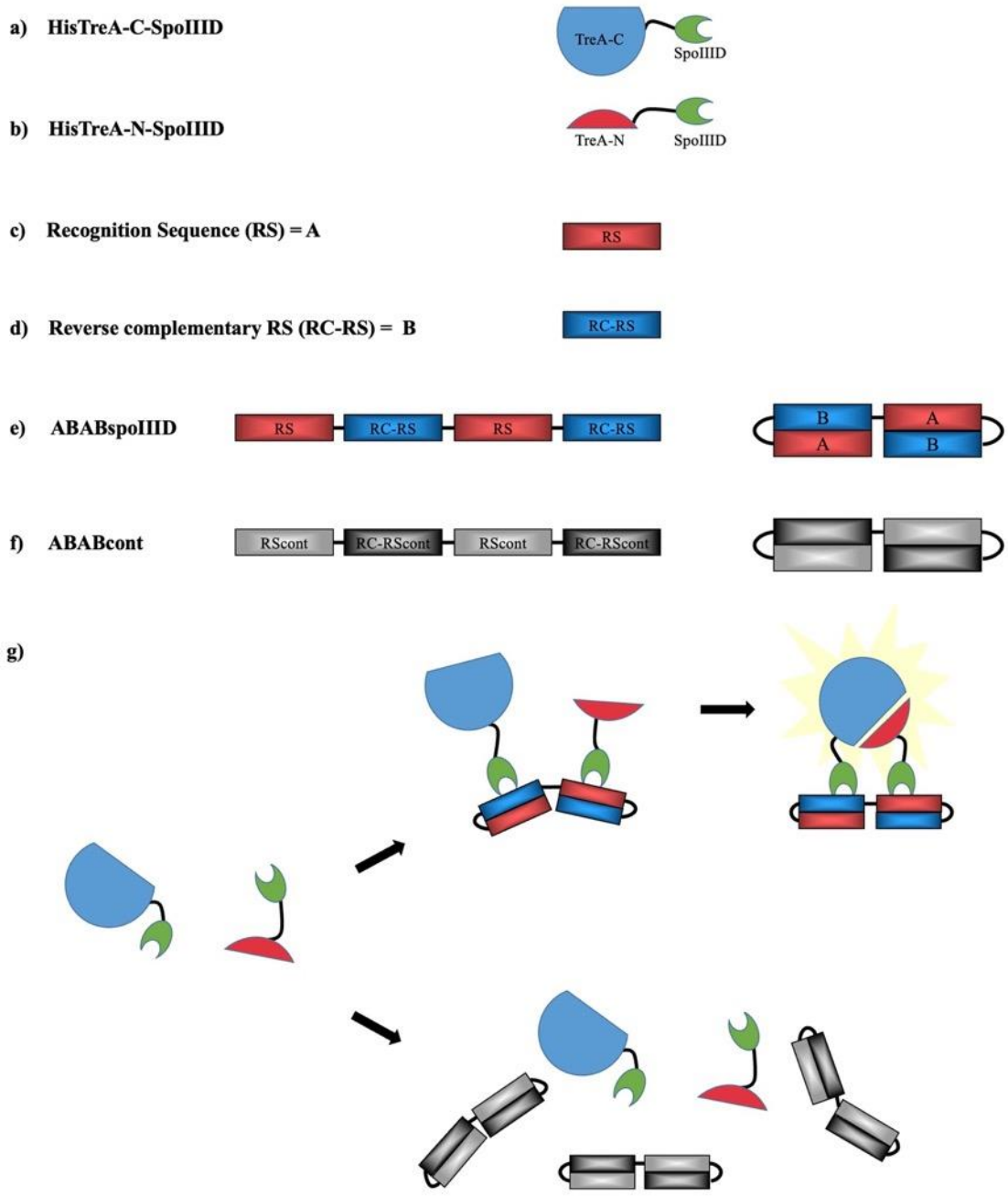

Figure 4. Schematic diagram depicting the comparison of complementation of fusion proteins HisTreA-N-SpoIIID and HisTreA-C-SpoIIID with hairpin-forming oligonucleotide

sequences ABABcont and ABABspoIIID. (a) Recombinant protein HisTreA-C-SpoIIID with the C-domain of trehalase and the DNA binding protein SpoIIID. **(b)** Recombinant protein HisTreA-N-SpoIIID with the N-domain of trehalase and the DNA binding protein SpoIIID. **(c)** Sequence specifically recognized by protein SpoIIID. **(d)** Reverse complementary sequence of SpoIIID recognition sequence. **(e)** Construction of hairpin-forming oligonucleotide ABABspoIIID and its hairpin formed structure with two specific recognition sites. 'RS' red box represents the recognition sequence, which is equal to the 'A' red box. 'RC-RS' blue box represents the reverse complementary sequence of the recognition sites, which is equal to the 'B' blue box. **(f)** Construction of hairpin-forming oligonucleotide ABABcont and its hairpin formed structure. **(g)** With the addition of hairpin formed ABABspoIIID, SpoIIID on each split trehalase protein specifically binds to the recognition site, respectively, resulting in the complementation of split trehalase domains and restoration of enzymatic activity. However, split fusion proteins are incapable of interacting with the hairpin formed ABABcont which has no specific recognition sites incorporated.

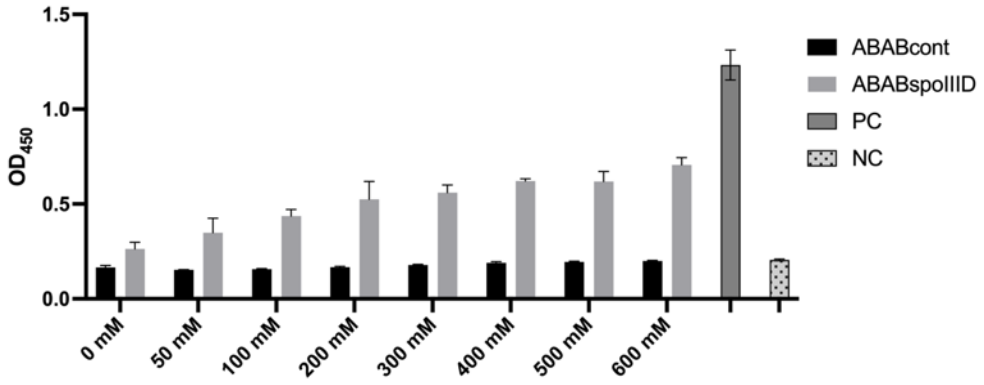

Figure 5. Comparison of complementation of fusion proteins HisTreA-N-SpoIIID and HisTreA-C-SpoIIID with hairpin-forming oligonucleotide sequences ABABcont and ABABspoIIID, analyzed by colorimetric enzymatic assay. The absorbance at 450 nm was measured by the spectrophotometer after a 90 min incubation at R/T. The positive control (PC) utilizes HisTreA, mimicking the successful restoration of the fusion proteins. The negative control (NC) utilizes water as the binding partner to the fusion proteins. Linear regression was performed on assays with hairpin-forming oligonucleotides ABABcont and ABABspoIIID within the salt concentration of 0 to 600 mM. At a 95% confidence level, the slopes of regression of ABABcont ($p < 0.001$) and ABABspoIIID ($p < 0.001$) are significantly different from zero. The linear regression slope comparison was then conducted at a 95% confidence level, and the resulting p value was less than 0.001, indicating a very significant difference between the two slopes.

5.2.2 Salt Titration Test with Oligonucleotide ABABspoIIID

To find the optimal concentration of salt leading to specific binding of HisTreA-C-SpoIIID and HisTreA-N-SpoIIID to the oligonucleotide ABABspoIIID containing the specific recognition sites, the concentration was expanded to 1 M in this additional test. Again, the activity increased with increasing salt concentration from 0 to 600 mM, reaching a maximum at 600 mM. With further salt added to the reaction, OD_{450} obtained after the 90 min incubation dropped at both 800 mM and 1 M of salt final concentrations. However, the results indicates that the optimal NaCl concentration for this specific protein-DNA interaction involving the fusion proteins HisTreA-C-SpoIIID and HisTreA-N-SpoIIID is around 600 mM (Figure 6).

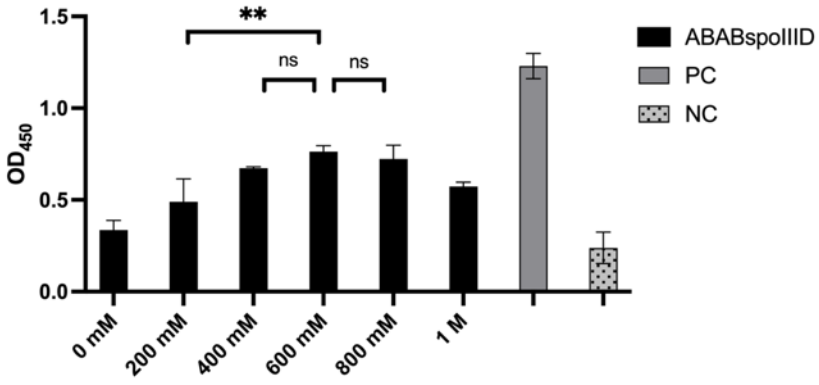

Figure 6. Comparison of complementation of fusion proteins HisTreA-N-SpoIIID and HisTreA-C-SpoIIID with hairpin-forming oligonucleotide sequence ABABspoIIID with the salt final concentration of 0 to 1 M, analyzed by colorimetric enzymatic assay. The absorbance

at 450 nm as measured by the spectrophotometer after a 90 min incubation at R/T. PC and NC were consistent with the previous experiment. One-way ANOVA was performed on groups with different salt concentration, and a p value < 0.001 was generated, indicating there are significant differences in the means in these groups. Tukey multiple comparisons of means were then conducted at a 95% confidence level. Very significant between-group difference is shown by '**' in the graph. No significant differences are shown by 'ns' in the graph.

5.2.3 Split Enzyme Fusion Proteins versus DNA Substrate Ratio Characterization

To investigate the effect of the ratio of split TreA fusion proteins versus DNA substrate involved in the binding reaction leading to complementation, hairpin-forming ABABspoIIID was selected as the binding partner of the fusion protein. In this experiment, the final concentration of background NaCl was set at 600 mM, and the molar ratio of the fusion proteins HisTreA-C-SpoIIID/HisTreA-N-SpoIIID to hairpin-forming ABABspoIIID was set up as 1:0.2, 1:0.4, 1:0.6, 1:0.8, 1:1 and 1:1.2, corresponding with the final molar concentration of the DNA substrate in the colorimetric enzymatic assays of 100 nM, 200 nM, 300 nM, 400 nM, 500 nM and 600 nM. The activity of the reaction was enhanced as the ratio of the fusion protein to treated ABABspoIIID decreased from 1:0.2 to 1:0.4 and reached a maximum at the ratio of 1:0.4. From this maximum, the activity continued to diminish as this ratio decreased, with the activity at the ratio of 1:1.2 at

the similar level as the initial ratio of 1:0.2 (Figure 7). This characterization experiment illustrated that an optimal restoration of enzymatic activity of trehalase could be achieved at the proposed ratio of fusion proteins to DNA substrate at 1:0.4.

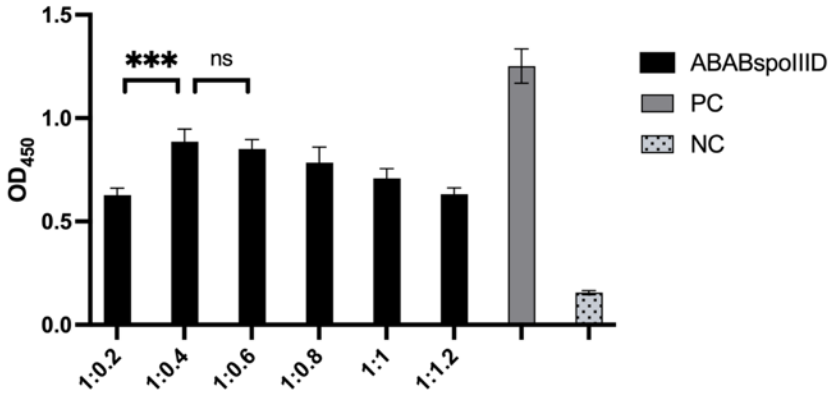

Figure 7. Comparison of complementation of fusion proteins HisTreA-N-SpoIIID and HisTreA-C-SpoIIID with hairpin-forming oligonucleotide sequence ABABspoIIID with different ratios of proteins to DNA substrate, analyzed by colorimetric enzymatic assay. The absorbance at 450 nm was measured by the spectrophotometer after a 90 min incubation at R/T. The positive control (PC) utilizes HisTreA mimicking the successful restoration of the fusion proteins. The negative control (NC) utilizes water instead of the oligonucleotide. One-way ANOVA was performed on groups with different ratios, and a p value < 0.001 was generated, indicating there are significant differences in the means in these groups. Tukey multiple comparisons of means were then conducted at a 95% confidence level. Very significant between-group difference is shown by '***' in the graph. No significant difference is shown by 'ns' in the

graph.

5.2.4 Complementation Experiments of Split Trehalase Fusion Proteins with Oligonucleotides Variants

Four oligonucleotides, ABABspoIIID, ABBAspoIIID, BABAspoIIID and BAABspoIIID, distinguished by differences in the directions of the double-stranded recognition sites at both ends, were utilized in this test at the optimal molar ratio of fusion proteins and DNA substrate determined by the previous ratio characterization experiment (Figure 8). Among the four hairpin-forming sequences above, the signal intensity after a 90 min incubation from the reactions involving ABABspoIIID and BAABspoIIID was significantly higher than that of the remaining two binding partners, indicating that the proposed complementation of the split trehalase fragments was better accommodated by the 3-dimensional complex formed by binding with ABABspoIIID and BAABspoIIID (Figure 9). However, no significant between-group difference was found between ABABspoIIID and BAABspoIIID (Figure 9). This variant test indicates that with the assistance of optimal salt final concentration and optimal ratio of DNA substrate addition, the direction of the recognition sequences generated within hairpin-forming ABABspoIIID was capable of reaching the highest binding activity with the split TreA spoIIID fusion proteins.

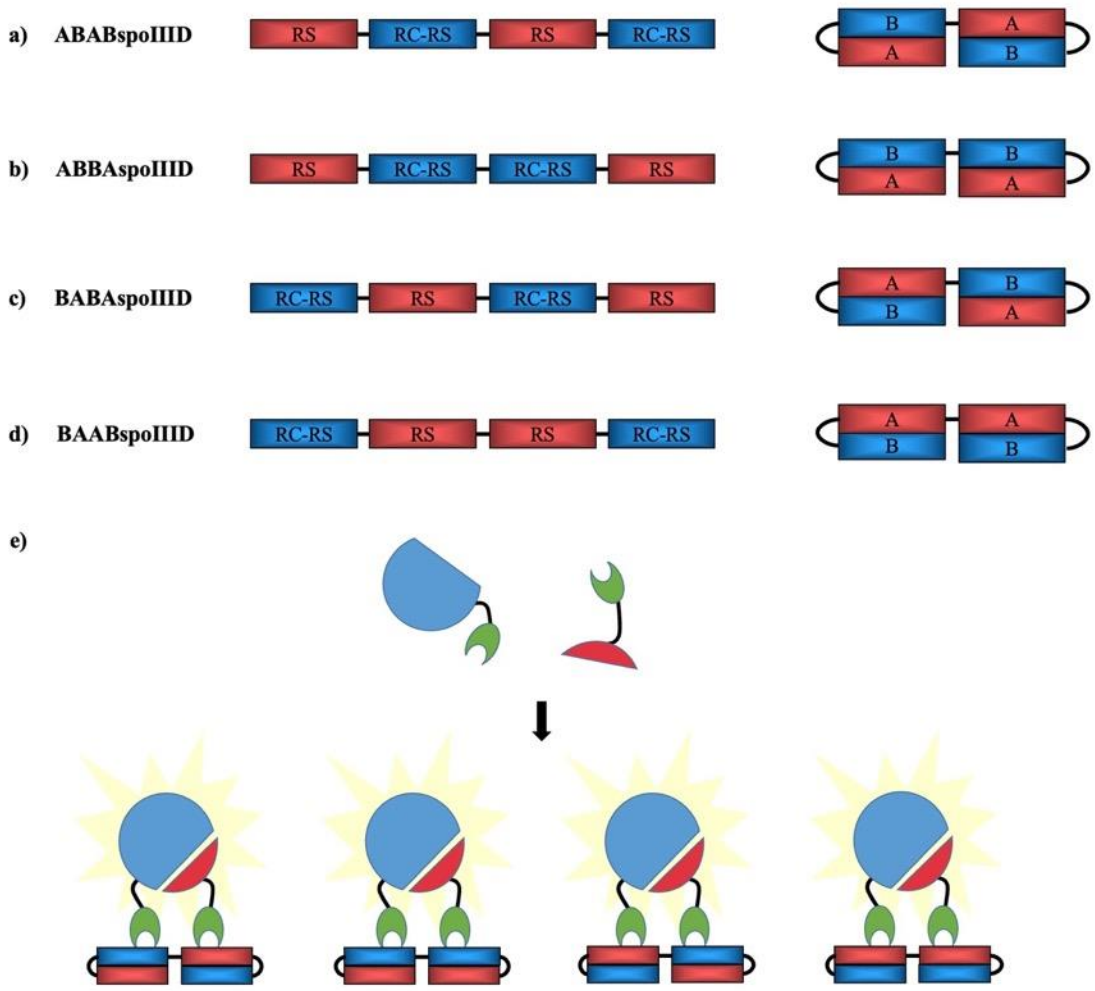

Figure 8. Schematic diagram depicting the comparison of complementation of fusion proteins HisTreA-N-SpoIIID and HisTreA-C-SpoIIID with four hairpin-forming oligonucleotide sequences with different orientation of the two recognition sites. Constructions and hairpin-formed structures of oligonucleotides ABABspoIIID **(a)** and its derived variants ABBAspoIIID **(b)**, BABAspoIIID **(c)** and BAABspoIIID **(d)** with recognition sites in different orientations are as shown. **(e)** Fusion proteins HisTreA-N-SpoIIID and HisTreA-C-SpoIIID specifically bind to the above four hairpin-formed structures, resulting in the

complementation of split trehalase domains and restoration of enzymatic activity.

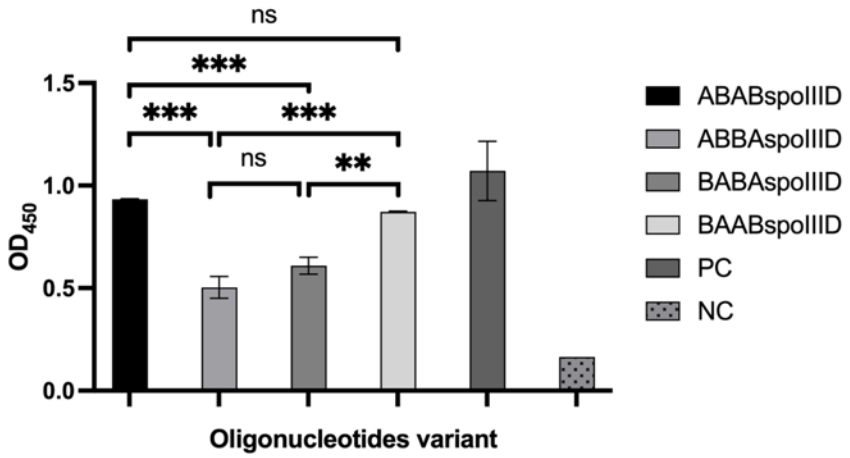

Figure 9. Comparison of complementation of fusion proteins HisTreA-N-SpoIIID and HisTreA-C-SpoIIID with four hairpin-forming oligonucleotide sequences with different orientation of the two recognition sites, analyzed by colorimetric enzymatic assay. The absorbance at 450 nm was measured by the spectrophotometer after a 90 min incubation at R/T. The positive control (PC) utilizes HisTreA, mimicking the successful restoration of the fusion proteins. The negative control (NC) utilizes water instead of the oligonucleotides. One-way ANOVA was performed, and a p value < 0.001 was generated, indicating there are significant differences in the means in the groups. Tukey multiple comparisons of means were then conducted at a 95% confidence level. The resulting p values indicate the very significant between-group differences for ABABspoIIID & ABBAspoIIID ($p < 0.001$), ABABspoIIID & BABAspoIIID ($p < 0.001$), ABBAspoIIID & BAABspoIIID ($p < 0.001$) and BABAspoIIID & BAABspoIIID (p

= 0.004) shown by '***' and '**' in the graph. No significant between-group differences for ABABspoIIID & BAABspoIIID (p = 0.857), and ABBAspoIIID & BABAspoIIID (p = 0.402) are shown by 'ns' in the graph.

5.2.5 Complementation Experiments of Split Trehalase Fusion Proteins with Double Stranded DNA with Tandem Recognition Sites and Different Linker lengths

In this experiment, double-stranded DNA with two specific recognition sequences in tandem and different linker lengths obtained by annealing oligonucleotides FF_DG74, FF_DG74+5T, FF_DG74+10T, FF_DG74+15T, FF_DG74+25T, and FF_DG74+30T with their corresponding complementary strands were utilized (Figure 10). The maximal OD_{450} after 90 min was observed in the assay of FF_DG74 with a linker length of four thymines (Figure 11). The activity of this protein-DNA binding decreased with each extension of five additional thymine. Linker lengths of 15 or higher resulted in activity levels indistinguishable from the negative control which has no DNA substrate added (Figure 11). The results indicated that with increasing linker length, the detected signal of the protein-DNA interaction decreases significantly, resulting in complete loss of complementation activity of split trehalase proteins.

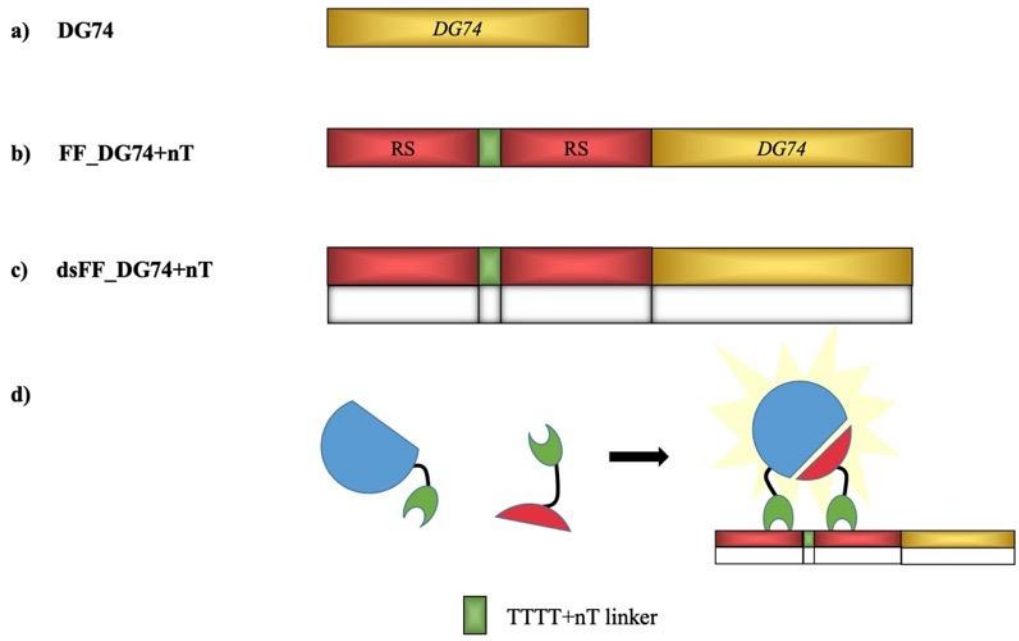

Figure 10. Schematic diagram depicting the comparison of complementation of fusion proteins HisTreA-N-SpoIIID and HisTreA-C-SpoIIID with double-stranded DNA (dsFF_DG74) with different linker lengths between the tandem recognition sites. (a) Construction of oligonucleotide DG74. **(b)** Construction of sequence FF_DG74+nT with a TTTT+nT linker between the incorporated tandem recognition sites shown as 'FF'. **(c)** Construction of double-stranded DNA dsFF_DG74+nT generated by annealing FF_DG74+nT and its corresponding complementary strand. **(d)** Fusion proteins HisTreA-N-SpoIIID and HisTreA-C-SpoIIID specifically bind to the two recognition sites on the dsFF_DG74+nT, resulting in the complementation of split trehalase domains and restoration of enzymatic activity.

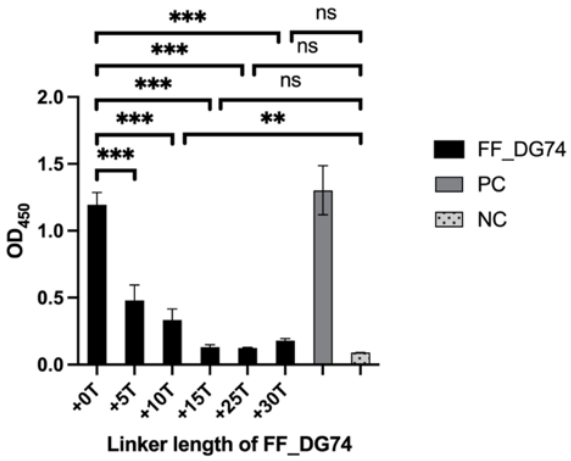

Figure 11. Comparison of complementation of fusion proteins HisTreA-N-SpoIIID and HisTreA-C-SpoIIID with double-stranded DNA (dsFF_DG74) with six different linker lengths between the tandem recognition sites analyzed by colorimetric enzymatic assay. The absorbance at 450 nm was measured by the spectrophotometer after a 90 min incubation at R/T. The positive control (PC) utilizes HisTreA, mimicking the successful restoration of the fusion proteins. The negative control (NC) utilizes water instead of the oligonucleotide. One-way ANOVA was performed, and a p value < 0.001 was generated, indicating there are significant differences in the means in the groups. Tukey multiple comparisons of means were then conducted at a 95% confidence level. The resulting p values indicate the very significant between-group differences for +0T & +5T ($p < 0.001$), +0T & +10T ($p < 0.001$), +0T & +15T ($p < 0.001$), +0T & +25T ($p < 0.001$), +0T & +30T ($p < 0.001$) and +10T & NC ($p = 0.006$) shown by '***' and '**' in the graph. No significant between-group differences for +15T & NC ($p = 0.986$), +25T & NC ($p = 0.993$) and +30T & NC ($p = 0.635$) are shown by 'ns' in the graph.

5.3 Complementation Assessment with PCR Products from *S. devriesei* and *E. coli* Colonies with ABSTA

5.3.1 Modification of Gram Type-Specific PCR

Six primer pairs consisting of DG74/Gram+, DG74/Gram-, FF_DG74/Gram+, FF_DG74/Gram-, FR_DG74/Gram+ and FR_DG74/Gram- were used in colony PCR of Gram-positive bacteria *S. devriesei* and Gram-negative bacteria *E. coli* to test the amplification specificity of primer pairs FF_DG74/Gram+ and FF_DG74/Gram- which had the SpoIIID recognition sequences incorporated in tandem (Figure 12). According to the sizes of the bands displayed on the agarose gel, *S. devriesei* colonies were successfully amplified by primer pairs DG74/Gram+ and FF_DG74/Gram+, while *E. coli* colonies were successfully amplified by primer pairs DG74/Gram- and FF_DG74/Gram-. Primer pairs FR_DG74/Gram+ and FR_DG74/Gram- containing the reverse complement of the recognition sequence failed to amplify *S. devriesei* or was amplified *E. coli* less efficiently (Figure 13a). To further explore the amplification specificity of primer pairs FF_DG74/Gram+ and FF_DG74/Gram- for Gram-positive and Gram-negative bacteria, FF_DG74/Gram+ was applied to *E. coli* colony PCR, while FF_DG74/Gram- was applied to *S. devriesei* colony PCR. At the annealing temperature of 65°C, the absence of the corresponding band on the agarose gel indicated that FF_DG74/Gram+ was incapable of amplifying *E. coli*. However, the appearance of light-colored bands corresponding to *S. devriesei*

indicated the possibility for the primer pair FF_DG74/Gram- to amplify *S. devriesei* non-specifically (Figure 13b). Subsequently, PCR with a gradient annealing temperature of 65 to 70°C was used to determine the optimal annealing temperature for the primer pair FF_DG74/Gram- to achieve specificity. According to the results of gel electrophoresis, when the annealing temperature was increased to 67°C, the non-specific bands from *S. devriesei* disappeared, while the amplification of FF_DG74/Gram- towards *E. coli* remained specific (Figure 13c). The series of tests in this section demonstrated that the primer pairs FF_DG74/Gram+ and FF_DG74/Gram- with tandem recognition sequences incorporated were both Gram type-specific; however, the optimal annealing temperature for the primer pair FF_DG74/Gram- appeared to be close to 67°C, which was different from 65°C for FF_DG74/Gram+.

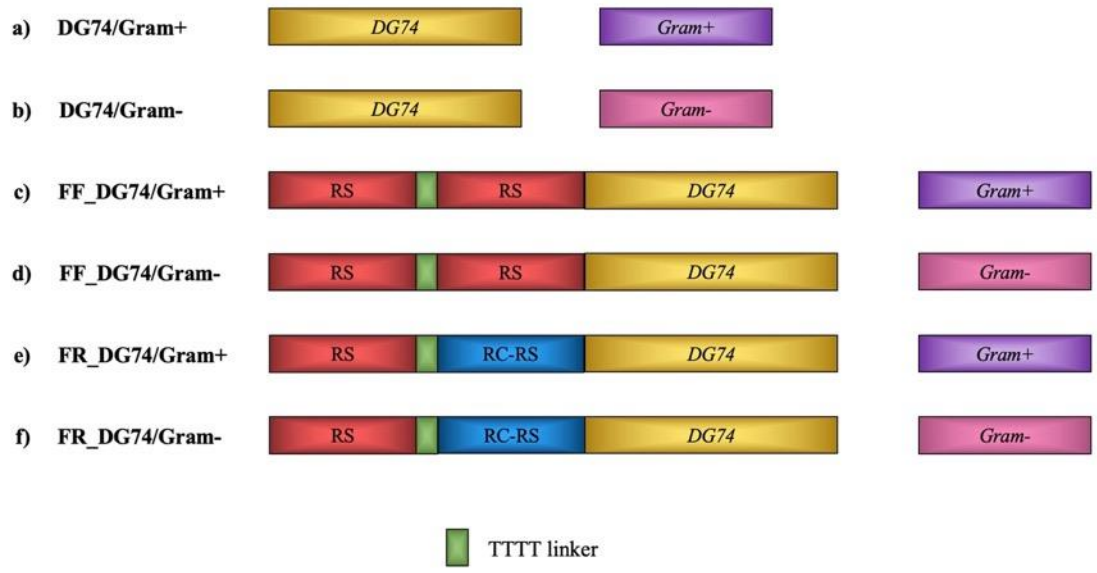

Figure 12. Constructions of primer pairs used in PCR confirmation of amplification specificity to Gram-positive and Gram-negative bacteria. (a) Primer pair consisting of Gram-positive-specific forward primer Gram+ and universal reverse primer DG74. **(b)** Primer pair consisting of Gram-negative-specific forward primer Gram- and primer DG74. **(c)** Primer pair consisting of primer Gram+ and tandem-recognition-sequence-incorporated primer FF_DG74. **(d)** Primer pair consisting of primer FF_DG74 and Gram-. **(e)** Primer pair consisting of primer Gram+ and primer FR_DG74 incorporated recognition sequence and reverse complementary sequence. **(f)** Primer pair consisting of primer FR_DG74 and Gram-. TTTT linker are used for the DG74-derived primers.

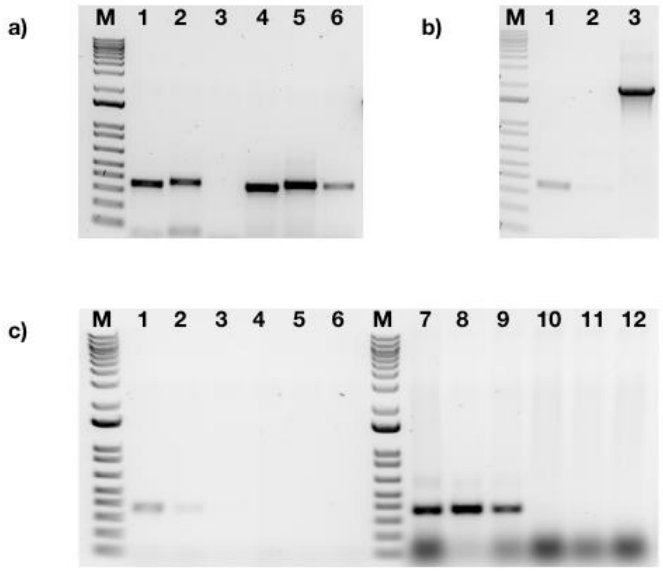

Figure 13. PCR confirmation of amplification specificity of primer pairs FF_DG74/Gram+ and FF_DG74/Gram- to Gram-positive and Gram-negative bacteria using six primer pairs. **(a)** Agarose gel showing the successful amplification of *S. devriesei* using primer pairs DG74/Gram+ and FF_DG74/Gram+ with bands corresponding to 355 bp (1) and 381 bp (2), respectively, as well as the successful amplification of *E. coli* using primer pairs DG74/Gram- and FF_DG74/Gram- with bands corresponding to 353 bp (4) and 379 bp (5), respectively. The primer pair FR_DG74/Gram+ failed to amplify *S. devriesei* (3), while FR_DG74/Gram- was less efficient in amplifying *E. coli* (6). **(b)** Agarose gel showing the non-specific amplification of *S. devriesei* using primer pair FF_DG74/Gram- (1) and the failed amplification of *E. coli* using primer pair FF_DG74/Gram+ (2). Vector pETDuet-1 was utilized as the positive control of the PCR (3). **(c)** Agarose gel showing the non-specific amplification of *S. devriesei* using primer pair FF_DG74/Gram- at 65°C (1) and 66°C (2), failed amplification at 67°C (3), 68°C (4), 69°C (5)

and 70°C (6); the specific amplification of *E. coli* using primer pair FF_DG74/Gram- at 65°C (7), 66°C (8) and 67°C (9), failed amplification at 68°C (10), 69°C (11) and 70°C (12). 1 Kb DNA ladder was utilized in all gels (M).

5.3.2 Specific Detection of Purified PCR Products with Recognition Sites Incorporated in Tandem

To investigate the complementation of split trehalase proteins with PCR products incorporated with recognition sites in tandem, purified and concentrated products of *S. devriesei* and *E. coli* colony PCR were added to the ABSTA at determined molar concentration. Compared to the endpoint OD_{450} corresponding to the double-stranded fragment dsFF_DG74, both *S. devriesei* amplicon from primer pair FF_DG74/Gram+ and *E. coli* amplicon from primer pair FF_DG74/Gram- showed evidence of complementation of the fusion proteins HisTreA-C-SpoIIID and HisTreA-N-SpoIIID, despite the fact that the activity of the latter is 56% of that of the former (Figure 10). ABSTAs corresponding to primer pairs DG74/Gram+ and DG74/Gram- without specific recognition sequences incorporated, however, demonstrated signal intensities close to reaction with no DNA substrate or using double-stranded fragment dsFR_DG74 as the substrate (Figure 14). No significance difference was found between assay of dsFR_DG74 and non-template control as well (Figure 14). This experiment demonstrated that when added at the optimal final

concentration, the purified and concentrated PCR products from *S. devriesei* and *E. coli* with tandem recognition sites could specifically trigger the complementation of the fusion proteins and generate detectable signals.

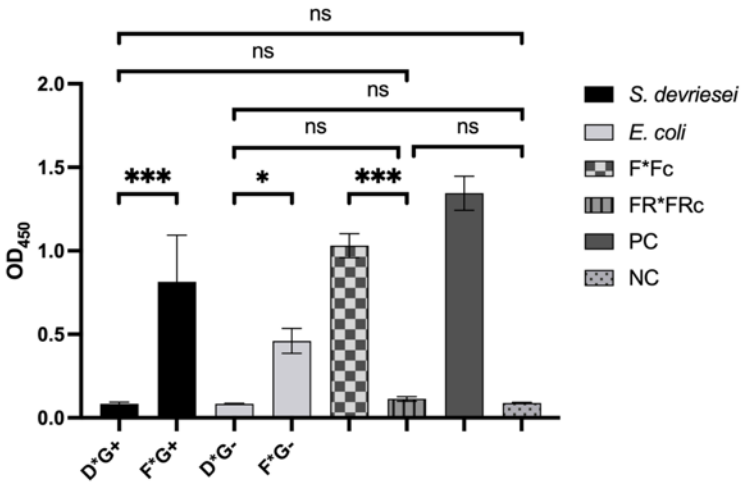

Figure 14. Complementation of fusion proteins HisTreA-N-SpoIIID and HisTreA-C-SpoIIID by purified colony PCR products of *S. devriesei* and *E. coli* amplified by four primer pairs analyzed by ABSTA. D*G-, F*G+, D*G+, F*G-, F*Fc and FR*FRc are the simplified versions of assays involving primer pairs DG74/Gram+, FF_DG74/Gram+, DG74/Gram-, FF_DG74/Gram-, and assays with dsFF_DG74 and dsFR_DG74, respectively. The absorbance at 450 nm was measured by the spectrophotometer after a 90 min incubation at R/T. The positive control (PC) utilizes HisTreA, mimicking the successful restoration of the fusion proteins. The negative control (NC) utilizes water as the binding partner to the fusion proteins. One-way ANOVA was performed, and a p value < 0.001 was generated, indicating there are significant differences in the means in the groups. Tukey multiple comparisons of means were then conducted at a 95%

confidence level. The resulting *p* values indicate the very significant between-group differences for D*G+ & F*G+ ($p < 0.001$), FF*FFc & FR*FRc ($p < 0.001$) shown by '***' in the graph, and significant between-group differences for D*G- & F*G- ($p = 0.014$) shown by '*'. No significant between-group differences for D*G+ & NC ($p = 1.0$), D*G+ & FR*FRc ($p = 0.999$), D*G- & NC ($p = 1.0$), D*G- & FR*FRc ($p = 0.999$) and FR*FRc & NC ($p = 1.0$) are shown by 'ns' in the graph.

5.3.3 Dilution Test of Purified PCR Products with Recognition Sites Incorporated in Tandem

Colony PCR was performed on *S. devriesei* using primer pairs DG74/Gram+ and FF_DG74/Gram+, and the corresponding purified and concentrated PCR products were used to determine the optimal composition of fusion proteins and PCR products with specific recognition sites incorporated. The products resulting from primer pair FF_DG74/Gram+ were further diluted 2-fold and 5-fold, respectively. According to the OD_{450} after 90 min, fusion proteins HisTreA-C-SpoIIID and HisTreA-N-SpoIIID demonstrated comparable complementation activity when reacted with diluted and undiluted PCR products with specific recognition sequences introduced. However, the signal levels obtained from the 2-fold dilution decreased by 23.4% compared to the undiluted one, while the decrease corresponding to the 5-fold dilution came to 42.4% (Figure 15). No detectable signal was observed in the ABSTA with amplicon from primer pair DG74/Gram+,

consistent with the non-DNA control. This experiment indicated that, the complementation activity of fusion proteins HisTreA-C-SpoIIID and HisTreA-N-SpoIIID was dependent on the amount of specific-recognition-site-incorporated PCR products in the reaction. As the final molar concentration of purified PCR products decreased due to dilution, so did the activity of such fusion proteins-DNA interactions.

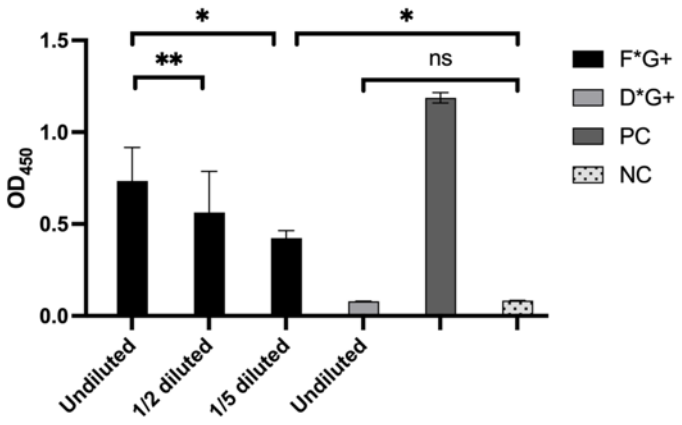

Figure 15. Comparison of complementation of fusion proteins HisTreA-N-SpoIIID and HisTreA-C-SpoIIID with dilutions of purified colony PCR products of *S. devriesei* amplified by two primer pairs analyzed by ABSTA. F*G+ and D*G+ are the simplified versions of assays involving primer pairs FF_DG74/Gram+ and DG74/Gram+, respectively. The absorbance at 450 nm was measured by the spectrophotometer after a 90 min incubation at R/T. The positive control (PC) utilizes HisTreA, mimicking the successful restoration of the fusion proteins. The negative control (NC) utilizes water instead of DNA substrate. One-way ANOVA was performed on F*G+ groups of Undiluted, 1/2 diluted, 1/5 diluted and NC, and a p value < 0.001 was generated,

indicating there are significant differences in the means in these groups. Tukey multiple comparisons of means were then conducted at a 95% confidence level. The resulting *p* values indicate the very significant between-group difference for Undiluted & 1/2 diluted ($p = 0.002$) shown by '**' in the graph; Significant between-group differences for Undiluted & 1/5 diluted ($p = 0.015$) and 1/5 diluted & NC ($p = 0.015$) are shown by '*' in the graph. Two-sample t-test was conducted between Undiluted D*G+ and NC at a 95% confidence level. No significant difference ($p = 0.074$) is shown by 'ns' in the graph.

5.3.4 Use of EDTA to Counter Inhibition of ABSTA by PCR Reagents

Inhibition of the ABSTA coming from the PCR mastermix was suspected. Therefore, the addition of EDTA to PCR products of *S. devriesei* colony PCR was tested to counter the bivalent cations in the mastermix and improve the ABSTA activity. Treated and untreated PCR reagents were added to the colorimetric enzymatic assays using the double-stranded fragment dsFF_DG74 as DNA substrate. After incubating for 90 min, the observed signal level with PCR reagents was considerably lower than that without PCR reagents, which was less than 50% of the latter. However, in the assays where the PCR reagents with EDTA at concentrations of 0.1 mM and 0.5 mM were added, the signals for both assays were strongly increased compared to the assay with untreated PCR reagents (Figure 16). Nonetheless, no significant difference was recorded between the activity

levels of the two above-mentioned EDTA-treated assays, which were both restored to more than 80% of the signal level of the dsFF_DG74-only assay (Figure 16). This experiment simulated the inhibition of ABSTA involving substrate dsFF_DG74 in the presence of PCR reagents, which was partially countered by incubating EDTA with the PCR reagents in advance of adding to the ABSTA.

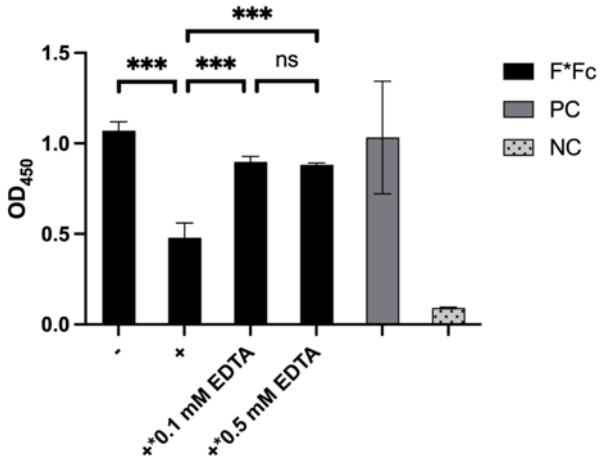

Figure 16. Complementation of fusion proteins HisTreA-N-SpoIIID and HisTreA-C-SpoIIID by double-stranded DNA (dsFF_DG74) without and with addition of EDTA to PCR reagents at two final molar concentrations analyzed by ABSTA. The presented positive (+), negative (-) and F*Fc are the simplified versions of assays with PCR reagents addition, no PCR reagents addition and dsFF_DG74, respectively. The absorbance at 450 nm was measured by the spectrophotometer after a 90 min incubation at R/T. The positive control (PC) utilizes HisTreA, mimicking the successful restoration of the fusion proteins. The negative control (NC) utilizes water instead of DNA substrate. Two-sample t-test was performed on - & + at a 95% confidence level. The resulting *p* values indicate the very significant difference for - & + ($p < 0.001$) shown

by '***' in the graph. One-way ANOVA was performed with groups of +, +*0.1 mM EDTA and +*0.5 mM EDTA, and a p value < 0.001 was generated, indicating there are significant differences in the means in these groups. Tukey multiple comparisons of means were then conducted at a 95% confidence level. The resulting p values indicate the very significant between-group differences for + & +*0.1 mM EDTA ($p < 0.001$) and + & +*0.5 mM EDTA ($p < 0.001$) shown by '***' in the graph; No significant differences for +*0.1 mM EDTA and +*0.5 mM EDTA ($p = 0.922$) are shown by 'ns' in the graph.

5.3.5 Titration of Unpurified PCR Products

To determine the optimal volume of unpurified colony PCR products to add to the reaction resulting in the highest activity resulting in complementation of the split trehalase fusion proteins, a titration experiment was carried out with the unpurified PCR products from the *S. devriesei* and *E. coli* colonies. The volumes of the two Gram type PCR products added to each colorimetric enzyme reaction ranged from 5, 10, 20, 30 and 40 µl. As demonstrated by a 90 min incubation, all the signal intensities generated from the complementation of the fusion proteins were low compared to the assay using dsFF_DG74 (Figure 17). Maximally 30% of that reference level was achieved. A slight increase of the corresponding signal intensity was observed compared to the negative control without the DNA substrate. With increasing volume of unpurified products from

5 µl to 30 µl, the OD_{450} at 90 min slowly rose, reaching a plateau at 30 µl (Figure 17). Subsequently, addition of 40 µl PCR product led to a modest decline in signal intensity for both bacteria. Nonetheless, the activity of the complementation of fusion proteins from the above-mentioned assays remained low, seeing that the ABSTA was negatively affected by PCR reagents that can be removed by purification.

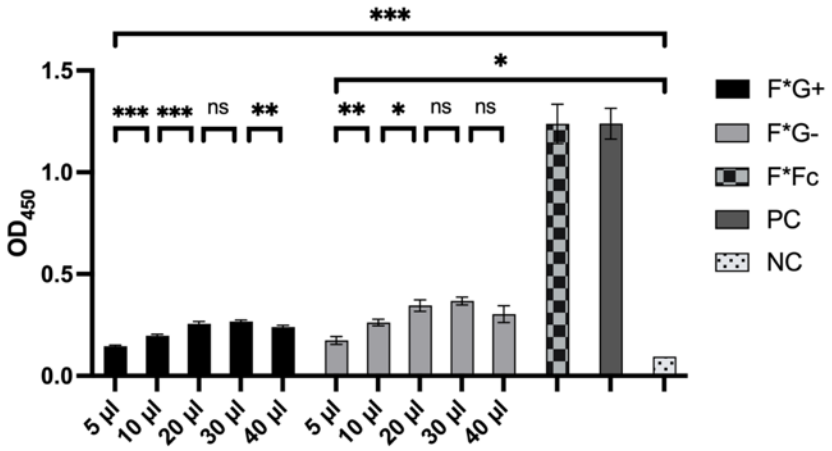

Figure 17. Complementation of fusion proteins HisTreA-N-SpoIIID and HisTreA-C-SpoIIID by specific-recognition-sequence-incorporated unpurified colony PCR products added to the reaction in different volumes analyzed by ABSTA. F*G+, F*G- and F*Fc are the simplified versions of assays involving primer pairs FF_DG74/Gram+, FF_DG74/Gram- and assay with dsFF_DG74, respectively. The absorbance at 450 nm was measured by the spectrophotometer after a 90 min incubation at R/T. The positive control (PC) utilizes HisTreA, mimicking the successful restoration of the fusion proteins. The negative control (NC) utilizes water instead of DNA substrate. One-way ANOVA was performed separately within groups belonging to F*G+ and F*G-.

The generated *p* values for both ANOVA ($p < 0.001$) indicate significant differences in the means within groups of F*G+ and F*G-. Tukey multiple comparisons of means were then conducted at a 95% confidence level. The resulting *p* values indicate the very significant between-group differences for NC & 5 µl F*G+ ($p < 0.001$), 5 µl F*G+ & 10 µl F*G+ ($p < 0.001$), 10 µl F*G+ & 20 µl F*G+ ($p < 0.001$), 30 µl F*G+ & 40 µl F*G+ ($p = 0.008$), and 5 µl F*G- & 10 µl F*G- ($p = 0.008$) shown by '***' and '**' in the graph; Significant between-group differences for NC & 5 µl F*G- ($p = 0.016$) and 10 µl F*G- & 20 µl F*G- ($p = 0.012$) are shown by '*'; No significant between-group differences for 20 µl F*G+ & 30 µl F*G+ ($p = 0.481$), 20 µl F*G- & 30 µl F*G- ($p = 0.852$), and 30 µl F*G- & 40 µl F*G- ($p = 0.059$) are shown by 'ns' in the graph.

5.3.6 Use of EDTA to Counter Inhibition of ABSTA by Unpurified PCR Products

In this experiment, EDTA was incubated with unpurified colony PCR products from *S. devriesei* and *E. coli* at final molar concentrations of 0, 0.1 mM, 0.3 mM, and 0.5 mM, respectively. The PCR products were then added to the colorimetric enzyme reaction at the optimal addition volume determined in test 5. 3. 5 to explore the utilization of EDTA to counter the inhibition. The assay with double-stranded DNA dsFF_DG74 was employed as a positive control for the complementation activity of split trehalase proteins by pure DNA substrate. After a 90 min incubation, the activity without EDTA was low compared to dsFF_DG74, consistent with the

observation in the previous experiment (Figure 18). However, except that the *E. coli* assay with 0.5 mM EDTA showed a significantly improved signal compared to the assay without EDTA added, none of the remaining assays experienced a distinguishable signal increase from the assay with 0 EDTA, remaining at 30% of the signal level corresponding to dsFF_DG74. This test thus demonstrates that the inhibition of the ABSTA by unpurified PCR products mix was not countered by EDTA.

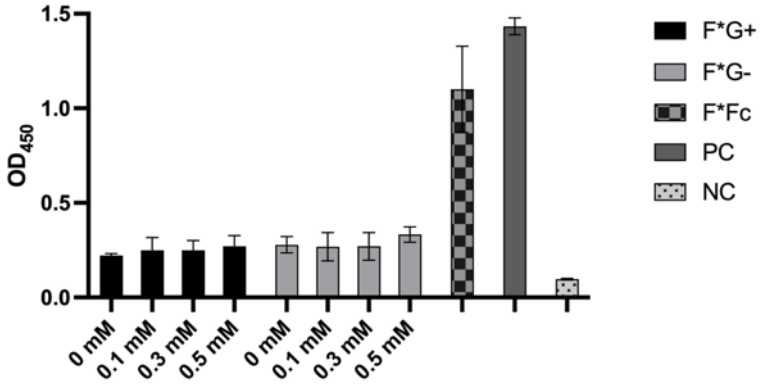

Figure 18. Complementation of fusion proteins HisTreA-N-SpoIIID and HisTreA-C-SpoIIID by specific-recognition-sequence-incorporated unpurified colony PCR products without and with addition of EDTA at three final molar concentrations analyzed by ABSTA. F*G+, F*G- and F*Fc are the simplified versions of FF_DG74/Gram+, FF_DG74/Gram- and double-stranded DNA dsFF_DG74, respectively. The absorbance at 450 nm was measured by the spectrophotometer after a 90 min incubation at R/T. The positive control (PC) utilizes HisTreA, mimicking the successful restoration of the fusion proteins. The negative control (NC) utilizes water instead of DNA substrate. One-way ANOVA was performed separately within groups

belonging to F*G+ and F*G-. The resulting p values for F*G+ ($p = 0.721$) and F*G- ($p = 0.541$) indicate no significant between-group differences in the means.

5.4 Sensitivity of Detection of Gram Type-Specific LAMP followed by ABSTA

5.4.1 *Staphylococcus* Specific LAMP Assay with Genomic DNA Extracted from Bacterial Culture

LAMP assays with *S. devriesei* gDNA with copy numbers ranging from 1.9×10^7 to 1.9 were set up after 10-fold serial dilutions of the initial DNA solution in sterile water, to determine the detection limit of the colorimetric enzymatic assays with split TreA and SpoIIID fusion proteins to these LAMP products. Indicated by the results of the 30 min LAMP reaction using the LAMPstaph primer set, the time required for exponential amplification of *S. devriesei* gDNA increased with higher dilutions. The melting curve of the negative control with the addition of water remained flat, indicating no dimers formation and self-amplifying in the LAMPstaph primer set, and the results were thus reliable (Figure 19a).

To confirm that *S. devriesei* gDNA corresponding to the above dilutions of copy numbers was successfully amplified by LAMPstaph, the LAMP products were subjected to gel electrophoresis. As shown in Figure 19b, as the copy number was reduced by the 10-fold serial dilution, the brightness of the band region indicating the primary size of the amplicon evenly decreased while the band corresponding to the negative control was absent, which was consistent with the above-mentioned fluorescent readings of the LAMP reactions.

In the colorimetric enzyme reaction using the above-mentioned LAMP products, the complementation of split fusion proteins of reactions using the undiluted, 10-fold diluted and 10^2-fold diluted DNA templates at 1.9×10^7, 1.9×10^6 and 1.9×10^5 copy numbers demonstrated the highest enzymatic activity which had the level comparable to positive control where the double-stranded DNA dsFF_DG74 was employed at the previously optimized final molar concentration. The complementation of fusion proteins HisTreA-C-SpoIIID and HisTreA-N-SpoIIID by LAMP amplicons decreased in subsequent reactions as the dilution fold increased. Nonetheless, the detected signal intensity corresponding to 1.9 of DNA copies remained 80% of the positive control (Figure 19c). This, it was demonstrated that the LAMPstaph primer set enabled a successful efficient amplification of gDNA from *S. devriesei*. Moreover, according to the colorimetric enzyme reaction incubated for 90 min, LAMP amplification of *S. devriesei* gDNA starting at 1.9 copies was sufficient to complement the fusion proteins and producing a detectable signal.

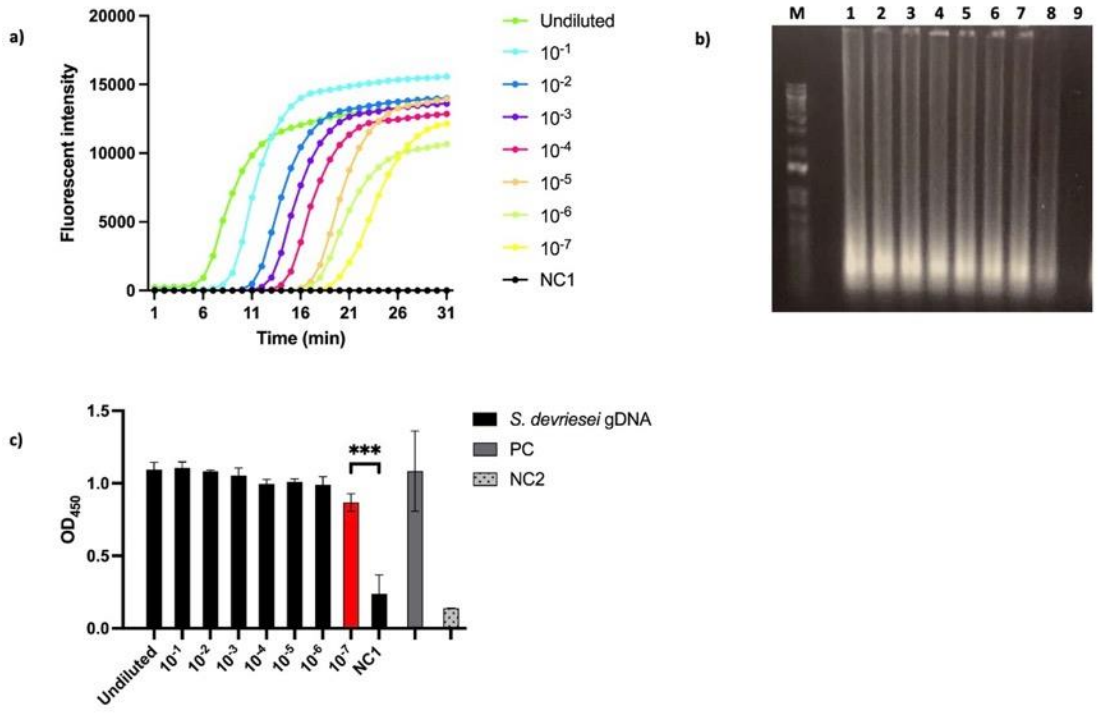

Figure 19. Sensitivity of detection of *S. devriesei* gDNA with LAMP followed by ABSTA. (a) LAMP assays using LAMPstaph primer set and serial dilutions of copy number of *S. devriesei* gDNA extracted from bacterial cultures. **(b)** Agarose gel electrophoresis confirmation of LAMP amplicons of *S. devriesei* gDNA at undiluted (1), 10-fold diluted (2), 10^2-fold diluted (3), 10^3-fold diluted (4), 10^4-fold diluted (5), 10^5-fold diluted (6), 10^6-fold diluted (7), 10^7-fold diluted (8) copy number using LAMPstaph primer sets with bands in the typical ladder-like pattern. Non-template LAMP product was used as negative control (NC1) (9). 1 Kb DNA ladder was utilized (M). **(c)** ABSTA showing the complementation of fusion proteins HisTreA-N-SpoIIID and HisTreA-C-SpoIIID by LAMP amplicons at different copy number of *S. devriesei* gDNA. The absorbance at 450 nm was measured by the spectrophotometer after a 90 min incubation at R/T. The positive control (PC) utilizes the double-stranded DNA dsFF_DG74 as the substrate for binding with fusion

proteins. The negative control (NC2) utilizes water instead of DNA substrate. Two-sample t-test was conducted between assays treated with gDNA dilution series and NC1 at a 95% confidence level. The resulting p values indicate that the mean difference for 10^{-7} & NC1 ($p < 0.001$) is significantly different from zero, which is shown by '***' in the graph. The limit of detection of ABSTA is indicated in red.

5.4.2 *Streptococcus* Specific LAMP Assay with Genomic DNA Extracted from Bacterial Culture

To explore the detection limit of colorimetric reactions using split trehalase fusion proteins and LAMP products with specific recognition sites incorporated, LAMP reactions with copy numbers of *S. uberis* gDNA from 2.4×10^7 to 2.4 were set up after 10-fold serial dilutions of the starting DNA solution. From the results of the 30 min LAMP assays using the above dilution sets, the gDNA of *S. uberis* was able to be successfully amplified by the primer set LAMPstrep as early as 7 min when added at the initial copy number of 2.4×10^7. As the dilution increased subsequently, the time required for successful amplification stepwise increased as well, ending up at 28 min corresponding to the 10^7-fold dilution and the end-point fluorescence intensity dropped by practically half. No amplification was detected in the negative control with added water, indicating that the primer set LAMPstrep did not form dimers and self-amplify, and the results were reliable

(Figure 20a).

The gel electrophoresis results using the above LAMP products were consistent with the LAMP assays, i.e., as the number of copies of gDNA added decreased due to 10-fold serial dilutions, the brightness of the area corresponding to the major amplicon size on band was reduced. The LAMP product from the negative control produced no bands on the agarose gel as expected (Figure 20b).

As shown in the 90 min colorimetric enzyme reaction using the above-mentioned LAMP products, assays with undiluted to 10^4-fold diluted DNA templates at copy numbers of 2.4×10^7 to 2.4×10^3 presented comparable signal levels of enzyme complementarity to the positive control using the double-stranded DNA dsFF_DG74. However, the signal level afterwards decreased with increasing dilution-fold, ending with 60% of the level at the undiluted set (Figure 20c). Demonstrated by the results of colorimetric reaction, LAMP amplification using the primer set LAMPstrep with 24 copies of the *S. uberis* gDNA template was sufficient to complement the fusion proteins and generate a detectable signal.

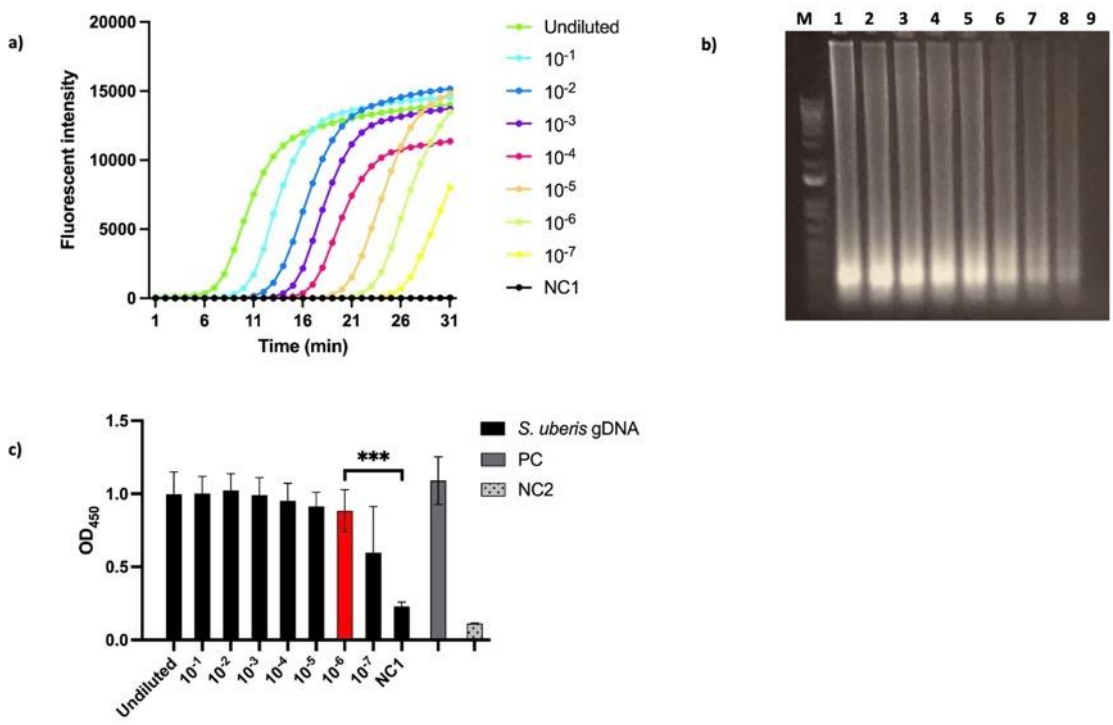

Figure 20. Sensitivity of detection of *S. uberis* gDNA with LAMP followed by ABSTA. (a) LAMP assays using LAMPstrep primer set and serial dilutions of copy number of *S. uberis* gDNA extracted from bacterial cultures. **(b)** Agarose gel electrophoresis confirmation of LAMP amplicons of *S. uberis* gDNA at undiluted (1), 10-fold diluted (2), 10^2-fold diluted (3), 10^3-fold diluted (4), 10^4-fold diluted (5), 10^5-fold diluted (6), 10^6-fold diluted (7), 10^7-fold diluted (8) copy number using LAMPstrep primer sets with bands in the typical ladder-like pattern. Non-template LAMP product was used as negative control (NC1) (9). 1 Kb DNA ladder was utilized (M). **(c)** ABSTA showing the complementation of fusion proteins HisTreA-N-SpoIIID and HisTreA-C-SpoIIID by LAMP amplicons at different copy number of *S. uberis* gDNA. The absorbance at 450 nm was measured by the spectrophotometer after a 90 min incubation at R/T. The positive control (PC) utilizes the double-stranded DNA dsFF_DG74 as the substrate for binding with fusion

proteins. The negative control (NC2) utilizes water instead of DNA substrate. Two-sample t-test was conducted between assays treated with gDNA dilution series and NC1 at a 95% confidence level. The resulting p values indicate that the mean difference for 10^{-6} & NC1 ($p < 0.001$) is significantly different from zero, which is shown by '***' in the graph. The limit of detection of ABSTA is indicated in red.

5.4.3 Gram-Negative Specific LAMP Assay with Genomic DNA Extracted from Bacterial Culture

The copy numbers of *E. coli* gDNA employed for LAMP assays were set from 1.0×10^7 to 1.0 by 10-fold serial dilutions. From the melting curves of 30 min LAMP, the primer set LAMPneg was capable of successfully amplifying *E. coli* gDNA early in this timeframe when starting reaction at a copy number of 1.0×10^7. The time to onset of amplicon production extended with subsequent dilutions increasing. No detectable amplification was observed in the negative control, indicating reliable results (Figure 21a).

In the agarose gel electrophoresis using the LAMP products described above, the bands corresponding to reactions with increasing dilutions of DNA copy numbers were progressively less bright in the region where the major size of amplicon was located, which was consistent with

fluorescence intensities at 30 min indicative of the amplicon amount (Figure 21b). The above LAMP products were added to the colorimetric enzyme assay using the SpoIIID fusion proteins. As illustrated by the incubation results after 90 min, the enzyme complementary activity resulting from protein-DNA binding by the specific recognition sites on the LAMP amplicons was comparable to the positive control, at initial DNA copy numbers of 1.0×10^7 to 10. However, the signal intensity corresponding to the LAMP product with a starting copy number of 1 dropped dramatically, less than 40% of the positive control (Figure 21c). The above-mentioned results based on *E. coli* gDNA indicated that 10 copies of DNA were sufficient to be successfully amplified by the primer set LAMPneg, and the signal intensity of enzyme colorimetric reaction using the SpoIIID fusion proteins and this LAMP product was capable of reaching a detected level.

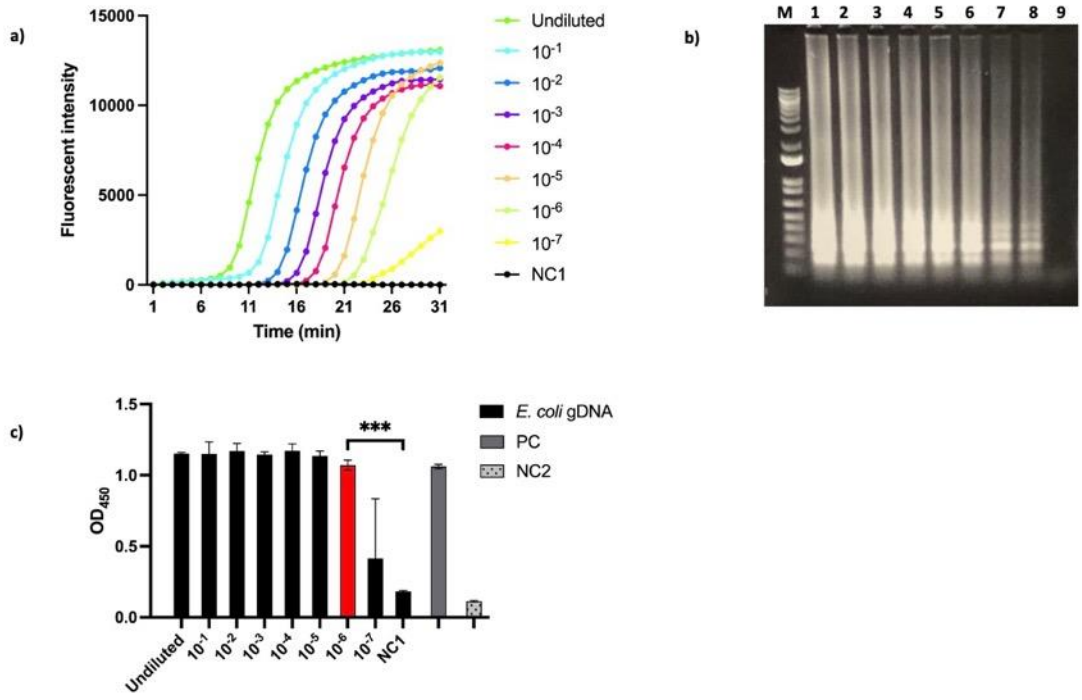

Figure 21. Sensitivity of detection of *E. coli* gDNA with LAMP followed by ABSTA. (a) LAMP assays using LAMPneg primer set and serial dilutions of copy number of *E. coli* gDNA extracted from bacterial cultures. **(b)** Agarose gel electrophoresis confirmation of LAMP amplicons of *E. coli* gDNA at undiluted (1), 10-fold diluted (2), 10^2-fold diluted (3), 10^3-fold diluted (4), 10^4-fold diluted (5), 10^5-fold diluted (6), 10^6-fold diluted (7), 10^7-fold diluted (8) copy number using LAMPneg primer sets with bands in the typical ladder-like pattern. Non-template LAMP product was used as negative control (NC1) (9). 1 Kb DNA ladder was utilized (M). **(c)** ABSTA showing the complementation of fusion proteins HisTreA-N-SpoIIID and HisTreA-C-SpoIIID by LAMP amplicons at different copy number of *E. coli* gDNA. The absorbance at 450 nm was measured by the spectrophotometer after a 90 min incubation at R/T. The positive control (PC) utilizes the double-stranded DNA dsFF_DG74 as the substrate for binding with fusion proteins. The negative

control (NC2) utilizes water instead of DNA substrate. Two-sample t-test was conducted between assays treated with gDNA dilution series and PBS (NC1) at a 95% confidence level. The resulting p values indicate that the mean difference for 10^{-6} & NC1 ($p < 0.001$) is significantly different from zero, which is shown by '***' in the graph. The limit of detection of ABSTA is indicated in red.

5.4.4 Detection of Staphylococci in Spiked Milk Samples with Primer Set LAMPstaph

In this experiment, the CFU/ml of the milk aliquot spiked with undiluted *S. devriesei* culture of $OD_{600} = 1$ and its 10-fold dilutions were 4.9×10^7, 4.9×10^6, 4.9×10^5, 4.9×10^4, 4.9×10^3, and 4.9×10^2, respectively. From the melting curves of the LAMP assays, the DNA template extracted from the milk with CFU/ml at 4.9×10^7 was capable of being amplified by the primer set LAMPstaph after 16 min. In comparison, the amplification corresponding to spiked milk with 4.9×10^6 CFU/ml was initiated after 19 min. As the dilution of bacterial culture used for spiking increased, the time needed for bacterial DNA to be amplified by primer set LAMPstaph was delayed. The end-point fluorescence intensity from the 10^2-fold dilution spiking reaction to the 10^3-fold dilution spiking reaction displayed a dramatic drop, being indistinguishable from the PBS control. The melting curve of the reaction with the addition of water did not rise, indicating no dimer was formed in this LAMP primer set and no self-amplify (Figure 22a).

The above-mentioned LAMP products were subjected to agarose gel electrophoresis to confirm the amplification by primer set LAMPstaph in LAMP assays. The band corresponding to the starting LAMP reaction showed the highest brightness at the size of the major amplicon. The brightness of lanes subsequently decreased as the CFU/ml of spiked milk samples serially decreased, while the band disappeared from 10^3-fold dilution, consistent with the observations from the LAMP curves (Figure 22b).

As illustrated by the colorimetric enzyme assays performed with the above-mentioned LAMP products, the amplicons corresponding to the spiked milk aliquots from 4.9×10^4 to 4.9×10^7 CFU/ml of *S. devriesei* were able to trigger the complementarity of the fusion proteins HisTreA-C-SpoIIID and HisTreA-N-SpoIII in a 90 min incubation. The restored enzymatic activity of split trehalase resulting from the set of 4.9×10^7 CFU/ml was the highest, yet lower than the signal corresponding to the positive control using double-stranded dsFF_DG74. Starting from the LAMP product corresponding to 4.9×10^3 CFU/ml, the generated signals were shown to be flat. These observations were consistent with the differences in the end-point fluorescence intensity of the LAMP assay (Figure 22c). With the DNA extracted from *S. devriesei*-spiked milk samples of CFU/ml $\geq 4.9 \times 10^4$, the fusion proteins HisTreA-C-SpoIIID and HisTreA-N-SpoIII were complemented by the corresponding recognition-site-incorporated LAMP products and produced detectable signal intensity.

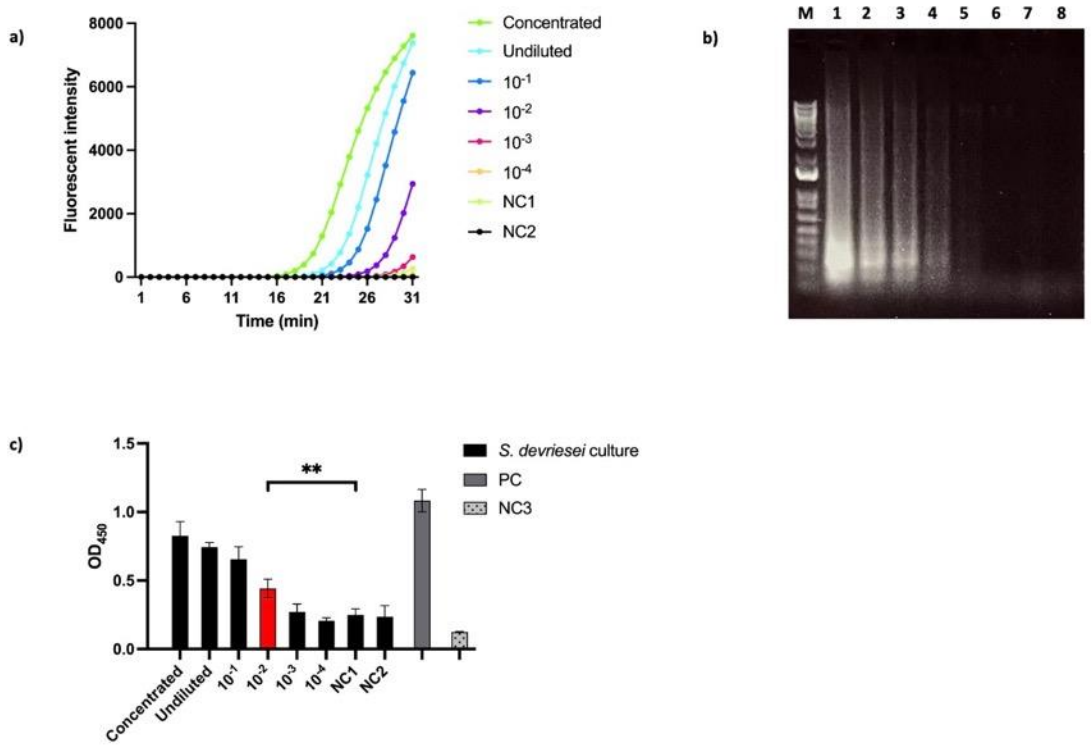

Figure 22. Sensitivity of detection of DNA extracted from *S. devriesei*-spiked milk with LAMPstaph followed by ABSTA. (a) LAMP assays using LAMPstaph primer set and DNA extracted from milk aliquots spiked with serial dilutions of *S. devriesei* culture at OD_{600} = 1. **(b)** Agarose gel electrophoresis confirmation of LAMP amplicons of DNA extracted from milk aliquots spiked with concentrated (1), undiluted (2), 10-fold diluted (3), 10^2-fold diluted (4), 10^3-fold diluted (5) and 10^4-fold diluted (6) *S. devriesei* culture of OD_{600} = 1 and PBS (NC1) (7) using LAMPstaph primer set with bands in the typical ladder-like pattern. Non-template LAMP product was used as negative control (NC2) (8). 1 Kb DNA ladder was utilized (M). **(c)** ABSTA showing the complementation of fusion proteins HisTreA-N-SpoIIID and HisTreA-C-SpoIIID by LAMP amplicons at different dilutions of *S. devriesei* culture of OD_{600} = 1. The absorbance at 450 nm

was measured by the spectrophotometer after a 90 min incubation at R/T. The positive control (PC) utilizes the double-stranded DNA dsFF_DG74 as the substrate for binding with fusion proteins. The negative control (NC3) utilizes water instead of DNA substrate. Two-sample t-test was conducted between assays treated with bacterial culture serial dilutions and PBS (NC1) at a 95% confidence level. The resulting *p* values indicate that the mean difference for 10^{-2} & NC1 (p = 0.007) is significantly different from zero, which is shown by '**' in the graph.

The limit of detection of ABSTA is indicated in red.

5.4.5 Detection of Streptococci in Spiked Milk Samples with Primer Set LAMPstrep

In this sensitivity experiment, the CFU/ml of the milk aliquot spiked with undiluted *S. uberis* culture of OD_{600} = 1 and its 10-fold dilutions were 2.0×10^7, 2.0×10^6, 2.0×10^5, 2.0×10^4, 2.0×10^3 and 2.0×10^2, respectively. As shown by the melting curves, DNA extracted from concentrated spiked milk corresponding to 2.0×10^7 CFU/ml was successfully amplified by primer set LAMPstrep at 16 min, resulting in peak endpoint fluorescence intensity. In contrast, the time required to amplify DNA templates from milk samples spiked with undiluted and 10-fold diluted culture was extended. The amplification curves of these two groups raised more slowly and ended with respective 58.8% and 35.5% of the fluorescent intensity of the starting group. With increasing

dilutions of the spiking culture, progressively flatter amplification curves were observed in groups corresponding to 10^2-fold, 10^3-fold and 10^4-fold dilutions. The LAMP melting curves remained flat for the PBS control and non-template control, indicating no contamination from streptococci in the unspiked milk and no dimer formation and self-amplify within the primers of LAMPstrep (Figure 23a).

Agarose gel electrophoresis was employed to confirm the amplification of the LAMP assays described above. Consistent with the end-point fluorescence intensities of the LAMP assay, the band corresponding to the starting CFU/ml of 2.0×10^7 displayed the highest brightness at the correct amplicon size of all reactions. This brightness subsequently decreased with the serial 10-fold reduction of CFU/ml in the spiked milk samples. The ladder-like band pattern turned undetectable starting from the LAMP amplicon corresponding to the 10^2-fold dilution, while LAMP products generated from PBS-spiked group and non-template LAMP reaction led to no bands on the agarose gel (Figure 23b).

The above-mentioned LAMP products were subjected to the colorimetric enzymatic assay to detect the difference in OD_{450} resulting from the complementation of the fusion proteins triggered by the binding with the recognition-site-incorporated amplicons. The detected endpoint OD_{450} of the assay corresponding to the initial CFU/ml of 2.0×10^7 reached 63.8% of the positive control. With the decrease of CFU/ml in spiked milk samples, the OD_{450} at 90 min demonstrated a decreasing trend consistent with the endpoint fluorescence intensities in the LAMP experiment. Starting from

the LAMP products corresponding to the 10^2-fold dilution, the signal levels derived from complemented split trehalase proteins were indistinguishable from those of the PBS control and the LAMP non-template control (Figure 23c). Therefore, with LAMP amplicons produced from *S. uberis*-spiked milk samples of CFU/ml ≥ 2.0×10^5, trehalase activity was restored by the complementation of fusion proteins HisTreA-C-SpoIIID and HisTreA-N- SpoIII and generated the detectable signal intensities.

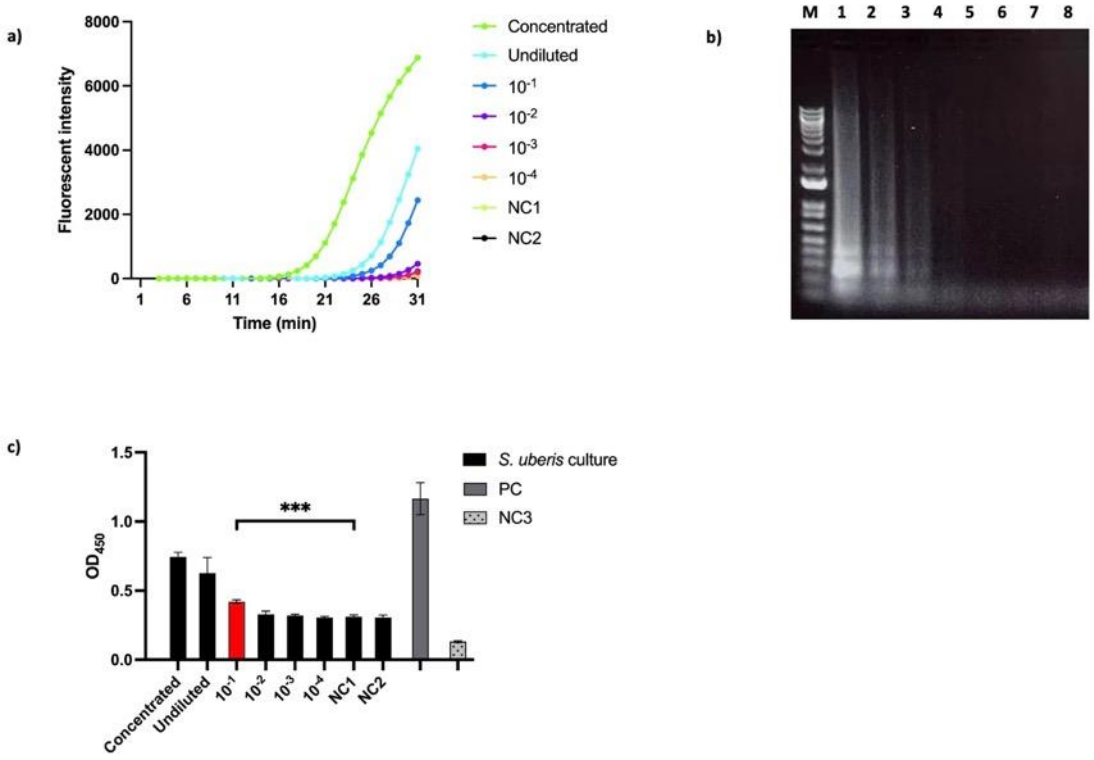

Figure 23. Sensitivity of detection of DNA extracted from *S. uberis*-spiked milk with LAMPstrep followed by ABSTA. (a) LAMP assays using LAMPstaph primer set and DNA extracted from milk aliquots spiked with serial dilutions of *S. uberis* culture at OD_{600} = 1. **(b)**

Agarose gel electrophoresis confirmation of LAMP amplicons of DNA extracted from milk aliquots spiked with concentrated (1), undiluted (2), 10-fold diluted (3), 10^2-fold diluted (4), 10^3-fold diluted (5) and 10^4-fold diluted (6) *S. uberis* culture of OD_{600} = 1 and PBS (NC1) (7) using LAMPstaph primer set with bands in the typical ladder-like pattern. Non-template LAMP product was used as negative control (NC2) (8). 1 Kb DNA ladder was utilized (M). **(c)** ABSTA showing the complementation of fusion proteins HisTreA-N-SpoIIID and HisTreA-C-SpoIIID by LAMP amplicons at different dilutions of *S. uberis* culture of OD_{600} = 1. The absorbance at 450 nm was measured by the spectrophotometer after a 90 min incubation at R/T. The positive control (PC) utilizes the double-stranded DNA dsFF_DG74 as the substrate for binding with fusion proteins. The negative control (NC3) utilizes water instead of DNA substrate. Two-sample t-test was conducted between assays treated with bacterial culture serial dilutions and PBS (NC1) at a 95% confidence level. The resulting *p* values indicate that the mean difference for 10^{-1} & NC1 ($p < 0.001$) is significantly different from zero, which is shown by '***' in the graph. The limit of detection of ABSTA is indicated in red.

5.4.6 Detection of *E. coli* in Spiked Milk Samples with Primer Set LAMPneg

E. coli bacterial culture at OD_{600} = 1 and its 10-fold serial dilutions were utilized for the milk aliquots spiking. Corresponding to undiluted, 10-fold diluted, 10^2-fold diluted, 10^3-fold diluted,

10^4-fold diluted, 10^5-fold diluted, and 10^6-fold diluted bacterial cultures, the CFU/ml in the milk samples were 1.1×10^7, 1.1×10^6, 1.1×10^5, 1.1×10^4, 1.1×10^3, 1.1×10^2 and 11, respectively. The melting curves obtained by LAMP using the above DNA template and the primer set LAMPneg showed that the amplification of the assay corresponding to the starting spiked milk sample of 1.1×10^7 CFU/ml occurred after 10 min (Figure 24a). The time for amplification for subsequent assays increased with increasing dilution fold, resulting in no rise detected corresponding to a spiked milk sample of 11 CFU/ml after 28 min of the reaction. The endpoint fluorescence intensity reached the highest level for the first three dilution series. In contrast, however, starting from the assay corresponding to the 1.1×10^4 CFU/ml, the detected intensity for the remaining dilutions decreased gradually. No amplification was observed from the LAMP non-template control using water, indicating no dimer formation and self-amplify among the components of primer set LAMPneg.

The amplification of the above-mentioned LAMP products was confirmed by agarose gel electrophoresis. The band located at the major amplicon size and the ladder-like pattern of the LAMP amplicons corresponding to undiluted, 10-fold diluted, and 10^2-fold diluted bacterial cultures exhibited the highest brightness (Figure 24b). As the CFU/ml in the spiked milk samples serially decreased, the brightness reduced accordingly. Consistent with the endpoint fluorescence intensity of LAMP assays, the LAMP products obtained from the PBS control and non-template control reactions demonstrated no bands on the gel.

The colorimetric enzymatic assay was applied to measure the signal levels resulting from the complementation of the fusion proteins. The OD_{450} after 90 min incubation for samples corresponding to CFU/ml of 1.1×10^7 and 1.1×10^6 were the highest among all assays, reaching 73.1% and 77.0% of the positive control, respectively (Figure 24c). Nonetheless, the endpoint OD_{450} corresponding to assays on 10^2-fold and 10^6-fold dilutions decreased rapidly as the CFU/ml in the spiked milk samples declined. With the DNA extracted from *E. coli*-spiked milk samples of CFU/ml ≥ 11 (corresponding to 10^6-fold dilution), the fusion proteins HisTreA-C-SpoIIID and HisTreA-N-SpoIII were complemented by the corresponding recognition-site-incorporated LAMP products.

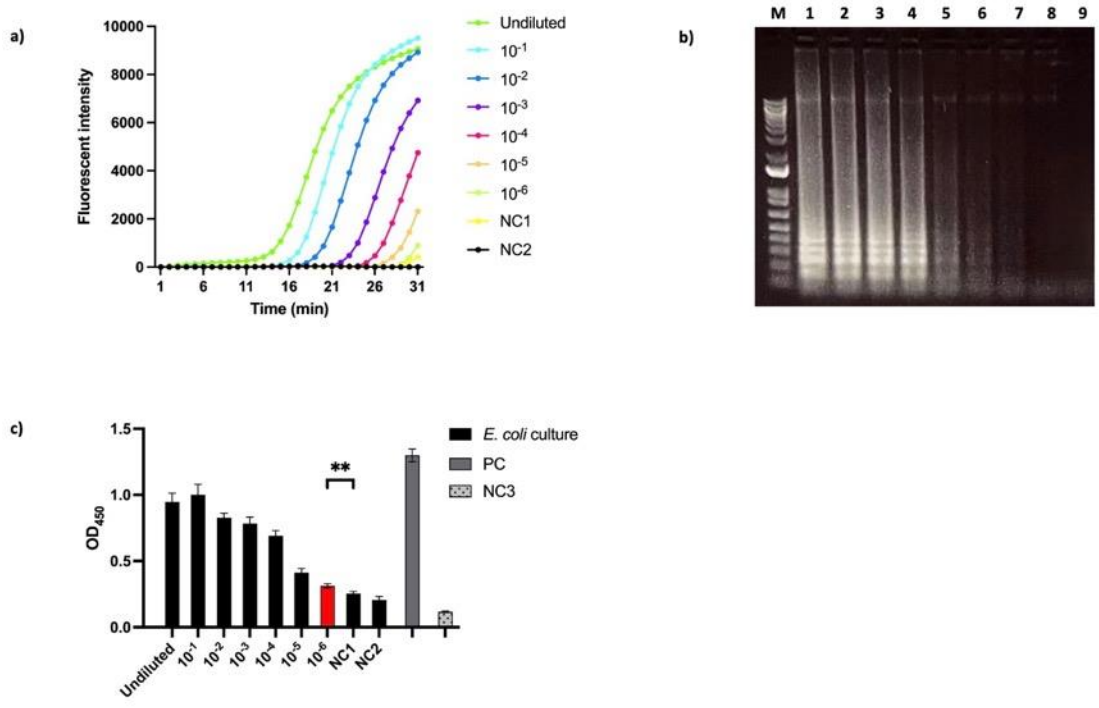

Figure 24. Sensitivity of detection of DNA extracted from *E. coli*-spiked milk with LAMPneg

followed by ABSTA. (a) LAMP assays using LAMPneg primer set and DNA extracted from milk aliquots spiked with serial dilutions of *E. coli* culture at OD_{600} = 1. **(b)** Agarose gel electrophoresis confirmation of LAMP amplicons of DNA extracted from milk aliquots spiked with undiluted (1), 10-fold diluted (2), 10^2-fold diluted (3), 10^3-fold diluted (4), 10^4-fold diluted (5) 10^5-fold diluted (6) 10^6-fold diluted (7) of *E. coli* culture of OD_{600} = 1 and PBS (NC1) (8) using LAMPneg primer set with bands in the typical ladder-like pattern. Non-template LAMP product was used as negative control (NC2) (9). 1 Kb DNA ladder was utilized (M). **(c)** ABSTA showing the complementation of fusion proteins HisTreA-N-SpoIIID and HisTreA-C-SpoIIID by LAMP amplicons at different dilutions of *E. coli* culture of OD_{600} = 1. The absorbance at 450 nm was measured by the spectrophotometer after a 90 min incubation at R/T. The positive control (PC) utilizes the double-stranded DNA dsFF_DG74 as the substrate for binding with fusion proteins. The negative control (NC3) utilizes water instead of DNA substrate. Two-sample t-test was conducted between assays treated with bacterial culture serial dilutions and PBS (NC1) at a 95% confidence level. The resulting p values indicate that the mean difference for 10^{-6} & NC1 (p = 0.006) is significantly different from zero, which is shown by '**' in the graph. The limit of detection of ABSTA is indicated in red.

5.5 Specificity of Detection of Gram Type-Specific LAMP

5.5.1 Specificity of the LAMPstaph Primer Set Evaluated on Genomic DNA Extracted from Multiple Bacterial Cultures

To explore the specificity of the LAMP assay using the LAMPstaph primer set, bacterial gDNA preparations were added to each LAMP reaction at respective 10^6 and 10^3 copies as the template. After a 30 min isothermal incubation, melting curves corresponding to reactions with 10^6 copies of *S. devriesei* and *S. aureus* gDNA raised up at the 11^{th} min and reached the highest fluorescence intensity at the 20^{th} min. On the other hand, successful amplification in the reactions with 10^3 gDNA copies of these two bacteria was detected at the 16^{th} min, ending with their respective highest fluorescence intensities at 26^{th} min. In contrast, no rise in the melting curves was seen for the remaining bacteria at either concentration, indicating that the gDNA of these bacteria was not amplified by LAMPstaph. No amplification occurred in the LAMP non-template control using water, due to the absence of primer dimer formation and self-amplification (Figure 25a).

Results consistent with the LAMP assays were observed in agarose gel electrophoresis. LAMP products corresponding to 10^6 and 10^3 copy numbers of gDNA of *S. devriesei* and *S. aureus* displayed the highest brightness at ladder-like pattern bands and the major amplicon size. LAMP products from the non-template control and other bacteria at both DNA copy numbers showed no

bands on the gel (Figure 25b).

5.5.2 Specificity of the LAMPstrep Primer Set Evaluated on Genomic DNA Extracted from Multiple Bacterial Cultures

Except that the primer set was changed to LAMPstrep, the other experimental setup was the same as the previous experiment. As shown by the LAMP curves, DNA templates corresponding to the two copy numbers of *S. uberis*, *S. dysgalactiae* and *Streptococcus* spp. were amplified by LAMPstrep primer set at the 11^{th} and 16^{th} min, respectively, reaching comparable levels of endpoint fluorescence intensity. On the contrary, the gDNA of the other bacteria failed to be amplified at either copy number, exhibiting melting curves remaining unchanged. No curve was found for the LAMP non-template control as well, indicating no dimer formation within this primer set and no self-amplify (Figure 25c).

The above-mentioned LAMP products were subsequently subjected to gel electrophoresis analysis. Among all the bacteria involved in the experiment, only the six assays corresponding to two copy numbers of streptococcus gDNA showed visible typical ladder-like pattern bands on the agarose gel. The bands for the LAMP product with 10^6 copy numbers were slightly brighter than the 10^3 ones throughout the pattern and at the major amplicon size. The band corresponding to the non-

template control disappeared according to no amplification (Figure 25d).

5.5.3 Specificity of the LAMPneg Primer Set Evaluated on Genomic DNA Extracted from Multiple Bacterial Culture

An identical experimental setup was conducted other than changing the primer set to LAMPneg in this experiment. As demonstrated in the melting curves, the gDNA of 10^6 copies of *E. coli* DH10β, *E. coli*, *Klebsiella* spp. and *Enterobacter* spp. was amplified by the LAMPneg primer set between the 8^{th} and 13^{th} min of the reaction, while the curves for 10^3 copies began to rise at the 18^{th} min, reaching comparable endpoint fluorescence intensities. Seeing from the amplification of the other bacteria, only the gDNA of 10^6 copies of *Corynebacterium* spp. was amplified at the 23^{rd} min by this primer set. Nonetheless, its end-point fluorescence intensity was less than half of the Gram-negative bacteria involved in this LAMP experiment. No dimer formation and self-amplify existed within the LAMPneg prime set due to no amplification for the LAMP non-template control was found (Figure 25e).

Illustrated by the agarose gel electrophoresis, certain brightness was shown in the ladder-like patterns corresponding to the post-amplified LAMP products. However, the brightness of patterns corresponding to 10^3 copies was slightly lower than 10^6 copies in terms of each Gram-negative

bacteria. Consistent with the LAMP curves, the overall brightness of patterns of *Corynebacterium* spp. at 10^6 copies was the lowest. No band was observed for the LAMPneg non-template control (Figure 25f). The specificity of detection of the above-mentioned three primer sets was summarized (Table 2).

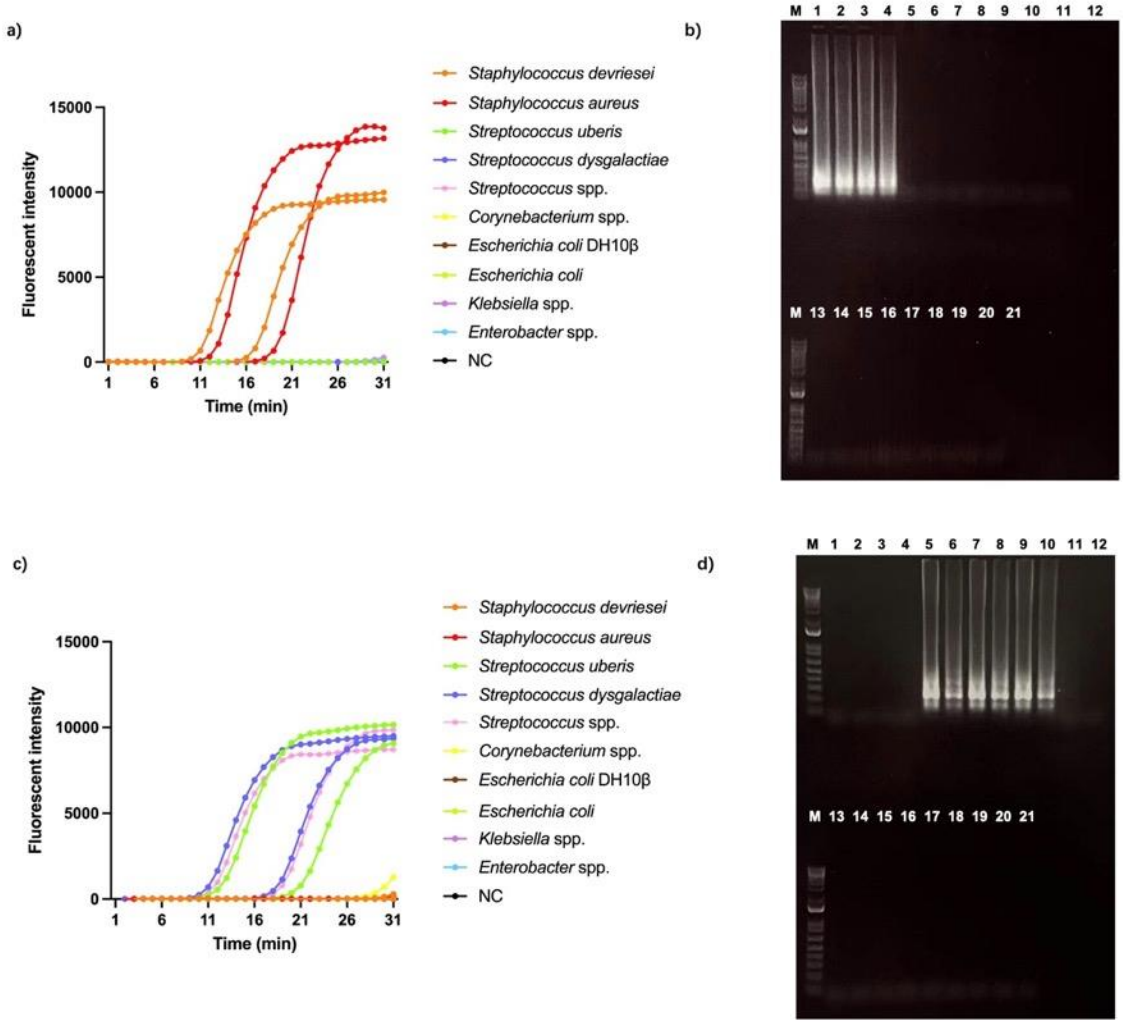

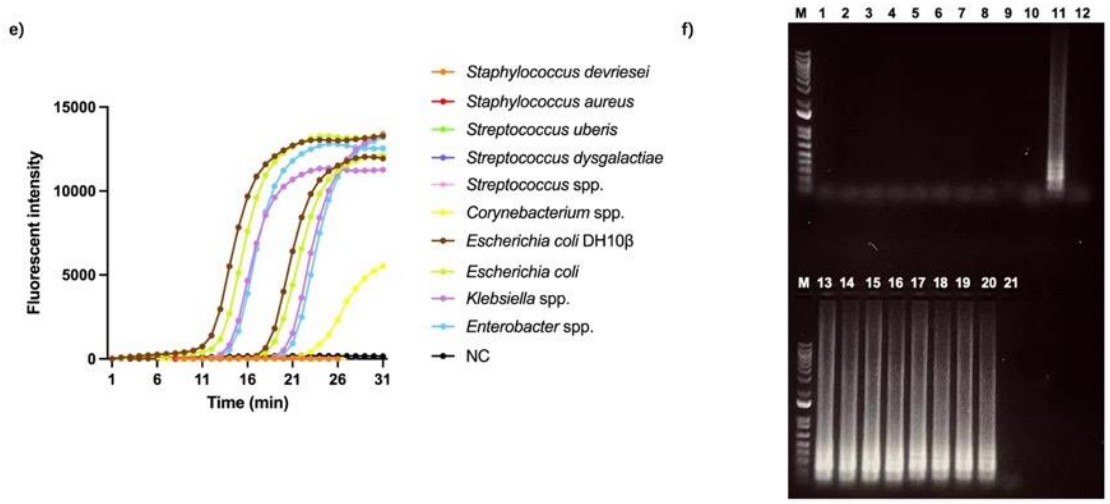

Figure 25. Specificity of detection of Gram-positive and Gram-negative genomic DNA by LAMPstaph, LAMPstrep and LAMPneg. LAMP assays using primer set LAMPstaph **(a)**, LAMPstrep **(c)** and LAMPneg **(e)** on gDNA at copy numbers of 10^6 and 10^3 extracted from multiple bacterial cultures. **(b) (d) (f)** Agarose gel electrophoresis confirmation of LAMP amplicons of gDNA of *S. devriesei* at 10^6 (1), *S. devriesei* at 10^3 (2), *S. aureus* at 10^6 (3), *S. aureus* at 10^3 (4), *S. uberis* at 10^6 (5), *S. uberis* at 10^3 (6), *S. dysgalactiae* at 10^6 (7), *S. dysgalactiae* at 10^3 (8) *Streptococcus* spp. at 10^6 (9), *Streptococcus* spp. at 10^3 (10), *Corynebacterium* spp. at 10^6 (11), *Corynebacterium* spp. at 10^3 (12), *E. coli* DH10β at 10^6 (13), *E. coli* DH10β at 10^3 (14), *E. coli* at 10^6 (15), *E. coli* at 10^3 (16), *Klebsiella* spp. at 10^6 (17), *Klebsiella* spp. at 10^3 (18), *Enterobacter* spp. at 10^6 (19) and *Enterobacter* spp. at 10^3 (20) copies using primer set LAMPstaph, LAMPstrep and LAMPneg with bands in the typical ladder-like pattern. Non-template LAMP was used as negative control (NC) (21). 1 Kb DNA ladder was utilized (M).

Table 2. Summary of the specificity of detection bacterial genomic DNA by three LAMP primer sets.

Bacterial Isolates	Primer Sets					
	LAMPstaph		LAMPstrep		LAMPneg	
	Genomic DNA copy numbers					
	10^6	10^3	10^6	10^3	10^6	10^3
Staphylococcus devriesei 1316	+	+	-	-	-	-
Staphylococcus aureus USA300	+	+	-	-	-	-
Streptococcus uberis 10501290	-	-	+	+	-	-
Streptococcus dysgalactiae 20304478	-	-	+	+	-	-
Streptococcus spp. 10107041	-	-	+	+	-	-
Corynebacterium spp. 40200255	-	-	-	-	+	-
Escherichia coli DH10β	-	-	-	-	+	+
Escherichia coli 10109298	-	-	-	-	+	+
Klebsiella spp. 10116692	-	-	-	-	+	+
Enterobacter spp. 11104490	-	-	-	-	+	+

* '+' indicates successful amplification; '-' indicates no amplification.

6. DISCUSSION

The purpose of this study was to develop Gram type-specific LAMP assays to detect DNA of bovine mastitis causing bacteria by employing the complementation of split-trehalase recombinant proteins. The function validation phase of recombinant split trehalase proteins involved the expression and purification of the respective proteins HisTreA-C-SpoIIID and HisTreA-N-SpoIIID from transformed *E. coli* BL21(DE3) cells, and the condition optimization of binding of fusion proteins with the designed SpoIIID-recognition-sequence-incorporated oligonucleotide and DNA. In a next step, the recognition sequences were introduced in tandem into Gram type-specific PCR primers, and the detection specificity of the conditional complementation of fusion proteins to colony PCR products of derived from bacteria of both Gram types was verified. To develop a detection method of bacterial DNA for point-of-care use, LAMP primer sets specific for *Staphylococcus*, *Streptococcus* and Gram-negative bacteria were designed based on the 16S rRNA genes of common bovine mastitis pathogens with the tandem specific recognition sequences introduced. The three sets of LAMP primers developed were subsequently utilized to amplify DNA extracted from bacterial cultures and spiked milk samples. Excellent detection sensitivity and specificity of the three LAMP assays were established with signals generated by the restoration of trehalase activity in a colorimetric enzymatic assay.

The novel and convenient method we developed is highly sensitive and specific for detecting the gDNA of the common bovine mastitis-causing *Staphylococcus*, *Streptococcus*, and Gram-negative

bacteria. This method preliminarily relies on a novel split trehalase platform through the specific recognition of a consensus sequence by the DNA-binding protein SpoIIID to detect PCR and LAMP amplicons. Essentially, this split trehalase platform is based on the detection of glucose produced by restoring the enzymatic capacity through complementation of split *E. coli* glycolytic enzyme trehalase (TreA). In this study, the glucose signal can reach detectable levels in the colorimetric enzymatic assay within 1.5 h. It has been demonstrated that immunoglobulins, whole pathogens and protein-protein binding and protein aggregation can be identified with high specificity by fusing the split trehalase with sensors with specificity for the corresponding analytes (95). More importantly, the split domains do not self-complement in the absence of analytes. SpoIIID, a transcript regulator during endospore formation process of *Bacillus subtilis*, was shown to bind a conserved DNA with high affinity in a monomeric form (78). The binding of SpoIIID as a monomer is critical in developing our method with regards to avoiding self-complementation of the fusion proteins, which contributed to the selection of SpoIIID among other choices of DNA-binding proteins. The above-mentioned study has demonstrated that split TreA is capable of complementing due to dimerization of the TreA fragments fused to analyte-sensing elements (protein-protein binding) (95). Therefore, in the case that no DNA substrate was added to the colorimetric assay of our study, self-complementation of split TreAs did not take place, because the fused SpoIIID remained as monomers. Based on this characteristic, the combination of split TreA platform and SpoIIID can be used to detect the added amplicons with SpoIIID specific recognition sequences incorporated, indicating presence or absence through the glucose signals generated by the conditional recovery of the trehalase capacity. The novelty of this combination

includes: (i) the complementation of split enzymes is triggered by the specific recognition of DNA-binding proteins to DNA, showing an overall specificity of the fusion protein reagents; (ii) the target analytes are DNA amplicons harboring specific recognition sequences in tandem, boosting the accuracy for the identification of common bovine mastitis-causing Gram-positive and Gram-negative bacteria at a molecular level; (iii) the released glucose can be detected within a short incubation time. Moreover, the glucose signal is very compatible with the existing glucometer on the market which is portable and compact, enhancing the potential for further development of this combination as point-of-care detection.

The sensitivity of detection of Gram type bacteria gDNA by three designed LAMP primer sets was validated with gDNA 10-fold serial dilutions along with the signals observed in ABSTA. It was seen that the undiluted gDNA could be amplified by the corresponding LAMP primer set within 10 min of the reaction and then reached the fluorescence intensity plateau (Figure 19a, 20a, 21a). Even with the 10^6-fold dilutions, the assays for the three primer sets yielded considerable amplicons, which was indicated by the comparable ABSTA signals with the positive control using double-stranded dsFF_DG74 as well (Figure 19c, 20c, 21c). It was noted that for the last dilution (whereby the gDNA copy number was estimated to be less than 10), the ABSTA signals corresponding to LAMPstrep and LAMPneg showed a dramatic drop with larger error bars. This might be due to no gDNA or few gDNA being added in one or two repeats of the triplicate. Therefore, based on the ABSTA results of the gDNA-based sensitivity test, the detection limits of LAMPstaph, LAMPstrep and LAMPneg for gDNA copy numbers correspond to 10^7-fold dilution,

10^6-fold dilution and 10^6-fold dilution, respectively.

Based on sensitivity tests of three LAMP assays using DNA extracted from bacteria-spiked milk, the minimum time required for amplification initialization was greatly extended compared to detection of gDNA. In the starting assays (milk with 10^7 CFU/ml of bacteria) using LAMPstaph and LAMPstrep, the exponential amplification required more than 16 min to start (Figure 22a, 23a). Such observations might be due to the inhibition of the LAMP, insufficient yield or purity of bacterial DNA by the extraction methods, or cell lysis difficulty of Gram-positive and Gram-negative bacteria. Previously, it has been demonstrated that bacterial DNA in spiked milk was mainly recovered from the milk pellet with some appearing in the fat fraction, which was confirmed by culturing different milk fractions on selective media and qPCR results (101). This distribution was caused by the aggregation of bacterial cells with milk fat globules, which could be observed in milk inoculated with both Gram-positive and Gram-negative bacteria but with a varying adhesion affinity by bacterial species (102-104). The presence of bacterial cells in the milk fat fraction could partly explain the longer amplification time for spiked milk DNA in this study since the fat layer was discarded during the DNA extraction procedure, which could have resulted in the partial loss of target bacterial DNA. Therefore, as the dilution of the bacterial culture increased, the amount of spiking bacteria in the cell pellet decreased, resulting in the signal disappearance from the LAMP assays corresponding to 10^2 or 10^3-fold culture dilutions (Figure 22a, 23a). Nonetheless, considering that DNA extraction efficiency was affected by milk fat which also severely interfered with pipetting operations, it was reasonable to abandon the fat layer in this

study (105).

In addition, the reduced sensitivity of the LAMP assay using DNA extracted from milk samples might be due to the presence and accumulation of inhibitors from milk in the eluted DNA products (106). Although LAMP was demonstrated to be more robust and more resistant to inhibitory agents than conventional PCR, it was noted that calcium ions in milk could enhance the inhibitory effect (107-110). This can be explained by the role of magnesium in the LAMP reaction. The activity of *Bst* DNA polymerase is affected by the divalent magnesium ions which facilitates the efficiency of incorporation of dNTPs and primer during polymerization. However, since they both are divalent cations, residual calcium ions in the DNA eluate might compete with magnesium ions to interfere with the magnesium-DNA polymerase interaction, resulting in the overall amplification reaction being suppressed (107). Other inhibitors present in milk that affected DNA amplification could be protein and fat, but the addition of chloroform-phenol and proteinase K should have led to their removal and degradation in the DNA extraction protocol of this study (111). The lipids could be released from the milk fat globules into the cell pellet by a shear force caused by a too high centrifugation speed (> 10,000 *g*) (106). However, it was reported that fat has a minor inhibitory effect on nucleic acid amplification, and the centrifugation speed used in the milk fractions separation step in this study was 6,700 *g* which should have prevented the rupture of milk fat globules (112). Therefore, in terms of the inhibitory agents, proteins and fats were not presumed to be responsible for the reduced amplification of the three LAMP assays using spiked-milk DNA.

The limited sensitivity of the above-mentioned three LAMP experiments could be resulting from the choice of method for DNA extraction. In this study, the phenol-chloroform method was employed based on a slight modification of the classical method (113). The addition of organic solvents aided in the removal of proteins and other cellular residues prior to DNA purification and ethanol was used to precipitate the DNA. However, assessment of the relative performance of DNA extraction protocols was determined by the final DNA yield, purity, and ability to remove inhibitors for subsequent molecular studies. It is worth mentioning that the 260/280 nm ratio measured by spectrophotometer for the extracted DNA (data not shown) was within the standard ratio range, indicating that protein impurities in milk and bacteria were effectively removed by the phenol-chloroform method. In contrast, the measured 260/230 nm ratio (data not shown) was constantly lower than the standard ratio, indicating that the DNA elutes were not thoroughly purified with chemical reagent contamination existing (114). Such measurement could be explained by the reagents used in the phenol-chloroform method combined with the inhibition presented in three LAMP assays. EDTA in the lysis buffer could have chelated magnesium, forming a complex and affecting the DNA polymerase activity; phenol existing in the organic solvent mixture could have hydrogen-bonded with the enzyme molecule, or denatured the polymerase; ethanol and isopropanol could have clumped DNA molecules (115). The presence of SDS, an ionic detergent, in the eluates could have contributed to the inhibition of polymerase activity as well (116). However, the nonionic surfactant Triton X-100, which was utilized instead of SDS in a study by Quigley et al., reported to cause PCR inhibition only at relative excess (116-117). In addition, in order to improve the efficiency of DNA precipitation by ethanol, sodium

acetate was used in the DNA extraction method described by Quigley et al. (117), which could be introduced in the phenol-chloroform method for further achieving an increase DNA yield.

A significant challenge was encountered in lysing Gram-positive bacteria to release sufficient target DNA, which could explain the difference in the amplification time delay of the two bacterial Gram types (Figure 22a, 23a, 24a). Compared with Gram-negative bacteria, the peptidoglycan layer on the cell wall of Gram-positive bacteria is thicker and more extensive in cross-linking (118-119). As a result, the cell wall of Gram-positive bacteria has higher strength and rigidity, making it more difficult for intracellular DNA release. Although the recommended bead-beating step was incorporated to mechanically break down the bacterial cell wall by shaking at a high speed in the presence of zirconium beads, the LAMP results continued to indicate a low yield of the targeted DNA from Gram-positive bacteria (120). In addition, in an attempt to improve the effect of enzymatic lysis on DNA release, we added lysozyme, lysostaphin and mutanolysin, which are capable of disrupting the peptidoglycan structure, to the cell pellet resuspension at the respective recommended concentrations (117, 121-122). Lysozyme is used for cell lysis of both Gram-positive and Gram-negative bacteria, while lysostaphin and mutanolysin are used to break down the cell wall of *Staphylococcus* and *Streptococcus*, respectively. Surprisingly, the subsequent LAMP assays with DNA extracted by this modified protocol were not improved (data not shown). This suggests that more combinations of different concentrations and working conditions of these three enzymes could be tested further, or that other enzymes or agents assisting cell lysis could be employed. Moreover, a boiling step could be applied before the addition of enzymes, which would

perhaps more effectively disrupt the cell wall of Gram-positive microorganisms as previously reported with respect to spiked-milk DNA extraction of both Gram types of bacteria (123-124).

To date, a number of commercial and non-commercial methods for DNA extraction from (bacterial-spiked) milk have been compared, with evaluation criteria related to the quality and yield of the isolated DNA and success in generating target bacterial amplicons (113, 117). In the present study, the pathogens were successfully detected in LAMP assays following the phenol-chloroform extraction method. However, it was noticed that the target DNA failed to be detected when pathogen levels in milk were relatively high, especially for the Gram-positive bacteria (10^3 CFU/ml of *S. devriesei* in milk; 10^4 CFU/ml of *S. uberis* in milk) (Figure 22a, c; 23a, c). Moreover, the long duration and limited repeatability of this DNA extraction method were deemed problematic. For example, when transferring the upper aqueous phase, the sandwiched protein layer was easily aspirated, resulting in inconsistent protein contamination control in different batches of DNA preparations.

In contrast, several commercial DNA extraction kits have been reported to achieve a certain balance between DNA yield, purity, molecular amplification, and labor requirements. These kits included QIAprep Spin Miniprep kit (Qiagen), DNeasy Blood and Tissue kit (Qiagen), SmartHelix First DNAid kit (ExVivon), Milk Bacterial Isolation kit (Norgen Biotek) and PowerFood™ Microbial DNA Isolation kit (MoBio Laboratories). Among them, the PowerFood™ Microbial DNA Isolation kit was shown to efficiently extract high-quality and high-purity DNA from two

Gram-type bacteria from spiked raw milk and lead to robust amplification of target gene templates in real-time PCR (113, 117). Due to time constraints, the testing of more single DNA extraction methods or the combinations of multiple methods was not realized in this study. Nonetheless, these strategies will be part of further development to optimize the extraction of high-quality DNA from bacteria-spiked milk.

The 16S rRNA gene consists of highly conserved regions flanked by variable regions (125). This fits well with our need for bacterial Gram-type identification. We designed universal primers based on conserved regions of the 16S rRNA genes with sufficient homology among but also enough differences between Gram-positive and Gram-negative bovine mastitis bacteria to minimize the number of primers required for the entire assay and ease the labor of LAMP reagents preparation. This is in contrast to other genus or species specific target genes, such as the *nuc* gene specific for *S. aureus*, the *PhoA* gene specific for *E. coli*, and the *UreD* gene specific for *K. pneumoniae*, which also have been employed in LAMP assays for detecting specific mastitis causative bacteria (126-127). The designed LAMP primer sets LAMPstaph, LAMPstrep and LAMPneg successfully discriminated 10 isolates of bovine mastitis pathogens in the specificity evaluation assays (Figure 25). With the inclusion of both a high copy number and a low copy number in the specificity experiments, the LAMP assay was negative when the non-specific gDNA was at a high copy number while the LAMP assay was positive when the specific gDNA was at a low copy number. Thus, the specificity of a single primer set to detect the corresponding bacteria was validated. Furthermore, the observed time required for specific gDNA amplification at both copy numbers

was consistent with the sensitivity test results of the gDNA-based LAMP assays. However, different from other primer sets, LAMPneg unexpectedly initiated amplification after 23 min for the gDNA of *Corynebacterium* spp. at the copy number of 10^6. Although this time was even later than that of the reactions using Gram-negative bacteria gDNA at 10^3 copies, the *Corynebacterium* spp. amplicons resulted in a lighter but detectable band on the subsequent agarose gel (Figure 25e, f). This exception was likely due to the fact that the *Corynebacterium* spp. were not considered in the 16S rRNA gene alignments when designing the three LAMP primer sets, resulting in the consensus for LAMPneg primers to have some binding affinity for the C*orynebacterium* spp. 16S rRNA gene sequence. Nevertheless, considering the maximal bacterial count for mastitis milk caused by *Corynebacterium* spp. was less than 10^5 CFU/ml, the level of gDNA found in the milk infected by this organism would be unlikely detected by LAMPneg in practice (128). Therefore, according to the amplification, the specificity of three proposed LAMP primer sets to detect gDNA of *Staphylococcus*, *Streptococcus* and Gram-negative bacteria were reliable. Further optimization for the detection specificity could include incorporating the 16S rRNA gene sequences of more pathogenic genes into the alignments for primer set design and using additional PCR reagents, such as DMSO, which was demonstrated to reduce non-specific LAMP amplification at low concentrations (129).

The proposed methodology combining DNA extraction, LAMP assay, and ABSTA successfully displayed high sensitivity and specificity for detecting target pathogens. However, like other similar studies, our method undoubtedly has limitations for our long-term goal of developing field-

oriented diagnostics (126). The complete procedure is time-consuming, requiring sophisticated experimental instruments and skilled personnel, especially when dealing with large-scale samples. For the purpose of on-farm use, some studies have provided new ideas for simplification of DNA extraction steps and more accessible storage and preparation of LAMP reaction reagents. In a published study of 2021 by Sivaprasad et al., tissue sample was slightly treated with lysis buffer and subjected to heating and centrifugation, with the resulting supernatant being directly used as the DNA template (130). Then, they optimized the LAMP reaction through adjusting the concentration of $MgSO_4$, dNTPs, the concentration ratio between inner primers, outer primers and loop primers, operating temperature and selecting another dye that indicated amplification. In addition, processed LAMP reagents (excluding *Bst* DNA polymerase) were demonstrated to retain activity after storage at room temperature after lyophilization, while a more recent study further indicated that the addition of sucrose in premixed LAMP reagents stabilized *Bst* DNA polymerase activity at room temperature, without the requirement for cold storage or freeze-dryer operation (131-132). The simplification of our methodology could be inspired by this single-step DNA extraction, customized LAMP assay, and optimized reagents preparation. More ideally, our proposed ABSTA and LAMP are expected to be integrated in one reaction using a closed tube LAMP technique, which is not only for a more convenient on-farm testing but also for avoiding the false positive results resulted from the LAMP products cross contamination (133). Notably, LAMP assays were all performed at 65ºC in our study. However, this operating temperature could be further reduced to 40ºC by applying phosphorothioate modification onto LAMP inner primers to reduce the thermal stability of the terminus extended dsDNA intermediates, with similar

sensitivity as operating at 65ºC (134). These reports offer opportunities for further optimizing our methodology combining ABSTA and LAMP, to make it a simpler, less time-consuming and highly cost-effective field-compatible diagnosis method.

Alternatives that enable visualization of LAMP results could be to use real-time PCR machine, turbidity measurement and UV fluorescence. The real-time PCR machine is used to confirm the identity of the amplified product based on the intercalation SYBR in double-stranded DNA and its resulting fluorescence. The turbidity of positive products can be evaluated by the naked eye or a turbidimeter. UV light excites the added dyes to exhibit distinguishable colors (135). The former two require specific laboratory equipment as it is difficult to distinguish by the naked eye when the contrast between the product and the background is minimal, which is not suitable for on-site testing. Prolonged exposure to UV light is also harmful to health (136). However, the signal readout of our ABSTA is derived from the specific binding of split enzyme fusion proteins and LAMP products, which strengthens the specificity of the detection. Currently, ABTSA requires a spectrophotometer for readouts, but the glucose signal it produces is very compatible with commercially available glucometers, which offers the potential for simple on-site quantification of the results using this technology. To solve the dependence on sophisticated equipment, some visualization methods employ LED light instead of UV light, and a novel detection of FAM- and biotin-labelled LAMP amplicons was reported (126, 133). Other methods to improve the POC detection of LAMP amplifications, including improvements to ABSTA, are bound to be developed.

In terms of combining ABSTA with PCR, the amplification specificity of Gram type-specific PCR primer pairs incorporated with SpoIIID-specific recognition sites in tandem was validated by colony PCR of *S. devriesei* and *E. coli* at the first step, with non-specific amplification eliminated by setting up a gradient of annealing temperature (Figure 13). A high signal level was obtained in ABSTA with the purified PCR product, while it decreased as expected with a decreasing product adding volume (Figure 14, 15). In contrast, the highest ABSTA signal obtained with the unpurified PCR product was around 50% of the purified one (Figure 15, 17). This finding indicated inhibition of ABSTA, and EDTA was employed in subsequent experiment to counter it. Since the binding of the fusion proteins HisTreA-C-SpoIIID and HisTreA-N-SpoIIID to DNA substrates is sensitive to the salt concentration of the reaction, changes in the salt concentration by other positively charged ions was assumed to be the reason for the inhibition. Given that the divalent magnesium ions were presented in PCR reagents, they were inferred to be an inhibitor of ABSTA with unpurified PCR products. EDTA, a widely used chelator for magnesium, was tested at concentrations of 0.1 mM to 0.5 mM in ABSTA with dsFF_DG74 DNA fragments and unpurified PCR products (Figure 16, 18). The addition of EDTA greatly enhanced the complementation of the dsFF_DG74-involved fusion proteins, which was surprisingly not observed in the unpurified product-involved reactions. A reasonable illustration for this difference could be that the inhibition of ABSTA by the unpurified PCR products might be caused systematically by one or more unknown inhibitors, even though the chelation of magnesium ions by EDTA indeed facilitated the complementation of split trehalase proteins when DNA substrate was present.

Although the positive results detected with ABSTA in this study validated the performance of recombinant split trehalase proteins in binding to DNA substrates and self-complementation, it was challenging to design the purification scheme for these proteins at the beginning of the project. After testing on-bench purification at native and denaturing conditions but failing to show high protein purity by SDS-PAGE, we turned to ÄKTA™ Go system, a compact liquid chromatography system for routine protein purification. The most considerable improvement of using this system was the significant increase in eluted protein yield. The subsequent dialysis protocol for refolding denatured proteins in high concentrations of guanidinium chloride was modified as well. The replacement frequency of the dialysis membrane was determined to be every 4-6 hr because protein aggregates blocked the diffusion pores. However, it is noted that the repeatability of the concentration and purity of the correctly refolded proteins was limited due to the high aggregation rate. Another alternative approach could have been using step-wise dialysis with high, moderate and low denaturant concentrations to alleviate the rapid protein aggregation and misfolding in one-step dialysis (137). In addition, the dialysis equipment could be another considerable factor affecting refolding efficiency. Using a commercial dialysis cylinder (dialysis sack) or dialysis cassette could have been a way to reduce the formation of aggregates (138).

Through testing the salt concentrations, the ratio of DNA substrates versus split trehalase fusion proteins, the orientation of tandem recognition sites, and the length of the linker between binding sites, conditions required for the complementation of fusion proteins HisTreA-C-SpoIIID and HisTreA-N-SpoIIID in the colorimetric enzymatic assay were optimized. Salt concentration was

considered critical to determining the specificity of protein-DNA binding to form site-specific complexes, and nonspecific binding increases at low salt concentrations (139-140). Therefore, the specific binding involved the hairpin-forming oligonucleotide ABABspoIIID and the non-specific involved the control oligonucleotide ABABcont were compared at a salt concentration gradient from 0 to 600 mM (Figure 5). It was noted that hairpin-formed ABABcont did not demonstrate non-specific binding to the fusion proteins in the salt concentration range tested in the experiments. However, 600 mM was identified as optimal molar concentration of NaCl for the protein-DNA specific binding by salt titration testing, at which the complementation of split proteins exhibited the highest activity (Figure 6). Another indispensable condition for achieving the best recovery of trehalase enzymatic activity was the molar ratio of fusion proteins to DNA substrate, which was finally determined to be 1:0.4 (Figure 7). Such signal changes could be explained by the assumption that when the DNA substrate concentration is very low, only limited DNA can bind to the fusion proteins, resulting in a low signal intensity generated by complementation. As the added DNA substrate increases, the binding of paired split enzyme fusion proteins to the same DNA increases until a dynamic equilibrium is reached, where the complementation could produce the maximal restoration of enzyme activity. As the concentration of DNA substrate continues to rise, this equilibrium is disrupted, lowering the possibility of binding two paired protein reagents on the same DNA molecule. Furthermore, oligonucleotide variants testing, and linker length testing allowed the subsequent tandem incorporation of recognition sequences to the Gram type-specific PCR primer pairs and LAMP primer sets in a reliable manner.

7. CONCLUSION

We determined the optimal salt concentration, protein reagents versus DNA substrate ratio, direction and linker length of tandem recognition sites required for split trehalase fusion proteins HisTreA-C-SpoIIID and HisTreA-N-SpoIIID to specifically bind to DNA substrate. This specific protein-DNA binding was further applied as Gram-type specific detecting method of purified colony PCR products by incorporating recognition sites to Gram-type specific primer pairs. By incorporating recognition sequences in *Staphylococcus*, *Streptococcus* and Gram-negative bacteria-specific LAMP primer sets, high specificity of detecting gDNA of these bacteria was demonstrated by these three respective LAMP assays. Promising sensitivity on gDNA detection was observed by combining LAMP assays with ABSTA fusion protein detection; with less desirable sensitivity when DNA was extracted from bacteria-spiked milk samples due to challenges with the DNA extraction from milk samples. Nevertheless, the milk DNA extraction method and LAMP operating requirements (e.g., reagents storage, running temperature) in this study could be continuously improved to enhance the potential of developing an accurate, rapid and user-friendly on-farm diagnostic method for either specific mastitis pathogens or for discrimination of IMI with Gram-positive or Gram-negative bacteria.

8. REFERENCES

1. Seegers, H., Fourichon, C., & Beaudeau, F. (2003). Production effects related to mastitis and mastitis economics in dairy cattle herds. *Veterinary Research*, *34*(5), 475-491.

2. De Vliegher, S., Fox, L. K., Piepers, S., McDougall, S., & Barkema, H. W. (2012). Invited review: Mastitis in dairy heifers: Nature of the disease, potential impact, prevention, and control. *Journal of Dairy Science*, *95*(3), 1025-1040.

3. Ruegg, P. L. (2017). A 100-Year Review: Mastitis detection, management, and prevention. *Journal of Dairy Science*, *100*(12), 10381-10397.

4. Kuang, Y., Tani, K., Synnott, A. J., Ohshima, K., Higuchi, H., Nagahata, H., & Tanji, Y. (2009). Characterization of bacterial population of raw milk from bovine mastitis by culture-independent PCR–DGGE method. *Biochemical Engineering Journal*, *45*(1), 76-81.

5. Contreras, G. A., & Rodríguez, J. M. (2011). Mastitis: comparative etiology and epidemiology. *Journal of Mammary Gland Biology and Neoplasia*, *16*(4), 339-356.

6. Radostits, O.M., Gay, C.C., Blood, D.C. & Hinchcliff, K.W. (2000) Bovine mastitis. *Veterinary Medicine: A Textbook of the Diseases of Cattle, Sheep, Pigs, Goats and Horses.* Elsevier Health

Sciences.

7. Riekerink, R. O., Barkema, H. W., Kelton, D. F., & Scholl, D. T. (2008). Incidence rate of clinical mastitis on Canadian dairy farms. *Journal of Dairy Science*, *91*(4), 1366-1377.

8. Dmitriev, A., Bhide, M., & Mikula, I. (2006). cpn60 gene-based multiplex-PCR assay for simultaneous identification of Streptococcal species. *Acta Veterinaria Brno*, *75*(2), 235-240.

9. Levison, L. J., Miller-Cushon, E. K., Tucker, A. L., Bergeron, R., Leslie, K. E., Barkema, H. W., & DeVries, T. J. (2016). Incidence rate of pathogen-specific clinical mastitis on conventional and organic Canadian dairy farms. *Journal of Dairy Science*, *99*(2), 1341-1350.

10. Graber, H. U., Casey, M. G., Naskova, J., Steiner, A., & Schaeren, W. (2007). Development of a highly sensitive and specific assay to detect Staphylococcus aureus in bovine mastitic milk. *Journal of Dairy Science*, *90*(10), 4661-4669.

11. De Buck, J., Ha, V., Naushad, S., Nobrega, D. B., Luby, C., Middleton, J. R., ... & Barkema, H. W. (2021). Non-aureus Staphylococci and bovine udder health: current understanding and knowledge gaps. *Frontiers in Veterinary Science*, *8*, 360.

12. Koivula, M., Pitkälä, A., Pyörälä, S., & Mäntysaari, E. A. (2007). Distribution of bacteria and

seasonal and regional effects in a new database for mastitis pathogens in Finland. *Acta Agriculturae Scand Section A*, *57*(2), 89-96.

13. Oliveira, L., Hulland, C., & Ruegg, P. L. (2013). Characterization of clinical mastitis occurring in cows on 50 large dairy herds in Wisconsin. *Journal of Dairy Science*, *96*(12), 7538-7549.

14. Riekerink, R. O., Barkema, H. W., Kelton, D. F., & Scholl, D. T. (2008). Incidence rate of clinical mastitis on Canadian dairy farms. *Journal of Dairy Science, 91*(4), 1366-1377.

15. Du Preez, J. H. (2000). Bovine mastitis therapy and why it fails: continuing education. *Journal of the South African Veterinary Association, 71*(3), 201-208.

16. Du Preez, J. H. (1989). Reasons why mastitis therapy is unsuccessful. *South African Journal of Dairy Science.*

17. Bhutto, A. L., Murray, R. D., & Woldehiwet, Z. (2012). California mastitis test scores as indicators of subclinical intra-mammary infections at the end of lactation in dairy cows. *Research in Veterinary Science, 92*(1), 13-17.

18. Cheng, W. N., & Han, S. G. (2020). Bovine mastitis: risk factors, therapeutic strategies, and alternative treatments—A review. *Asian-Australasian Journal of Animal Sciences, 33*(11), 1699.

19. Ganda, E. K., Bisinotto, R. S., Lima, S. F., Kronauer, K., Decter, D. H., Oikonomou, G., ... & Bicalho, R. C. (2016). Longitudinal metagenomic profiling of bovine milk to assess the impact of intramammary treatment using a third-generation cephalosporin. *Scientific Reports, 6*(1), 1-13.

20. Barlow, J. (2011). Mastitis therapy and antimicrobial susceptibility: a multispecies review with a focus on antibiotic treatment of mastitis in dairy cattle. *Journal of Mammary Gland Biology and Neoplasia, 16*(4), 383-407.

21. Hossain, M. K., Paul, S., Hossain, M. M., Islam, M. R., & Alam, M. G. S. (2017). Bovine mastitis and its therapeutic strategy doing antibiotic sensitivity test. *Austin J Vet Sci Anim Husb, 4*(1), 1030.

22. Erskine, R. J. (2020). Mastitis in Cattle. *MSD Vet Manual. https://www.msdvetmanual.com/reproductive-system/mastitis-in-large-animals/mastitis-in-cattle [last modified May 2020].*

23. Rainard, P., Foucras, G., Fitzgerald, J. R., Watts, J. L., Koop, G., & Middleton, J. R. (2018). Knowledge gaps and research priorities in Staphylococcus aureus mastitis control. *Transboundary and Emerging Diseases, 65*, 149-165.

24. Wilson, C. D., Agger, N., Gilbert, G. A., Thomasson, C. A., & Tolling, S. T. (1986). Field trials with cefoperazone in the treatment of bovine clinical mastitis. *The Veterinary Record, 118*(1), 17-19.

25. EFSA Panel on Biological Hazards (BIOHAZ), Ricci, A., Allende, A., Bolton, D., Chemaly, M., Davies, R., ... & Herman, L. (2017). Risk for the development of Antimicrobial Resistance (AMR) due to feeding of calves with milk containing residues of antibiotics. *EFSA Journal, 15*(1), e04665.

26. Koskinen, M. T., Wellenberg, G. J., Sampimon, O. C., Holopainen, J., Rothkamp, A., Salmikivi, L., ... & Pyörälä, S. (2010). Field comparison of real-time polymerase chain reaction and bacterial culture for identification of bovine mastitis bacteria. *Journal of Dairy Science, 93*(12), 5707-5715.

27. Ganda, E. K., Bisinotto, R. S., Decter, D. H., & Bicalho, R. C. (2016). Evaluation of an on-farm culture system (Accumast) for fast identification of milk pathogens associated with clinical mastitis in dairy cows. *PloS One*, *11*(5), e0155314.

28. Ashraf, A., Imran, M., Yaqub, T., Tayyab, M., Shehzad, W., Mingala, C. N., & Chang, Y. F. (2018). Development and validation of a loop-mediated isothermal amplification assay for the detection of Mycoplasma bovis in mastitic milk. *Folia Microbiologica, 63*(3), 373-380.

29. Ashraf, A., & Imran, M. (2018). Diagnosis of bovine mastitis: from laboratory to farm. *Tropical Animal Health and Production, 50*(6), 1193-1202.

30. Harmon, R. J. (1994). Physiology of mastitis and factors affecting somatic cell counts. *Journal of Dairy Science, 77*(7), 2103-2112.

31. Viguier, C., Arora, S., Gilmartin, N., Welbeck, K., & O'Kennedy, R. (2009). Mastitis detection: current trends and future perspectives. *Trends in Biotechnology, 27*(8), 486-493.

32. Sargeant, J. M., Leslie, K. E., Shirley, J. E., Pulkrabek, B. J., & Lim, G. H. (2001). Sensitivity and specificity of somatic cell count and California Mastitis Test for identifying intramammary infection in early lactation. *Journal of Dairy Science, 84*(9), 2018-2024.

33. Muhammad, G., Naureen, A., Asi, M. N., & Saqib, M. (2010). Evaluation of a 3% surf solution (surf field mastitis test) for the diagnosis of subclinical bovine and bubaline mastitis. *Tropical Animal Health and Production, 42*(3), 457-464.

34. Smolenski, G., Haines, S., Kwan, F. Y. S., Bond, J., Farr, V., Davis, S. R., ... & Wheeler, T. T. (2007). Characterisation of host defence proteins in milk using a proteomic approach. *Journal of Proteome Research, 6*, 207-215.

35. De Vliegher, S., Fox, L. K., Piepers, S., McDougall, S., & Barkema, H. W. (2012). Invited review: Mastitis in dairy heifers: Nature of the disease, potential impact, prevention, and control. *Journal of Dairy Science, 95*(3), 1025-1040.

36. Wichmann, F., Udikovic-Kolic, N., Andrew, S., & Handelsman, J. (2014). Diverse antibiotic resistance genes in dairy cow manure. *MBio, 5*(2), e01017-13.

37. Ganda, E. K., Bisinotto, R. S., Decter, D. H., & Bicalho, R. C. (2016). Evaluation of an on-farm culture system (Accumast) for fast identification of milk pathogens associated with clinical mastitis in dairy cows. *PloS One*, *11*(5), e0155314.

38. Lago, A., & Godden, S. M. (2018). Use of rapid culture systems to guide clinical mastitis treatment decisions. *Veterinary Clinics: Food Animal Practice*, *34*(3), 389-412.

39. Graber, H. U., Casey, M. G., Naskova, J., Steiner, A., & Schaeren, W. (2007). Development of a highly sensitive and specific assay to detect Staphylococcus aureus in bovine mastitic milk. *Journal of Dairy Science*, *90*, 4661-4669.

40. Koskinen, M. T., Wellenberg, G. J., Sampimon, O. C., Holopainen, J., Rothkamp, A., Salmikivi, L., ... & Pyörälä, S. (2010). Field comparison of real-time polymerase chain reaction and bacterial culture for identification of bovine mastitis bacteria. *Journal of Dairy Science*, *93*(12), 5707-5715.

41. Martins, S. A., Martins, V. C., Cardoso, F. A., Germano, J., Rodrigues, M., Duarte, C., ... & Freitas, P. P. (2019). Biosensors for on-farm diagnosis of mastitis. *Frontiers in Bioengineering and Biotechnology*, 186.

42. Zhao, Y., Chen, F., Li, Q., Wang, L., & Fan, C. (2015). Isothermal amplification of nucleic acids. *Chemical Reviews, 115*(22), 12491-12545.

43. Zou, Y., Mason, M. G., & Botella, J. R. (2020). Evaluation and improvement of isothermal amplification methods for point-of-need plant disease diagnostics. *PloS One, 15*(6), e0235216.

44. Cornelissen, J. B. W. J., De Greeff, A., Heuvelink, A. E., Swarts, M., Smith, H. E., Van der Wal, F. J., & 1Health4Food—Dutch Mastitis Diagnostics Consortium. (2016). Rapid detection of Streptococcus uberis in raw milk by loop-mediated isothermal amplification. *Journal of Dairy Science*, *99*(6), 4270-4281.

45. Lee, P. L. M. (2017). DNA amplification in the field: Move over PCR, here comes LAMP. *Molecular Ecology Resources, 17*(2), 138-141.

46. Nagamine, K., Hase, T., & Notomi, T. J. M. C. P. (2002). Accelerated reaction by loop-mediated isothermal amplification using loop primers. *Molecular and Cellular Probes, 16*(3), 223-229.

47. Ashraf, A., & Imran, M. (2018). Diagnosis of bovine mastitis: from laboratory to farm. *Tropical Animal Health and Production, 50*(6), 1193-1202.

48. Parida, M., Sannarangaiah, S., Dash, P. K., Rao, P. V. L., & Morita, K. (2008). Loop mediated isothermal amplification (LAMP): a new generation of innovative gene amplification technique; perspectives in clinical diagnosis of infectious diseases. *Reviews in Medical Virology, 18*(6), 407-421.

49. Notomi, T., Mori, Y., Tomita, N., & Kanda, H. (2015). Loop-mediated isothermal amplification (LAMP): principle, features, and future prospects. *Journal of Microbiology, 53*(1), 1-5.

50. Tomita, N., Mori, Y., Kanda, H., & Notomi, T. (2008). Loop-mediated isothermal amplification (LAMP) of gene sequences and simple visual detection of products. *Nature Protocols, 3*(5), 877-882.

51. Notomi, T., Okayama, H., Masubuchi, H., Yonekawa, T., Watanabe, K., Amino, N., & Hase, T. (2000). Loop-mediated isothermal amplification of DNA. *Nucleic Acids Research, 28*(12), e63-e63.

52. Tie, Z., Chunguang, W., Xiaoyuan, W., Xinghua, Z., & Xiuhui, Z. (2012). Loop-mediated

isothermal amplification for detection of Staphylococcus aureus in dairy cow suffering from mastitis. *Journal of Biomedicine and Biotechnology, 2012.*

53. Bosward, K. L., House, J. K., Deveridge, A., Mathews, K., & Sheehy, P. A. (2016). Development of a loop-mediated isothermal amplification assay for the detection of Streptococcus agalactiae in bovine milk. *Journal of Dairy Science, 99*(3), 2142-2150.

54. Luscombe, N. M., Austin, S. E., Berman, H. M., & Thornton, J. M. (2000). An overview of the structures of protein-DNA complexes. *Genome Biology, 1*(1), 1-37.

55. Afek, A., Schipper, J. L., Horton, J., Gordân, R., & Lukatsky, D. B. (2014). Protein− DNA binding in the absence of specific base-pair recognition. *Proceedings of the National Academy of Sciences, 111*(48), 17140-17145.

56. Murphy IV, F. V., & Churchill, M. E. (2000). Nonsequence-specific DNA recognition: a structural perspective. *Structure, 8*(4), R83-R89.

57. Murphy, F. V., Sweet, R. M., & Churchill, M. E. (1999). The structure of a chromosomal high mobility group protein–DNA complex reveals sequence-neutral mechanisms important for non-sequence-specific DNA recognition. *The EMBO Journal, 18*(23), 6610-6618.

58. Agback, P., Baumann, H., Knapp, S., Ladenstein, R., & Härd, T. (1998). Architecture of nonspecific protein–DNA interactions in the Sso7d–DNA complex. *Nature Structural Biology*, 5(7), 579-584.

59. Pingoud, A., & Jeltsch, A. (2001). Structure and function of type II restriction endonucleases. *Nucleic Acids Research, 29*(18), 3705-3727.

60. Inukai, S., Kock, K. H., & Bulyk, M. L. (2017). Transcription factor–DNA binding: beyond binding site motifs. *Current Opinion in Genetics & Development, 43*, 110-119.

61. Sayle, R. A., & Milner-White, E. J. (1995). RASMOL: biomolecular graphics for all. *Trends in Biochemical Sciences, 20*(9), 374-376.

62. Rohs, R., Jin, X., West, S. M., Joshi, R., Honig, B., & Mann, R. S. (2010). Origins of specificity in protein-DNA recognition. *Annual Review of Biochemistry, 79*, 233-269.

63. Aravind, L., Anantharaman, V., Balaji, S., Babu, M. M., & Iyer, L. M. (2005). The many faces of the helix-turn-helix domain: transcription regulation and beyond. *FEMS Microbiology Reviews, 29*(2), 231-262.

64. Daniels, D. S., Woo, T. T., Luu, K. X., Noll, D. M., Clarke, N. D., Pegg, A. E., & Tainer, J. A.

(2004). DNA binding and nucleotide flipping by the human DNA repair protein AGT. *Nature Structural & Molecular Biology, 11*(8), 714-720.

65. Suzuki, M., Yagi, N., & Gerstein, M. (1995). DNA recognition and superstructure formation by helix-turn-helix proteins. *Protein Engineering, Design and Selection, 8*(4), 329-338.

66. Gajiwala, K. S., & Burley, S. K. (2000). Winged helix proteins. *Current Opinion in Structural Biology, 10*(1), 110-116.

67. Gajiwala, K. S., Chen, H., Cornille, F., Roques, B. P., Reith, W., Mach, B., & Burley, S. K. (2000). Structure of the winged-helix protein hRFX1 reveals a new mode of DNA binding. *Nature, 403*(6772), 916-921.

68. Janin, J., Rodier, F., Chakrabarti, P., & Bahadur, R. P. (2007). Macromolecular recognition in the protein data bank. *Acta Crystallographica Section D: Biological Crystallography, 63*(1), 1-8.

69. Ades, S. E., & Sauer, R. T. (1995). Specificity of minor-groove and major-groove interactions in a homeodomain-DNA complex. *Biochemistry, 34*(44), 14601-14608.

70. Tucker-Kellogg, L., Rould, M. A., Chambers, K. A., Ades, S. E., Sauer, R. T., & Pabo, C. O. (1997). Engrailed (Gln50→ Lys) homeodomain–DNA complex at 1.9 Å resolution: structural basis

for enhanced affinity and altered specificity. *Structure, 5*(8), 1047-1054.

71. Pabo, C. O., & Sauer, R. T. (1992). Transcription factors: structural families and principles of DNA recognition. *Annual Review of Biochemistry, 61*(1), 1053-1095.

72. Siggers, T. W., Silkov, A., & Honig, B. (2005). Structural alignment of protein–DNA interfaces: insights into the determinants of binding specificity. *Journal of Molecular Biology, 345*(5), 1027-1045.

73. Kroos, L. (2007). The Bacillus and Myxococcus developmental networks and their transcriptional regulators. *Annual Review of Genetics, 41*, 13-39.

74. Losick, R., & Stragier, P. (1992). Crisscross regulation of cell-type-specific gene expression during development in B. subtilis. *Nature, 355*(6361), 601-604.

75. Errington, J. (1993). Bacillus subtilis sporulation: regulation of gene expression and control of morphogenesis. *Microbiological Reviews, 57*(1), 1-33.

76. Halberg, R., & Kroos, L. (1994). Sporulation regulatory protein SpoIIID from Bacillus subtilis activates and represses transcription by both mother-cell-specific forms of RNA polymerase. *Journal of Molecular Biology, 243*(3), 425-436.

77. Zhang, B., Daniel, R. A., Errington, J., & Kroos, L. (1997). Bacillus subtilis SpoIIID protein binds to two sites in the spoVD promoter and represses transcription by sigmaE RNA polymerase. *Journal of Bacteriology, 179*(3), 972-975.

78. Himes, P., McBryant, S. J., & Kroos, L. (2010). Two regions of Bacillus subtilis transcription factor SpoIIID allow a monomer to bind DNA. *Journal of Bacteriology, 192*(6), 1596-1606.

79. Kunkel, B., Kroos, L., Poth, H., Youngman, P., & Losick, R. (1989). Temporal and spatial control of the mother-cell regulatory gene spoIIID of Bacillus subtilis. *Genes & Development, 3*(11), 1735-1744.

80. Eichenberger, P., Fujita, M., Jensen, S. T., Conlon, E. M., Rudner, D. Z., Wang, S. T., ... & Eisen, J. A. (2004). The program of gene transcription for a single differentiating cell type during sporulation in Bacillus subtilis. *PLoS Biology, 2*(10), e328.

81. Tullius, T. (1995). Homeodomains: together again for the first time. *Structure, 3*(11), 1143-1145.

82. Robinson, P. K. (2015). Enzymes: principles and biotechnological applications. *Essays in Biochemistry, 59*, 1.

83. Paul, M. J., Primavesi, L. F., Jhurreea, D., & Zhang, Y. (2008). Trehalose metabolism and signaling. *Annual Review of Plant Biology, 59*, 417.

84. Gibson, R. P., Gloster, T. M., Roberts, S., Warren, R. A. J., Storch de Gracia, I., García, Á., ... & Davies, G. J. (2007). Molecular basis for trehalase inhibition revealed by the structure of trehalase in complex with potent inhibitors. *Angewandte Chemie International Edition, 46*(22), 4115-4119.

85. Sacktor, B. (1968). Trehalase and the transport of glucose in the mammalian kidney and intestine. *Proceedings of the National Academy of Sciences of the United States of America, 60*(3), 1007.

86. Ouyang, Y., Xu, Q., Mitsui, K., Motizuki, M., & Xu, Z. (2009). Human trehalase is a stress responsive protein in Saccharomyces cerevisiae. *Biochemical and Biophysical Research Communications, 379*(2), 621-625.

87. Shukla, E., Thorat, L. J., Nath, B. B., & Gaikwad, S. M. (2015). Insect trehalase: physiological significance and potential applications. *Glycobiology, 25*(4), 357-367.

88. Elbein, A. D., & Mitchell, M. (1973). Levels of glycogen and trehalose in Mycobacterium

smegmatis and the purification and properties of the glycogen synthetase. *Journal of Bacteriology, 113*(2), 863-873.

89. Shimakata, T., & Minatogawa, Y. (2000). Essential role of trehalose in the synthesis and subsequent metabolism of corynomycolic acid in Corynebacterium matruchotii. *Archives of Biochemistry and Biophysics, 380*(2), 331-338.

90. Kaasen, I., McDougall, J., & Strøm, A. R. (1994). Analysis of the otsBA operon for osmoregulatory trehalose synthesis in Escherichia coli and homology of the OtsA and OtsB proteins to the yeast trehalose-6-phosphate synthase/phosphatase complex. *Gene, 145*(1), 9-15.

91. Maruta, K., Hattori, K., Nakada, T., Kubota, M., Sugimoto, T., & Kurimoto, M. (1996). Cloning and sequencing of trehalose biosynthesis genes from Rhizobium sp. M-ll. *Bioscience, Biotechnology, and Biochemistry, 60*(4), 717-720.

92. Henrissat, B., & Bairoch, A. (1993). New families in the classification of glycosyl hydrolases based on amino acid sequence similarities. *Biochemical Journal, 293*(3), 781-788.

93. Boos, W., Ehmann, U., Forkl, H., Klein, W., Rimmele, M., & Postma, P. (1990). Trehalose transport and metabolism in Escherichia coli. *Journal of Bacteriology, 172*(6), 3450-3461.

94. Horlacher, R., Uhland, K., Klein, W., Ehrmann, M., & Boos, W. (1996). Characterization of a cytoplasmic trehalase of Escherichia coli. *Journal of Bacteriology, 178*(21), 6250-6257.

95. Drikic, M., & De Buck, J. (2018). Split trehalase as a versatile reporter for a wide range of biological analytes. *Biotechnology and Bioengineering, 115*(5), 1128-1136.

96. Gera, K., & McIver, K. S. (2013). Laboratory growth and maintenance of Streptococcus pyogenes (the Group A Streptococcus, GAS). *Current Protocols in Microbiology*, *30*(1), 9D-2.

97. Michel, A., Koch-Koerfges, A., Krumbach, K., Brocker, M., & Bott, M. (2015). Anaerobic growth of Corynebacterium glutamicum via mixed-acid fermentation. *Applied and Environmental Microbiology*, *81*(21), 7496-7508.

98. Caguiat, J. J. (2014). Generation of Enterobacter sp. YSU auxotrophs using transposon mutagenesis. *Journal of Visualized Experiments*, (92), e51934.

99. Klausegger, A., Hell, M., Berger, A., Zinober, K., Baier, S., Jones, N., ... & Kofler, B. (1999). Gram type-specific broad-range PCR amplification for rapid detection of 62 pathogenic bacteria. *Journal of Clinical Microbiology*, *37*(2), 464-466.

100. Durfee, T., Nelson, R., Baldwin, S., Plunkett III, G., Burland, V., Mau, B., ... & Blattner, F. R.

(2008). The complete genome sequence of Escherichia coli DH10B: insights into the biology of a laboratory workhorse. *Journal of Bacteriology*, *190*(7), 2597-2606.

101. Stinson, L. F., Ma, J., Rea, A., Dymock, M., & Geddes, D. T. (2021). Centrifugation does not remove bacteria from the fat fraction of human milk. *Scientific Reports*, *11*(1), 1-8.

102. Sun, L., Dicksved, J., Priyashantha, H., Lundh, Å., & Johansson, M. (2019). Distribution of bacteria between different milk fractions, investigated using culture-dependent methods and molecular-based and fluorescent microscopy approaches. *Journal of Applied Microbiology*, *127*(4), 1028-1037.

103. ALI-VEHMAS, T. E. R. H. I., Westphalen, P., Myllys, V., & Sandholm, M. (1997). Binding of Staphylococcus aureus to milk fat globules increases resistance to penicillin-G. *Journal of Dairy Research*, *64*(2), 253-260.

104. Douëllou, T., Galia, W., Kerangart, S., Marchal, T., Milhau, N., Bastien, R., ... & Sergentet-Thevenot, D. (2018). Milk fat globules hamper adhesion of enterohemorrhagic Escherichia coli to enterocytes: in vitro and in vivo evidence. *Frontiers in Microbiology*, *9*, 947.

105. Mertens, K., Freund, L., Schmoock, G., Hänsel, C., Melzer, F., & Elschner, M. C. (2014). Comparative evaluation of eleven commercial DNA extraction kits for real-time PCR detection of

Bacillus anthracis spores in spiked dairy samples. *International Journal of Food Microbiology*, *170*, 29-37.

106. Lima, S. F., Bicalho, M. L. D. S., & Bicalho, R. C. (2018). Evaluation of milk sample fractions for characterization of milk microbiota from healthy and clinical mastitis cows. *PLoS One*, *13*(3), e0193671.

107. Bickley, J., Short, J. K., McDowell, D. G., & Parkes, H. C. (1996). Polymerase chain reaction (PCR) detection of Listeria monocytogenes in diluted milk and reversal of PCR inhibition caused by calcium ions. *Letters in Applied Microbiology*, *22*(2), 153-158.

108. Stedtfeld, R. D., Stedtfeld, T. M., Kronlein, M., Seyrig, G., Steffan, R. J., Cupples, A. M., & Hashsham, S. A. (2014). DNA extraction-free quantification of Dehalococcoides spp. in groundwater using a hand-held device. *Environmental Science & Technology*, *48*(23), 13855-13863.

109. Sun, Y., Quyen, T. L., Hung, T. Q., Chin, W. H., Wolff, A., & Bang, D. D. (2015). A lab-on-a-chip system with integrated sample preparation and loop-mediated isothermal amplification for rapid and quantitative detection of Salmonella spp. in food samples. *Lab on a Chip*, *15*(8), 1898-1904.

110. Kaneko, H., Kawana, T., Fukushima, E., & Suzutani, T. (2007). Tolerance of loop-mediated isothermal amplification to a culture medium and biological substances. *Journal of Biochemical and Biophysical Methods*, *70*(3), 499-501.

111. Powell, H. A., Gooding, C. M., Garrett, S. D., Lund, B. M., & McKee, R. A. (1994). Proteinase inhibition of the detection of Listeria monocytogenes in milk using the polymerase chain reaction. *Letters in Applied Microbiology*, *18*(1), 59-61.

112. Wilson, I. G. (1997). Inhibition and facilitation of nucleic acid amplification. *Applied and Environmental Microbiology*, *63*(10), 3741-3751.

113. JERŠEK, A. K. N. T. B. (2014). Evaluation of different methods for DNA extraction from milk. *Journal of Food and Nutrition Research (ISSN 1336-8672)*, *53*(2), 97-104.

114. Usman, T., Yu, Y., Liu, C., Fan, Z., & Wang, Y. (2014). Comparison of methods for high quantity and quality genomic DNA extraction from raw cow milk. *Genet Mol Res*, *13*(2), 3319-3328.

115. Hedman, J., & Rådström, P. (2013). Overcoming inhibition in real-time diagnostic PCR. *Methods in Molecular Biology (Clifton, N.J.), 943*, 17–48.

116. Weyant, R. S., Edmonds, P., & Swaminathan, B. (1990). Effect of ionic and nonionic detergents on the Taq polymerase. *Biotechniques*, *9*(3), 308-309.

117. Quigley, L., O'Sullivan, O., Beresford, T. P., Paul Ross, R., Fitzgerald, G. F., & Cotter, P. D. (2012). A comparison of methods used to extract bacterial DNA from raw milk and raw milk cheese. *Journal of Applied Microbiology*, *113*(1), 96-105.

118. Cabeen, M. T., & Jacobs-Wagner, C. (2005). Bacterial cell shape. *Nature Reviews Microbiology*, *3*(8), 601-610.

119. Vollmer, W., & Holtje, J. V. (2004). The architecture of the murein (peptidoglycan) in gram-negative bacteria: vertical scaffold or horizontal layer (s)?. *Journal of Bacteriology*, *186*(18), 5978-5987.

120. Odumeru, J., Gao, A., Chen, S., Raymond, M., & Mutharia, L. (2001). Use of the bead beater for preparation of Mycobacterium paratuberculosis template DNA in milk. *Canadian Journal of Veterinary Research*, *65*(4), 201.

121. Mahalanabis, M., Al-Muayad, H., Kulinski, M. D., Altman, D., & Klapperich, C. M. (2009). Cell lysis and DNA extraction of gram-positive and gram-negative bacteria from whole blood in a disposable microfluidic chip. *Lab on a Chip*, *9*(19), 2811-2817.

122. Raven, K. E., Girgis, S. T., Akram, A., Blane, B., Leek, D., Brown, N., & Peacock, S. J. (2021). A common protocol for the simultaneous processing of multiple clinically relevant bacterial species for whole genome sequencing. *Scientific Reports*, *11*(1), 1-8.

123. Ripon, M. H., Hasan, M., Ahasan, M. M., Alam, M. W., & Kabir, S. (2011). Comparison of three different methods of genomic DNA extraction from gram positive and gram negative bacteria. *J. Expt. Biosci*, *2*(1), 55-60.

124. Junior, J. C. R., Tamanini, R., Soares, B. F., de Oliveira, A. M., de Godoi Silva, F., da Silva, F. F., ... & Beloti, V. (2016). Efficiency of boiling and four other methods for genomic DNA extraction of deteriorating spore-forming bacteria from milk. *Semina: Ciências Agrárias*, *37*(5), 3069-3078.

125. Jenkins, C., Ling, C. L., Ciesielczuk, H. L., Lockwood, J., Hopkins, S., McHugh, T. D., ... & Kibbler, C. C. (2012). Detection and identification of bacteria in clinical samples by 16S rRNA gene sequencing: comparison of two different approaches in clinical practice. *Journal of Medical Microbiology*, *61*(4), 483-488.

126. Griffioen, K., Cornelissen, J., Heuvelink, A., Adusei, D., Mevius, D., van der Wal, F. J., & 1Health4Food–Dutch Mastitis Diagnostics Consortium. (2020). Development and evaluation of 4

loop-mediated isothermal amplification assays to detect mastitis-causing bacteria in bovine milk samples. *Journal of Dairy Science*, *103*(9), 8407-8420.

127. Sheet, O. H., Grabowski, N. T., Klein, G., & Abdulmawjood, A. (2016). Development and validation of a loop mediated isothermal amplification (LAMP) assay for the detection of Staphylococcus aureus in bovine mastitis milk samples. *Molecular and Cellular Probes*, *30*(5), 320-325.

128. Hahne, J., Kloster, T., Rathmann, S., Weber, M., & Lipski, A. (2018). Isolation and characterization of Corynebacterium spp. from bulk tank raw cow's milk of different dairy farms in Germany. *PLoS One*, *13*(4), e0194365.

129. Wang, D. G., Brewster, J. D., Paul, M., & Tomasula, P. M. (2015). Two methods for increased specificity and sensitivity in loop-mediated isothermal amplification. *Molecules*, *20*(4), 6048-6059.

130. Sivaprasad, V., Satish, L., Mallikarjuna, G., Chandrakanth, N., Josepha, A. M., & Moorthy, S. M. (2021). A Field-Friendly Loop-Mediated Isothermal Amplification (FF-LAMP) method for rapid detection of Nosema bombycis in silkworm, Bombyx mori. *Invertebrate Survival Journal*, 66-74.

131. Wong, Y. P., Othman, S., Lau, Y. L., Radu, S., & Chee, H. Y. (2018). Loop-mediated

isothermal amplification (LAMP): a versatile technique for detection of micro-organisms. *Journal of Applied Microbiology*, *124*(3), 626-643.

132. Lee, P. Y., Wong, Y. P., Othman, S., & Chee, H. Y. (2021). Room-temperature stable loop-mediated isothermal amplification (LAMP) reagents to detect leptospiral DNA. *Asian Biomedicine*, *15*(4), 183-189.

133. Karthik, K., Rathore, R., Thomas, P., Arun, T. R., Viswas, K. N., Dhama, K., & Agarwal, R. (2014). New closed tube loop mediated isothermal amplification assay for prevention of product cross-contamination. *MethodsX*, *1*, 137-143.

134. Cai, S., Jung, C., Bhadra, S., & Ellington, A. D. (2018). Phosphorothioated primers lead to loop-mediated isothermal amplification at low temperatures. *Analytical Chemistry*, *90*(14), 8290-8294.

135. Fischbach, J., Xander, N. C., Frohme, M., & Glökler, J. F. (2015). Shining a light on LAMP assays' A comparison of LAMP visualization methods including the novel use of berberine. *Biotechniques*, *58*(4), 189-194.

136. Bista, B. R., Ishwad, C., Wadowsky, R. M., Manna, P., Randhawa, P. S., Gupta, G., ... & Vats, A. (2007). Development of a loop-mediated isothermal amplification assay for rapid detection of

BK virus. *Journal of Clinical Microbiology*, *45*(5), 1581-1587.

137. Yamaguchi, H., & Miyazaki, M. (2014). Refolding techniques for recovering biologically active recombinant proteins from inclusion bodies. *Biomolecules*, *4*(1), 235-251.

138. Sørensen, H. P., Sperling-Petersen, H. U., & Mortensen, K. K. (2003). Dialysis strategies for protein refolding: preparative streptavidin production. *Protein Expression and Purification*, *31*(1), 149-154.

139. Record Jr, M. T., Ha, J. H., & Fisher, M. A. (1991). Analysis of equilibrium and kinetic measurements to determine thermodynamic origins of stability and specificity and mechanism of formation of site-specific complexes between proteins and helical DNA. *Methods in Enzymology, 208*, 291-343.

140. von Hippel, P. H. (2007). From “simple” DNA-protein interactions to the macromolecular machines of gene expression. *Annual Review of Biophysics and Biomolecular Structure, 36*, 79.